PREPARATION, CHARACTERISATION, STABILITY, AND APPLICATION OF TOCOTRIENOL NANOEMULSION STABILISED BY PEA PROTEIN ISOLATE AND FLAXSEED GUM COMPLEXES

By

TEOW SHUH JUN

Thesis Submitted to the School of Graduate Studies, Universiti Putra Malaysia, in Fulfilment of the Requirements for the Degree of Doctor of Philosophy

December 2023

FSTM 2023 15

Abstract of thesis presented to the Senate of Universiti Putra Malaysia in fulfilment of the requirement for the degree of Doctor of Philosophy

PREPARATION, CHARACTERISATION, STABILITY, AND APPLICATION OF TOCOTRIENOL NANOEMULSION STABILISED BY PEA PROTEIN ISOLATE AND FLAXSEED GUM COMPLEXES

By

TEOW SHUH JUN

December 2023

Chair : Professor Tan Chin Ping, PhD
Faculty : Food Science and Technology

In recent times, there has been a growing demand for full plant-based encapsulating agents to replace the commonly used animal-based or synthetic emulsifiers. However, native pea protein isolate (PPI) has the major drawback of low solubility at neutral pH and unable to stabilize emulsion under storage period. Tocotrienol-rich fraction (TRF) derived from red palm oil has gained significant attention due to its health benefits. However, incorporating it into food products has been challenging due to its poor water solubility. Therefore, this study aimed to enhance the solubility of native PPI followed by complexation with flaxseed gum (FG) to create a stable delivery system to form TRF-based nanoemulsions.

Firstly, the solubility of treated pea protein isolate (TPPI) was enhanced through pH adjustment and thermal treatment. TRF-based oil-in-water nanoemulsions were prepared under pH 6 using 2% w/w of soluble treated pea protein isolate- flaxseed gum (TPPI-FG) complexes at different ratios (ranging from 3:1 to 11:1). The results indicated that the nanoemulsion prepared using TPPI-FG (3:1) exhibited the highest stability, as evidenced by its increased viscosity, emulsifying activity index, and emulsion stability index. During a 7-day storage study, the nanoemulsion stabilized by TPPI-FG (3:1) remained the most stable, with only a slight increase in droplet size, the lowest rise in polydispersity index, and creaming index. The morphology study further revealed that no coalescence was observed in this nanoemulsion.

Subsequently, the optimized TPPI-FG (3:1) stabilized nanoemulsion was spray-dried using different core-to-wall ratios, wall material compositions, and mixing ratios. The microcapsule formed at a 1:4 M ratio exhibited higher microencapsulation efficiency (MEE), improved water solubility index, increased retention of tocopherol and tocotrienol, and excellent flowability. When the 1:4 core-to-wall ratio was employed, Maltodextrin (M) was mixed with starch sodium octenyl succinate (OSS) and inulin

(INU) at mixing ratios of 9:1 and 8:2, to create microcapsules. It was observed that the 1:4 M:OSS (8:2) microcapsule achieved the highest MEE, retained the most tocopherol and tocotrienol, demonstrated excellent flowability, and exhibited low cohesiveness. This microcapsule also possessed the highest sphericity, featuring a smooth and dense external surface without cracks.

Next, the optimised TRF-based microcapsule produced from the 1:4 M:OSS (8:2) ratio were examined for storage stability, release characteristics, and bioaccessibility of tocotrienol. Over 13 weeks of storage at 40 °C, the microcapsules displayed a slight increase in cohesiveness and lightness, along with a minor decrease in MEE, yellowness, and chroma. Additionally, the microcapsule remained stable against oxidation during storage, as indicated by a low peroxide value, and degradation of tocopherol and tocotrienol isomers. These microcapsules proceed to be stable under various ionic strengths (ranging from 0 to 200 mM) and pH (ranging from 3 to 9). Furthermore, they exhibited higher bioaccessibility and release compared to bulk oil.

Finally, the optimised TRF-based microcapsules were added to mayonnaises (M-mayo) and stored at 4 °C for one month. M-mayo remained stable throughout storage, showing only a slight increase in lightness, redness, yellowness, firmness, consistency, and viscosity. By the fourth week, M-mayo had a low peroxide value and minimal degradation of tocopherol and tocotrienol isomers. Sensory evaluation indicated that M-mayo received the highest rating for color, while other sensory attributes (aroma, taste, creaminess, sourness, and overall acceptability) received similar ratings with other samples. This demonstrated that M-mayo is equally well-liked as the original mayonnaise. In conclusion, this study successfully addresses the challenge of incorporating TRF into food products using a fully plant-based emulsifier. The optimized delivery system shows excellent stability, bioaccessibility, and acceptance, making it a promising approach for enhancing the nutritional value of food products.

Keywords: Protein-polysaccharide complex, Tocotrienol-rich fraction, Microencapsulation, Pea protein isolate, flaxseed gum

SGD: GOAL 3: Good Health and Well-Being

Abstrak tesis yang dikemukakan kepada Senat Universiti Putra Malaysia sebagai memenuhi keperluan untuk ijazah Doktor Falsafah

PENYEDIAAN, PENCIRIAN, KESTABILAN DAN APLIKASI NANOEMULSI TOKOTRIENOL YANG DISTABIL OLEH KOMPLEKS PROTIN PEA TERASING DAN GAM BIJI FLAX

Oleh

TEOW SHUH JUN

Disember 2023

Pengerusi : Profesor Tan Chin Ping, PhD
Fakulti : Sains dan Tekonolgi Makanan

Sejak kebelakangan ini, terdapat permintaan yang semakin meningkat untuk agen pengkapsulan berasaskan tumbuhan untuk menggantikan pengemulsi berasaskan haiwan atau sintetik yang biasa digunakan. Walau bagaimanapun, pengasingan protein pea asli (PPI) mempunyai kelemahan iaitu keterlarutan yang rendah pada pH neutral dan tidak dapat menstabilkan emulsi dalam tempoh penyimpanan. Pecahan kaya tokotrienol (TRF) yang diperoleh daripada minyak sawit merah telah mendapat perhatian yang ketara kerana manfaat kesihatannya. Walau bagaimanapun, memasukkannya ke dalam produk makanan telah mencabar kerana keterlarutan airnya yang lemah. Oleh itu, kajian ini bertujuan untuk meningkatkan keterlarutan PPI asli diikuti dengan pengkompleksan dengan gam biji flax (FG) untuk mewujudkan sistem penghantaran yang stabil untuk membentuk nanoemulsi berasaskan TRF.

Pertama, keterlarutan pengasingan protin pea yang dirawat (TPPI) telah dipertingkatkan melalui pelarasan pH dan rawatan haba. Nanoemulsi minyak dalam air berasaskan TRF telah disediakan di bawah pH 6 menggunakan 2% b/b kompleks pengasingan protin pea yang dirawat -gum biji flaxis (TPPI-FG) larut pada nisbah yang berbeza (antara 3:1 hingga 11:1). Keputusan menunjukkan bahawa nanoemulsi yang disediakan menggunakan TPPI-FG (3:1) mempamerkan kestabilan tertinggi, seperti yang dibuktikan oleh peningkatan kelikatan, indeks aktiviti pengemulsi, dan indeks kestabilan emulsi. Semasa kajian penyimpanan selama 7 hari, nanoemulsi yang distabilkan oleh TPPI-FG (3:1) kekal paling stabil, dengan hanya sedikit peningkatan dalam saiz titisan, kenaikan terendah dalam indeks polidispersiti, dan indeks krim. Kajian morfologi seterusnya mendedahkan bahawa tiada penyatuan diperhatikan dalam nanoemulsi ini.

Selepas itu, nanoemulsi stabil TPPI-FG (3:1) yang dioptimumkan telah disembur-kering menggunakan nisbah teras-ke-dinding yang berbeza, komposisi bahan dinding, dan nisbah campuran. Mikrokapsul yang terbentuk pada nisbah 1:4 maltodekstrin (M)

mempamerkan kecekapan mikroenkapsulasi (MEE) yang lebih tinggi, indeks keterlarutan air yang lebih baik, pengekalan tokoferol dan tokotrienol yang tidak berubah, dan kebolehaliran yang sangat baik. Apabila nisbah teras-ke-dinding 1:4 digunakan, M dicampur dengan kanji sodium octenyl succinate (OSS) dan inulin (INU) pada nisbah campuran 9:1 dan 8:2, untuk menghasilkan mikrokapsul. Telah diperhatikan bahawa mikrokapsul 1:4 M:OSS (8:2) mencapai MEE tertinggi, mengekalkan tokoferol dan tokotrienol yang paling banyak, menunjukkan kebolehliran yang sangat baik, dan mempamerkan kepaduan yang rendah. Mikrokapsul ini juga mempunyai sfera tertinggi, menampilkan permukaan luar yang licin dan padat tanpa retak.

Seterusnya, mikrokapsul berasaskan TRF yang dioptimumkan yang dihasilkan daripada nisbah 1:4 M:OSS (8:2) telah diperiksa untuk kestabilan penyimpanan, ciri pelepasan, dan bioakses tocotrienol. Lebih 13 minggu penyimpanan pada 40 °C, mikrokapsul menunjukkan sedikit peningkatan dalam kepaduan dan kecerahan, bersama-sama dengan penurunan kecil dalam MEE, kekuningan dan kroma. Selain itu, mikrokapsul kekal stabil terhadap pengoksidaan semasa penyimpanan, seperti yang ditunjukkan oleh nilai peroksida yang rendah, dan degradasi isomer tokoferol dan tokotrienol. Mikrokapsul ini terbukti stabil di bawah pelbagai kekuatan ionik (antara 0 hingga 200 mM) dan pH (antara 3 hingga 9). Tambahan pula, mereka mempamerkan bioakses dan pelepasan yang lebih tinggi berbanding minyak pukal.

Akhirnya, mikrokapsul berasaskan TRF yang dioptimumkan telah ditambah kepada mayonis (M-mayo) dan disimpan pada suhu 4 ° C selama satu bulan. M-mayo kekal stabil sepanjang penyimpanan, hanya menunjukkan sedikit peningkatan dalam kecerahan, kemerahan, kekuningan, ketegasan, konsistensi dan kelikatan. Menjelang minggu keempat, M-mayo mempunyai nilai peroksida yang rendah dan degradasi minimum isomer tokoferol dan tokotrienol. Penilaian deria menunjukkan bahawa M-mayo menerima penarafan tertinggi untuk warna, manakala atribut deria lain (aroma, rasa, krim, masam dan penerimaan keseluruhan) menerima penilaian yang sama dengan sampel lain. Ini menunjukkan bahawa M-mayo sangat digemari seperti mayonis asli. Kesimpulannya, kajian ini berjaya menangani cabaran untuk memasukkan TRF ke dalam produk makanan menggunakan pengemulsi berasaskan tumbuhan sepenuhnya. Sistem penyampaian yang dioptimumkan menunjukkan kestabilan, bioakses dan penerimaan yang sangat baik, menjadikannya pendekatan yang menjanjikan untuk meningkatkan nilai pemakanan produk makanan.

Kata Kunci: Kompleks protin-polisakarida, Pecahan kaya tokotrienol, Mikroenkapsulasi, Pengasingan protin pea, Gam biji flax

SGD: MATLAMAT 3: Kesihatan dan Kesejahteraan yang Baik

ACKNOWLEDGEMENTS

First and above all, I would like to express my deepest and most sincere gratitude to my supervisor, Prof. Dr. Tan Chin Ping, for his unwavering and friendly guidance, constructive discussions, valuable advice, precious suggestions, understanding, and constant support throughout the experimental and thesis phases. His contribution played a pivotal role in the success of this research.

I extend my special thanks to my co-supervisors, Dr. Tan Tai Boon, Dr. Khor Yih Phing, and Dr. Masni Mat Yusoff for their continuous support, practical suggestions, and great engagement in my research. I am genuinely grateful for their insightful comments and meaningful discussions, which greatly assisted me in completing my research.

I also want to express my sincere appreciation to all my fellow lab mates, especially Choy Hey Weng and Ng Siang Keat in the Fats and Oil Laboratory for their invaluable assistance and guidance. My deepest gratitude also goes to the laboratory staff at the Faculty of Food Science and Technology in Universiti Putra Malaysia, particularly Mr Shawal and Ms Suraya. Their help, friendship, advice, support, and understanding have been immensely valuable.

Last but certainly not least, I would like to express my deepest appreciation to my beloved parents, who always believed in me and provided unwavering faith, confidence, unconditional love and support. I also extend my gratitude to the rest of my extended family for their care, prayers, encouragement, and love. To all those who indirectly contributed to this research, your kindness means a great deal to me. Thank you very much.

This thesis was submitted to the Senate of Universiti Putra Malaysia and has been accepted as fulfilment of the requirement for the degree of Doctor of Philosophy. The members of the Supervisory Committee were as follows:

Tan Chin Ping, PhD
Professor
Faculty of Food Science and Technology
Universiti Putra Malaysia
(Chairman)

Tan Tai Boon, PhD
Senior Lecturer
Faculty of Food Science and Technology
Universiti Putra Malaysia
(Member**)**

Masni binti Mat Yusoff, PhD
Senior Lecturer
Faculty of Food Science and Technology
Universiti Putra Malaysia
(Member)

Khor Yih Phing, PhD
Lecturer
Faculty of Food Science and Technology
Universiti Putra Malaysia
(Member)

_____
ZALILAH MOHD SHARIFF, PhD
Professor and Dean
School of Graduate Studies
Universiti Putra Malaysia

Date: 8 May 2025

TABLE OF CONTENTS

		Page
ABSTRACT		i
ABSTRAK		iii
ACKNOWLEDGEMENTS		v
APPROVAL		vi
DECLARATION		viii
LIST OF TABLES		xv
LIST OF FIGURES		xvii
LIST OF ABBREVIATIONS		xviii
CHAPTER		
1	**INTRODUCTION**	1
	1.1 Background	1
	1.2 Problem statement	3
	1.3 Objectives	3
2	**LITERATURE REVIEW**	5
	2.1 Plant-Based Protein Emulsifier	5
	2.1.1 Pea Protein	5
	2.2 Plant-Based Polysaccharide Emulsifier	6
	2.2.1 Flaxseed Gum (FG)	7
	2.3 Complexation between Protein and Polysaccharides	7
	2.3.1 Synergistic Effect of Protein-polysaccharides Complexes	7
	2.3.2 Applications of Protein-polysaccharide Complexes in Food Industry	8
	2.4 Tocotrienol-Rich Fraction (TRF)	8
	2.4.1 Solubility	9
	2.4.2 Absorption Capacity	10
	2.5 Nanoemulsions	10
	2.5.1 Stability and Application of Nanoemulsions in Food	12
	2.6 Physiochemical Characterization of Nanoemulsions	14
	2.6.1 Zeta Potential	14
	2.6.2 Particle Size Distribution (PSD)	14
	2.6.3 Polydispersity Index (PDI)	14
	2.6.4 pH Profile	15
	2.6.5 Viscosity	15
	2.6.6 Storage Stability	16
	2.7 Spray drying	16
	2.7.1 Maltodextrin (M)	17
	2.7.2 Starch Sodium Octenyl Succinate (OSS)	17
	2.7.3 Inulin (INU)	18
	2.8 Characterization of Microcapsule	19
	2.8.1 Microencapsulation Efficiency (MEE)	19
	2.8.2 Moisture Content (MC)	19
	2.8.3 Water Activity (A_w)	19
	2.8.4 Flowability and Cohesiveness	19

2.8.5 Peroxide Value (PV) 20
2.9 Application of Tocotrienol Microcapsule in Food Matrix 20
2.9.1 Mayonnaise 20
2.10 Summary 21

3 PREPARATION OF STABLE TOCOTRIENOL-RICH NANOEMULSIONS USING PEA PROTEIN ISOLATE-FLAXSEED GUM COMPLEXES 22
3.1 Introduction 24
3.2 Materials and Methods 24
3.2.1 Materials 24
3.2.2 pH-Shifting and Thermal Treatment of PPI 24
3.2.2.1 Protein Solubility 24
3.2.3 Formation of TPPI-FG Complexes 25
3.2.3.1 Turbidimetric Measurement 25
3.2.4 Preparation of TRF-based Nanoemulsions 25
3.2.4.1 Zeta Potential Measurement 26
3.2.4.2 Droplet Size Distribution and Polydispersity Index (PDI) 26
3.2.4.3 Viscosity 26
3.2.4.4 pH 26
3.2.4.5 Emulsion Activity Index (EAI) and Emulsion Stability Index (ESI) 27
3.2.4.6 Creaming Index (CI) 27
3.2.4.7 Short-term Storage Study 27
3.2.4.8 Transition Electron Microscopy (HR-TEM) 28
3.2.5 Statistical Analysis 28
3.3 Results and Discussion 28
3.3.1 Effect of pH-shifting and Thermal Treatment on Protein Solubility 28
3.3.2 Characterization of TPPI-FG Complexes 29
3.3.2.1 Turbidimetric Measurement 29
3.3.2.2 Zeta Potential 31
3.3.3 Characterization of Nanoemulsions 32
3.3.3.1 Droplet Size Distribution and Polydispersity Index (PDI) 32
3.3.3.2 Zeta Potential 33
3.3.3.3 Viscosity and pH 33
3.3.3.4 Emulsion Activity Index (EAI) and Emulsion Stability Index (ESI) 34
3.3.3.5 Short-term Storage Study 36
3.3.3.6 Morphology 37
3.4 Conclusion 40

4 OPTIMIZATION AND CHARACTERIZATION OF TOCOTRIENOL-RICH FRACTION-BASED MICROCAPSULES PRODUCE BY SPRAY DRYING USING DIFFERENT CORE-TO-WALL RATIOS, 41

WALL MATERIAL COMPOSITIONS AND MIXING RATIOS
4.1 Introduction 41
4.2 Materials and Methods 42
4.2.1 Materials 42
4.2.2 Preparation of TPPI-FG Complex 43
4.2.3 Preparation of TRF-based Microcapsules 43
4.2.4 Spray Drying 44
4.2.4.1 Microencapsulation Efficiency (MEE) 44
4.2.4.2 Moisture Content (MC) 45
4.2.4.3 Water Activity(A_w) 45
4.2.4.4 Flowability and Cohesiveness 45
4.2.4.5 Water Solubility Index (WSI) and Water Absorption Index (WAI) 46
4.2.4.6 Colour 47
4.2.4.7 Tocopherol and Tocotrienol Content Analysis 47
4.2.4.8 Scanning Electron Microscopy (SEM) 48
4.2.5 Statistical Analysis 48
4.3 Results and Discussion 48
4.3.1 Microencapsulation Efficiency (MEE) 48
4.3.2 Moisture Content (MC) 49
4.3.3 Water Activity (A_w) 49
4.3.4 Flowability and Cohesiveness 49
4.3.5 Water solubility index (WSI) and water absorption index (WAI) 50
4.3.6 Colour 51
4.3.7 Tocopherol and Tocotrienol content Retention 53
4.3.8 Scanning Electron Microscopy (SEM) 55
4.4 Conclusions 56

5 DETERMINATION OF THE STORAGE STABILITY, RELEASE CHARACTERISTICS, AND BIOACCESSIBILITY OF THE TOCOTRIENOL-RICH FRACTION ENCAPSULATED IN MALTODEXTRIN-STARCH SODIUM OCTENYL SUCCINATE MICROCAPSULES 58
5.1 Introduction 58
5.2 Materials and Methods 59
5.2.1 Materials 59
5.2.2 Preparation of TPPI-FG Complex 60
5.2.3 Preparation of TRF-based Microcapsule 60
5.2.4 Spray Drying 60
5.2.5 Storage Stability 60
5.2.5.1 Microencapsulation Efficiency (MEE) 60
5.2.5.2 Moisture Content (MC) 60
5.2.5.3 Water Activity (A_w) 60
5.2.5.4 Flowability and Cohesiveness 61

5.2.5.5 Colour 61
5.2.5.6 Reconstitution Properties 61
5.2.5.7 Peroxide Value (PV) 61
5.2.5.8 Tocopherol and Tocotrienol Content Analysis 62
5.2.6 Release Characteristics 62
5.2.6.1 Effect of Ionic Strength 62
5.2.6.2 Effect of pH 63
5.2.7 *In vitro* Digestion 63
5.2.7.1 Bio-Accessibility and Percentage of Release 64
5.2.8 Statistical Analysis 64
5.3 Results and Discussion 64
5.3.1 Storage Stability 64
5.3.1.1 Microencapsulation Efficiency (MEE) 65
5.3.1.2 Moisture Content (MC) 65
5.3.1.3 Water Activity (A_w) 65
5.3.1.4 Flowability and Cohesiveness 65
5.3.1.5 Colour 66
5.3.1.6 Reconstitution Properties 66
5.3.1.7 Peroxide Value (PV) 68
5.3.1.8 Degradation of Tocopherol and Tocotrienol 68
5.3.2 Release Characteristics 71
5.3.2.1 Effect of Ionic Strength 71
5.3.2.2 Effect of pH 71
5.3.3 Percentage of TRF Release and Bioaccessibility after *In Vitro* Digestion 72
5.4 Conclusions 74

6 THE EFFECT OF STORAGE STABILITY OF TOCOTRIENOL-RICH FRACTION (TRF) ENCAPSULATED IN MALTODEXTRIN-STARCH SODIUM OCTENYL SUCCINATE MICROCAPSULES ON MAYONNAISE MATRIX 75
6.1 Introduction 76
6.2 Materials and Methods 76
6.2.1 Materials 76
6.2.2 Preparation of TRF-based microcapsule 77
6.2.3 Preparation of TRF-fortified Mayonnaise 77
6.2.4 Storage Stability 78
6.2.4.1 Colour 78
6.2.4.2 pH 78
6.2.4.3 Viscosity 78
6.2.4.4 Texture 78
6.2.4.5 Peroxide Value (PV) 78
6.2.4.6 Tocopherol and Tocotrienol Content Analysis 79
6.2.5 Sensory Evaluation 79

6.2.6 Statistical Analysis 80
6.3 Results and Discussion 80
6.3.1 Storage Stability 80
6.3.1.1 Colour 80
6.3.1.2 pH 81
6.3.1.3 Viscosity 83
6.3.1.4 Texture 83
6.3.1.5 Peroxide Value (PV) 85
6.3.1.6 Degradation of Tocopherol and Tocotrienol 85
6.3.2 Sensory Evaluation 87
6.4 Conclusions 88

7 SUMMARY, CONCLUSIONS AND FUTURE RECOMMENDATIONS 89

REFERENCES 91
APPENDICES 114
BIODATA OF STUDENT 125
LIST OF PUBLICATIONS 126

LIST OF TABLES

Table		Page
2.1	Comparison of high-energy method emulsification processes. Adapted from Håkansson & Rayner, (2018).	11
3.1	Critical pHs associated with the complexation of treated pea protein isolate-flaxseed gum at different ratios.	31
3.2	Characterization of fresh nanoemulsions produced using treated pea protein isolate-flaxseed gum complexes with different ratios.	35
4.1	Formulations of TRF-based microcapsules produced by spray-drying using different core-to-wall ratios, wall material compositions and mixing ratios.	44
4.2	Classification of microcapsules flowability based on the Carr Index (1965) and Hausner ratio (1967).	46
4.3	Characterization of treated pea protein isolate-flaxseed gum complex stabilized TRF-based microcapsules produced by spray-drying core-to-wall ratios, wall material compositions and mixing ratios.	52
4.4	Tocopherol and tocotrienol content analysis of TRF-based microcapsules produced by spray-drying using different core-to-wall ratios, wall material compositions and mixing ratios.	54
5.1	Physical stability of TRF-based microcapsule produced by wall material of M:OSS (8:2) stored at 40 °C for 13 weeks.	67
5.2	Oxidative stability of TRF-based microcapsule produced by wall material of M:OSS (8:2) stored at 40 °C for 13 weeks.	70
5.3	Release characteristic of spray-dried TRF-based microcapsule as a function of ionic strength and pH.	72
6.1	Formulations of TRF-fortified mayonnaises.	77
6.2	The effect of storage on the pH and colour of different mayonnaise samples.	80
6.3	The effect of storage on the texture and viscosity of different mayonnaise samples.	84
6.4	The effect of storage on the peroxide value and degradation of tocopherol and tocotrienol on different mayonnaise samples.	86

6.5 Sensory attributes of TRF-fortified mayonnaise samples based on hedonic ratings (n = 60)*. 87

LIST OF FIGURES

Figure		Page
2.1	Chemical structure of tocotrienol and tocopherol (Source: Aggarwal et al., 2010).	9
3.1	Solubility of native (—●—) and treated (—■—) pea protein isolate at different pH.	29
3.2	Turbidity of treated pea protein isolate-flaxseed gum complexes with different ratios as a function of pH.	31
3.3	Zeta potential of treated pea protein isolate-flaxseed gum complexes with different ratios as a function of pH.	32
3.4	(a) Droplet size distribution; (b) polydispersity index; (c) zeta potential; and (d) creaming index changes of nanoemulsions produced using treated pea protein isolate-flaxseed gum complexes with different ratios stored for 7 days at 25 ^{o}C.	37
3.5	TEM micrographs of TRF-based nanoemulsions prepared with different treated pea protein isolate-flaxseed gum complexes ratios (a) 3:1; (b) 5:1; (c) 7:1; (d) 9:1 and (e) 11:1. Scale bar represent 100 nm.	39
4.1	SEM micrographs of TRF-based microcapsules prepared at 1:4 core-to-wall ratio with different wall material compositions and mixing ratios (a) M:OSS (9:1); (b) M:OSS (8:2); (c) M:INU (9:1); (d) M:INU (8:2) and (e) M. Scale bar represent 10 µm.	56
5.1	Bioaccessibility and release of tocotrienol-rich fraction (TRF) from bulk oil and microcapsule after *in vitro* digestion.	74
6.1	Fresh mayonnaise samples prepared from different formulations: (a) Control mayonnaise (C-mayo); (b) Mayonnaise containing TRF-based microcapsule (M-mayo); (c) Mayonnaise containing TRF bulk oil (O-mayo).	81

LIST OF ABBREVIATIONS

ΔE	Total colour difference
a*	Green or red
ANOVA	Analysis of variance
A_w	Water activity
b*	Blue or yellow
C	Chroma
CFDA	China Food and Drug Administration
CI	Carr index
CIE	International Commission on Illumination
C-mayo	Control mayonnaise
EAI	Emulsion activity index
ESI	Emulsion stability index
FDA	U S Food and Drug Administration
FG	Flaxseed gum
GRAS	Generally Recognized As Safe
HCl	Hydrochloride acid
HPLC	High-performance liquid chromatography
HR	Hausner ratio
INU	Inulin
L*	Lightness
M	Maltodextrin
MC	Moisture content
MEE	Microencapsulation efficiency
M-mayo	Mayonnaise containing TRF-based microcapsule

NaCl	Sodium chloride
NaOH	Sodium hydroxide
O/W	Oil-in-water
O-mayo	Mayonnaise containing TRF bulk oil
OSS	Starch sodium octenyl succinate
PDI	Polydispersity index
pH_c	Soluble complex
pH_{opt}	Optimal complexation
$pH_{\phi 1}$	Insoluble complex
$pH_{\phi 2}$	Dissolution of complexes
pI	Isoelectric point
PPI	Pea protein isolate
PV	Peroxide value
RDA	Recommended dietary allowance
SEM	Scanning electron microscope
SGF	Stimulated gastric fluids
SIF	Stimulated intestinal fluids
SO	Surface oil
SSF	Simulated saliva fluids
TEM	Transmission electron microscopy
TO	Total oil
TPPI	Treated pea protein isolate
TRF	Tocotrienol-rich fraction
WAI	Water absorption index
WSI	Water solubility index

CHAPTER 1

INTRODUCTION

1.1 Background

Presently, consumer demands for healthier and natural food products have spurred the food industry to seek natural ingredient replacements for synthetic ones. Consequently, numerous studies have investigated the performance of natural emulsifiers relative to synthetic ones (Arancibia et al., 2017; Gumus et al., 2017; McClements et al., 2017; McClements & Gumus, 2016). Natural ingredients are derived from animal-based and plant-based, the latter has gained a lot of attention as it is more sustainable agricultural production, environmentally friendly, and lowers harmful gas emissions (Bryant, 2022).

Pea protein isolate (PPI) stands out as an outstanding plant-based protein due to its high nutritive value and abundance of raw materials (Li et al., 2024). It is a potential emulsifier because of its amphiphilic macromolecular nature, comprising both polar and nonpolar regions. It consists of legumin (11S) and vicilin (7S), which is attributed to emulsifying and gelling properties (Lam et al., 2018). Additionally, PPI is known for "clean" ingredients, high nutritive value, and low allergenicity (Walia & Chen, 2020). Furthermore, PPI possesses health benefits, which help to reduce blood pressure, regulate intestinal bacteria, and act as an antioxidant (Zou & Akoh, 2015b). Pea protein was incorporated into food products to produce emulsion (Kim et al., 2022; Zha et al., 2019), plant-based meat (Bryant, 2022; Desiderio et al., 2023), edible film (Farshi et al., 2024) and enriched bread (Moretton et al., 2023).

Flaxseed gum (FG), a water-soluble plant-based polysaccharide boasting excellent water-holding capacity and rheological properties, effectively stabilizes O/W emulsions (Wang et al., 2010). It is widely applied in food systems owing to its functional properties, including thickening and gelling (Sun et al., 2022). In addition, FG possesses health benefits such as preventing obesity, enhancing lipid metabolism, and preventing metabolic syndrome (Luo et al., 2019).

Palm oil is renowned for its rich vitamin E content, known to possess potent antioxidant properties with diverse benefits for biological activities (Pierpaoli et al., 2010; Sen et al., 2010). Vitamin E comprises two major constituents, tocopherols, and tocotrienols, sharing similar chemical structures featuring a chromane ring and an alkyl side chain (Goh et al., 2015). Both tocopherols and tocotrienols encompass four distinct variants, namely alpha (α-), beta (β-), gamma (γ-), and delta (δ-), distinguished by the number and position of methyl groups attached to the chromane rings (Aggarwal et al., 2010).

Extensive research highlights the pivotal role of tocopherols and tocotrienols in preventing various diseases, including atherosclerosis, neurodegeneration, cancer, and aging, driven by the adverse effects of reactive oxygen and nitrogen species that promote

oxidation (Park et al., 2010; Sen et al., 2010). Tocotrienols exhibit superior bioactivity compared to tocopherols (Peh et al., 2016). Despite their nutritional benefits, the hydrophobic nature of tocotrienols, low aqueous solubility, and limited intestinal permeability following oral ingestion pose formidable challenges in integrating them into aqueous-based foods (Fu et al., 2014; Goh et al., 2015; McClements & Xiao, 2012). Furthermore, the susceptibility of polyunsaturated tocotrienols to oxidation under environmental stressors such as heat, light, and oxygen hinders their bioactivity and leads to the formation of undesirable reaction products (Ko et al., 2010). Therefore, an efficient delivery system is crucial to enhance the stability of tocotrienols during storage and environmental stress.

Nanoemulsions offer a promising solution to address the solubility and intestinal permeability limitations of tocotrienols (Yang & McClements, 2013). Nanoemulsions are isotropic dispersed systems comprising two immiscible liquids, typically an oil phase dispersed in an aqueous phase or vice versa, forming nanoscale droplets (Simonazzi et al., 2018). These nanoscale delivery systems feature average oil droplet diameters of 10–100 nm and are generally recognized as safe (GRAS) for use in food. They are easily prepared, exhibit high physical and chemical stability, and enhance the bioavailability of lipid components (Walker et al., 2015; Yi et al., 2015).

However, liquid nanoemulsions have a limited shelf-life and are susceptible to microbial spoilage during storage. Additionally, the handling, bulk transport, and application of liquid nanoemulsions in dry food systems are constrained (Teo et al., 2021). Consequently, the conversion of nanoemulsions into a dry form through microencapsulation has become essential to overcome these limitations. Spray drying is the most widely employed method for encapsulation, renowned for its economic efficiency, flexibility, and effectiveness (Fang & Bhandari, 2012). This technique is particularly suitable for encapsulating heat-sensitive bioactive compounds due to its high drying rates and short residence time (Araujo-Díaz et al., 2017). Moreover, spray drying can dehydrate microcapsules to less than 3% of their final water content to minimize physical and chemical deterioration (Gharsallaoui et al., 2007).

The choice of wall materials for spray drying must consider factors such as low viscosity, high water solubility, excellent film-forming properties, and efficient drying properties (Turchiuli et al., 2014). Maltodextrin (M), a hydrolysed starch, is widely favored for encapsulation due to its favorable water solubility, oxidative stability, and low viscosity (Jafari et al., 2008). Starch sodium octenyl succinate (OSS), derived from tapioca, boasts high encapsulation efficiency, and emulsions prepared using M and OSS exhibit low viscosity (Carneiro et al., 2013). Inulin (INU), a dietary fiber, remains undigested in the small intestine but can be partially or completely degraded by colonic microbiota to promote human health (Tripodo & Mandracchia, 2019).

Mayonnaise, a creamy, white condiment with a thick texture, Mayonnaise, a creamy, white condiment with a thick texture, is commonly used with salads, sandwiches, and as a dipping sauce. Mayonnaise is a form of water-in-oil (W/O) emulsion prepared at low pH conditions (Mattia et al., 2015). Traditional mayonnaise typically consists of a high amount of oil (65 to 85%), egg yolk (as an emulsifier), lemon juice or vinegar (for pH

regulation and flavour), and seasonings (sugar, salt, and mustard) (Rashed et al., 2017; Di Mattia et al., 2015). With the rise of the healthy eating trend, mayonnaises have been fortified with natural antioxidants such as resveratrol, tocopherol, and rosemary essential oil (Abdolmaleki et al., 2019; Rabbani et al., 2021). In this study, mayonnaise was selected for fortification with tocotrienol microcapsules to assess the oxidative and storage stability of tocotrienol.

1.2 Problem statement

Pea protein isolate has great potential to produce nanoemulsion as it poses excellent foaming and emulsifying properties attributed to its amphiphilic nature (Jiang et al., 2019). However, the low solubility nature of native PPI at neutral conditions has become the major challenge that limits its emulsifying properties and functionality (Li et al., 2024; Sha et al., 2021). To overcome this problem, pH-shirting, and thermal treatment were applied to alter the conformation of the protein structure in this study. A study found that alkaline pH-treated pea protein improved the antioxidant activity and emulsification of oil-in-water (O/W) emulsions (Jiang et al., 2019). To further enhance the nanoemulsion stability, the treated PPI was complexed with FG by electrostatic interaction. The interactions between protein and polysaccharide improve the surface wettability and hydrophobicity of proteins, which promote higher complex adsorption at the interphase of the nanoemulsion (Li et al., 2024). Some studies have demonstrated that emulsion stability can be enhanced by utilizing protein-polysaccharide complexes to increase the thickness of the interfacial layer through electrostatic interaction (Berton-Carabin et al., 2014; Jourdain et al., 2009; Wong et al., 2011; Li et al., 2024). Additionally, FG poses high water-holding capacity and thickening properties which increase the viscosity of the aqueous phase to prevent oil droplet aggregation (Sun et al., 2022).

As for now, there are limited literature studies that have explored the effect of pH-shirting and thermal treatment on PPI. To the best of our knowledge, no study was done using the treated PPI to form a complex with FG and the emulsifying properties remain unknown. There is no exploration done on the formation of tocotrienol-rich fraction (TRF) based nanoemulsions using the TPPI-FG complex. Furthermore, the impact of wall materials on the encapsulation efficiency and stability of TRF-based microcapsules remains unclear. Additionally, the stability of TRF after incorporation into a food system has yet to be explored.

1.3 Objectives

The objectives of this study were as follows:

1. To prepare stable tocotrienol-rich nanoemulsions using treated TPPI-FG complexes.
2. To optimize and characterize tocotrienol-rich fraction-based microcapsules generated through spray drying using different core-to-wall ratios, wall material compositions, and mixing ratios.

3. To determine the storage stability, release characteristics, and bioaccessibility of the TRF encapsulated in M:OSS microcapsules.
4. To examine the effect of storage and mayonnaise matrix on the stability of TRF encapsulated in M:OSS microcapsules.

CHAPTER 2

LITERATURE REVIEW

2.1 Plant-Based Protein Emulsifier

Natural emulsifiers fall into categories such as surfactants, phospholipids, proteins, polysaccharides, and solid particles (Donsì & Velikov, 2019). Protein emulsifiers are amphiphilic molecules that form interfacial films at O/W interfaces (Foegeding & Davis, 2011; Lam & Nickerson, 2013; Plankensteiner et al., 2024). The amphiphilic nature of proteins reduces interfacial tension and stabilizes the O/W interface (Burger & Zhang, 2019). During emulsification, effective protein emulsifiers rapidly migrate to the interface, with their hydrophobic portions facing the oil phase and hydrophilic portions orienting toward the aqueous phase. Proteins unfold and adsorb at the interface, creating a viscoelastic film around oil droplets to prevent coalescence and flocculation (Karaca et al., 2011; Shevkani et al., 2015; Plankensteiner et al., 2024).

The advantages of using protein emulsifiers include high nutritive value, biocompatibility, biodegradability, and GRAS status (Wu et al., 2011). Protein emulsifiers are commonly derived from both plant and animal sources. Soybean (lecithin), gliadin, and zein are among the most common plant-based protein emulsifiers, while animal-based options include milk protein (whey protein), casein, eggs, gelatin, and collagen (Amine et al., 2014; Arancibia et al., 2017; Kibici & Kahveci, 2019; O'Sullivan et al., 2016; Ozcelik et al., 2019; Stone et al., 2015; Tarhini et al., 2017; Caihua Liu et al., 2024; Feng et al., 2022).

Plant-based proteins have gained popularity due to their sustainability, safety, and appeal to specific consumer groups such as vegans and vegetarians (Walia & Chen, 2020). Plant-based proteins are poised to be a promising alternative in the future, capable of replacing allergenic and/or animal-source emulsifiers (Burger & Zhang, 2019). Therefore, this study focused on plant-based protein emulsifiers, specifically PPI.

2.1.1 Pea Protein

Leguminous plants have gained recent popularity as natural emulsifiers due to their sustainability, functional attributes, high natural abundance, and cost-effectiveness, which are known as a clean source of protein (Abi-Melhem & Hassoun, 2023). Pea, soybean, lupin, and peanut belong to leguminous plants (Richard et al., 2015). Among all, peanut and soybean were associated with major allergic concerns as they were found to have 16 allergens and 8 allergens registered by the World Health Organisation/International Union of Immunological Societies (WHO/IUIS) Allergen Nomenclature Subcommittee (Cabanillas et al., 2018). Unlike peanut and soybean, only 3 allergens were isolated from peas, which are *Pisum sativum* (Pis s) 1, Pis s 2, and Pis s 3 (Cabanillas et al., 2018). Pea protein is not associated with major allergic concerns

(Walia & Chen, 2020). Pea protein is not labeled as a potential food allergen by the European Union, Canada, or the United States (Lavine & Ben-Shoshan, 2019).

Peas consist of approximately 20 to 30% protein, with 65 to 80% of it being globulins and 10 to 20% albumins (Karaca et al., 2011; Li et al., 2024). Globulins, particularly legumin and vicilin proteins (Lam et al., 2018; Makri et al., 2005). The PPI or pea protein concentrates typically contain 3 to 10% carbohydrate, 0.5 to 3.5% lipid, and 4 to 9% moisture (Karaca et al., 2011). The hydrophobic albumin fraction demonstrates foaming and emulsifying properties, as it tends to adsorb at the O/W interface (Burger & Zhang, 2019). Conversely, low-molecular-weight hydrophilic albumins play a lesser role in emulsification. Among the globulin fraction, vicilin is responsible for creating stable emulsions, while legumin proteins can enhance emulsion capacities (Koyoro & Powers, 1987), although vicilin can disrupt the adsorption of legumin at the interface due to its higher surface activity (Dagorn-Scaviner et al., 1986). Pea protein possesses both foaming and emulsifying properties because it possesses both polar and nonpolar regions, making it an amphiphilic macromolecule (Jiang et al., 2019).

However, their low solubility poses a challenge in efficiently delivering nutrients in food (Almajwal et al., 2019). Various approaches have been employed to enhance pea protein solubility, including alkaline pH treatment (Jiang et al., 2019) and a combination of ultrasound and pH-shifting treatment (Almajwal et al., 2019). The emulsion formed using alkaline pH–treated pea protein demonstrated improved antioxidant activity and O/W emulsion stability (Jiang et al., 2019). Additionally, the functional properties of PPI were enhanced following ultrasound and pH-shifting treatment, resulting in increased surface hydrophobicity, solubility, and particle size reduction to below 100 nm (Almajwal et al., 2019). Another study reported that ultrasonic treatment helps to unfold the compact PPI structures, enhancing its ability to adsorb at the oil-water interphase, thus improving the emulsifying properties (Li et al., 2024). Therefore, PPI was selected in this study owing to its great potential emulsifying and foaming capacity due to the presence of amphiphilic properties as well as its sustainability, high natural abundance, cost-effectiveness, and suitability for a vegan diet.

2.2 Plant-Based Polysaccharide Emulsifier

Polysaccharides, also known as hydrocolloids or gums, are typically soluble in water and have moderate surface activity, making them effective emulsion stabilizers by increasing the viscosity of the continuous phase (Bueno et al., 2009). Increased viscosity reduces droplet collisions in the dispersed phase, delaying phase separation (Benichou et al., 2002; Cameron et al., 1991; Huang et al., 2001; Makri et al., 2005) Furthermore, these large molecules can form thick hydrophilic layers around droplets, requiring higher surface loads compared to emulsifiers like surfactants or proteins (Ozturk & McClements, 2016). Polysaccharides stabilize emulsions through steric and electrostatic repulsion mechanisms. This type of emulsifier typically requires a larger quantity compared to other emulsifiers (Donsì & Velikov, 2019). Commonly studied polysaccharides include gum Arabic (Bai et al., 2016), modified starches (Donsì, Wang, et al., 2011; Sharif et al., 2017; Zhang et al., 2016), pectin (Guerra-Rosas et al., 2017), and FG (Liu et al., 2018).

2.2.1 Flaxseed Gum (FG)

Flaxseed consists mainly of FG, with a small protein fraction, and its polysaccharides are composed of 75% w/w arabinoxylans and 25% w/w rhamnogalacturonans, representing the neutral and acidic fractions, respectively (Cui & Mazza, 1996; Ding et al., 2018; Elboutachfaiti et al., 2017). It is commonly obtained as a by-product of the flax oil industry (Liu et al., 2018). It is water-soluble, with the mucilaginous material (soluble gum) obtained from the outermost layer of the hull through water soaking (Liang et al., 2018). Flaxseed gum boasts excellent rheological properties, including emulsification, thickening, and weak gelling properties, along with a high water-holding capacity. As a result, it finds extensive application in the food, cosmetic, and pharmaceutical industries as an additive (Liu, Shim, Poth, et al., 2016; Liu, Shim, Shen, et al., 2016). Flaxseed gum serves as an O/W emulsion stabilizer, while the flaxseed protein mainly acts as an emulsifier (Liu et al., 2017; Wang et al., 2010). The complex of flaxseed gum and whey protein isolates demonstrates improvement in the emulsion's physical stability by restricting the polymer orientational mobility of β-carotene emulsion (Xu et al., 2017).

2.3 Complexation between Protein and Polysaccharides

2.3.1 Synergistic Effect of Protein-polysaccharides Complexes

The formation of a network in protein-polysaccharide complexes is crucial in enhancing the stability and rheological characteristics of food products (Benichou et al., 2002). Extensive studies have demonstrated the synergistic effect of these complexes in improving emulsion stability by creating a thicker interfacial layer through electrostatic interactions (Berton-Carabin et al., 2014; Huck-Iriart et al., 2011; Yap et al., 2001; Wei & Huang, 2019). Furthermore, polysaccharides can alter the charge of the protein-polysaccharide complexes, enhancing the electrostatic, steric, and thermal stabilization of the emulsion (Li et al., 2024). Another finding reported that the complexation between soy protein isolate and soy hull polysaccharide was mainly governed by electrostatic, hydrophobic, and hydrogen bonding interactions attributed to the tryptophan and tyrosine residues inside protein molecules (Wang et al., 2020).

Typically, two methods are employed to prepare protein-polysaccharide complexes. In the complex model, protein-polysaccharide complexes are initially formed through electrostatic interaction and are subsequently employed as emulsifiers (complex model) to produce emulsions. In the layer-by-layer model, proteins are added first to create protein-emulsified O/W emulsions, followed by the addition of polysaccharides to form an additional outer layer around the droplets (Berton-Carabin et al., 2014). These two methods have a significant impact on interfacial properties, particularly thickness and compactness (Berton-Carabin et al., 2014; Liu et al., 2020).

Protein-polysaccharide complexes work synergistically, with proteins primarily serving as emulsifiers in O/W emulsions, while polysaccharides function as emulsion stabilizers by increasing the medium's viscosity to retard emulsion coalescence (Benichou et al.,

2002; Cameron et al., 1991; Huang et al., 2001; Makri et al., 2005). Based on previous findings, FG possesses desirable viscosity, emulsifying properties, and weak gelling properties, making it suitable for use as a thickener, emulsifier, and stabilizer in food (Zhang et al., 2013). Combining FG with whey protein isolate (Liu et al., 2015) and soybean protein isolate (Liu, Shim, Po et al., 2016), was found to enhance emulsion stability. In the case of whey protein isolate and FG complexes, increasing the FG concentration led to increased gel strength. However, when FG concentration exceeded 0.5% (w/w), gel strength decreased due to thermodynamic incompatibility, resulting in excessive phase separation (Zhang et al., 2013). These findings were consistent with the study of cold-set whey protein isolate-FG gels produced by adding calcium chloride or sodium chloride (NaCl) at a fixed ionic strength (150 mM). This study reported that increasing the amount of FG reduced both gel strength and water-holding capacity, leading to phase separation in whey protein isolate and FG mixtures (Kuhn et al., 2011).

2.3.2 Applications of Protein-polysaccharide Complexes in Food Industry

To ensure food safety and quality, the food industry often applies thermal processing techniques like pasteurization and sterilization to eliminate spoilage microorganisms (Kato et al., 1989). However, protein emulsifiers lose their emulsifying ability at high temperatures due to denaturation, causing their structure to unfold and deviate from their native state. When proteins are bound to polysaccharides through covalent bonds, destabilization caused by adverse environmental conditions, such as heat, acidic pH, and high electrolyte concentrations, is minimized because the adsorbed protein layer is protected (Dickinson, 2009). Another study found that the emulsifying activity of protein-polysaccharides complexes decreased when exposed to heat at 90 ^{o}C at a rate of 3 °C/min and then immediately cooled to 20 °C. However, significant emulsifying activity was restored in such heated complexes (Kato et al., 1989).

2.4 Tocotrienol-Rich Fraction (TRF)

Tocotrienol, another member of vitamin E, was discovered in 1960 (Pennock, 1964; Whittle et al., 1966). Unlike tocopherol, tocotrienol has been found to exhibit higher bioactivity (Peh et al., 2016) and potent anticancer activity (Pierpaoli et al., 2010). As shown in Figure 2.1, both components share a chromane ring and an alkyl side chain (Goh et al., 2015). They are further categorized into four derivatives: alpha (α-), beta (β), gamma (γ-), and delta (δ-), each distinguished by the number and position of methyl groups attached to the chromane rings (Aggarwal et al., 2010).

Palm TRF, derived from palm oil, comprises approximately 23% a-tocopherol, 25% α-tocotrienol, 2% β-tocotrienol, 35% γ-tocotrienol, and 15% δ-tocotrienol (Zou & Akoh, 2015). The TRF boasts exceptional antioxidant properties and has shown promise in various therapeutic applications, including anti-tumor, anti-cancer, anti-inflammatory, anti-aging, neuroprotective, and cholesterol-lowering effects (Abu-Fayyad et al., 2018; Budin et al., 2009; Goh et al., 2015; Musa et al., 2017; Sen et al., 2010). Owing to these health benefits, TRF has been incorporated into supplements and food products (Tan et al., 2018a; Zou & Akoh, 2015). However, the susceptibility of polyunsaturated

tocotrienols to degradation when exposed to environmental stressors such as heat, light, or oxygen poses a challenge, leading to reduced bioactivity and the formation of undesirable reaction products (Liang et al., 2018).

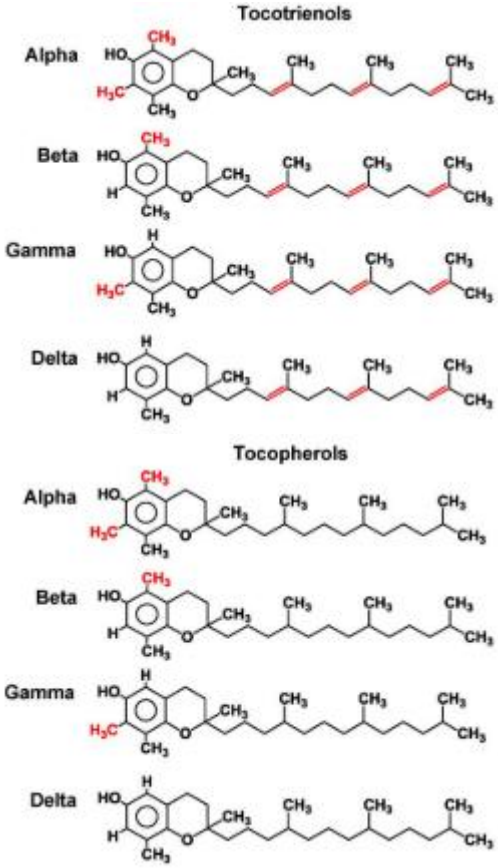

Figure 2.1. Chemical structure of tocotrienol and tocopherol (Source: Aggarwal et al., 2010).

2.4.1 Solubility

Tocotrienol, being highly hydrophobic, exhibits limited aqueous solubility and poor intestinal permeability when orally ingested (Fu et al., 2014; Goh et al., 2015; McClements & Xiao, 2012). Its lipophilic nature presents challenges when attempting to enrich aqueous-based foods and beverages with tocotrienols. To address these challenges, nanoemulsions have emerged as a promising water-soluble delivery system for enhancing the solubility of tocotrienols (Fu et al., 2014).

2.4.2 Absorption Capacity

While the absorption and metabolism of Vitamin E are well-studied, an understanding of its absorption and bioavailability in the human system remains incomplete (Fu et al., 2014). Previous studies have indicated that tocotrienols are not completely absorbed and exhibit limited bioavailability in rats (Peh et al., 2016). In rats, the bioavailability of alpha-tocotrienol was approximately 28%, while that of both gamma- and delta-tocotrienols was 9%. This study investigated the time required for alpha-, gamma-, and delta-tocotrienols to reach peak plasma concentration in both rats and humans. In rats, the time to peak plasma concentration was found to be 3.3, 3.0, and 2.8 h for α-, γ-, and δ-tocotrienols, respectively, with half-lives of 3 h for α-tocotrienol and 2 h for γ- and δ-tocotrienols (Yap & Yuen, 2004). In humans, the estimated half-lives in plasma were 2.3, 4.4, and 4.3 h for α-, γ-, and δ-tocotrienols, respectively (Yap et al., 2021), while the half-lives of α- and γ-tocopherols were 57 and 13 h, respectively (Leonard et al., 2005). Given the limited bioavailability of lipid-soluble tocotrienols in humans, the development of an effective delivery system is crucial. According to drug delivery systems technology, emulsions have been shown to enhance the absorption of fat-soluble compounds (Gao & Morozowich, 2006). The formation of tocotrienol emulsions has been found to improve absorption, leading to higher plasma concentrations of tocotrienols (Fu et al., 2014).

2.5 Nanoemulsions

Nanoemulsions, often referred to as submicron emulsions, nanoscale emulsions, mini-emulsions, or colloidal emulsions (McClements & Rao, 2011), are defined as biphasic colloidal disperse systems in the submicron size range, where one liquid phase is intimately dispersed as fine droplets in another liquid phase. This definition encompasses simple O/W or W/O emulsion systems (Donsì & Velikov, 2019). The crucial emulsifying agents required for forming nanoemulsions typically fall into categories such as surfactant molecules, solid particles, or (bio)polymers. These agents create a thin film surrounding each emulsion droplet at the intermediate phase or interphase (Kumar & Kumar, 2018).

In recent years, nanoemulsions have gained popularity over conventional emulsions, particularly after being designated as GRAS food ingredients (Peh et al., 2016). Nanoemulsions containing encapsulated oils often appear transparent or slightly turbid, with transparency largely dependent on the nanoemulsion's size. The size, often referred to as the mean droplet diameter, can vary based on different literature sources but typically falls within the range of 10 nm to 100 nm or 500 nm (Donsì & Velikov, 2019; Peh et al., 2016). The submicron size of nanoemulsions significantly enhances the dispersibility, bioaccessibility, and bioavailability of compounds by increasing the surface area and providing protection and controlled release for a wide array of substances (Donsì et al., 2013; Donsì & Velikov, 2019; Kumar & Kumar, 2018). Additionally, nanoemulsions offer a high capacity for loading lipophilic active compounds, making them suitable for various applications (Simonazzi et al., 2018). Nanoemulsions have proven effective in improving the solubility and intestinal permeability of tocotrienols (Peh et al., 2016), α-tocopherol (Kong et al., 2011),

cannabidiol (Nakano et al., 2019), β-carotene (Yuan et al., 2008), and curcumin (Wang et al., 2008).

Generally, nanoemulsion can be formed using both high-energy and low-energy emulsification methods. High-energy methods are commonly used to create food-grade nanoemulsions, as they require substantial mechanical energy to break down large droplets into nano-sized ones. Utilizing high-energy methods offers several advantages, including the ability to use lower emulsifying agent concentrations and achieve greater control over particle size, stability, and emulsion colour (Graves et al., 2005; Gursoy & Benita, 2004). The high-energy methods encompass high-pressure homogenization, microfluidization, rotor-stator emulsification, ultrasonication, and membrane emulsification. A detailed comparison of high-energy emulsification methods is provided in Table 2.1 (Håkansson & Rayner, 2018).

In contrast, low-energy methods require lower energy, relying on the internal chemical energy of the system under gentle stirring conditions to form nanoemulsions. Low-energy emulsification methods include two approaches:

(1) Self-emulsification method: nanoemulsions are formed through the turbulence generated by surfactant molecules that rapidly diffuse from the dispersed phase to the continuous phase.
(2) Phase inversion emulsification method: nanoemulsions result from the spontaneous curvature of surfactant leading to phase transition (Kumar et al., 2019).

However, these low-energy methods are less suitable for producing food-grade nanoemulsions due to their reliance on high emulsifying agent concentrations, which could potentially affect taste and safety (Komaiko & Mcclements, 2016).

Table 2.1: Comparison of high-energy method emulsification processes.

Type	Source of energy	Breakup mechanism	Energy density (kJ/m^2)	Viscosity range (mPas)
High-pressure homogenization	Pump	• Turbulent inertial • Turbulent viscous • Cavitation	10^4-10^6	1-200
Rotor-stator mixer	Rotor	• Turbulent inertial • Turbulent viscous • Laminar viscous	10^3-10^5	20-500

Table 2.1: Continued.

Microfludization	Pump	• Turbulent inertial • Turbulent viscous • Cavitation	10^4-10^6	1-200
Ultrasonication	Ultrasound	• Cavitation	10^3-10^5	Low to medium
Membrane emulsification	Trans-membrane pressure	• Laminar viscous	10-10^3	Low to medium

[Adapted from Håkansson & Rayner, (2018)].

In this study, a high-pressure homogenization method was employed to prepare TRF-based nanoemulsion. This method utilizes a high-pressure homogenizer to further reduce the coarse emulsion droplets into smaller sizes with a narrow distribution. This reduction is achieved by forcing the emulsion through a valve, creating a narrow gap of 10 to 100 µm under high pressure (50 to 200 MPa) (Håkansson & Rayner, 2018). Initially, the emulsion fluid passes through the valve to accelerate its velocity to 100 m/s, resulting in an elongational flow at the valve entrance. The high velocity reduces the local pressure below the vapor point, forming cavitation bubbles. As these bubbles move downstream in the valve, they are exposed to higher local pressure and burst, generating shock waves. These fluids flow as laminar or transitional flow within the narrow gap. Upon entering a larger outlet chamber, a jet is formed (Gothsch et al., 2015), and the kinetic energy is converted into turbulence. Breakup of the emulsion droplets occurs in the jet generated downstream of the gap (Bisten & Schuchmann, 2016; Kelemen et al., 2014). High-pressure homogenization methods enable the production of nanoemulsions with droplet sizes below 500 nm, ensuring stability during storage and the retention of desired properties (Håkansson, 2018). Numerous studies have reported enhanced delivery systems, bioactivity, physical properties, and stability using the high-pressure homogenization method for various compounds such as quercetin (Melchior et al., 2023), rosehip (*Rosa canina* L.) nectar (Saricaoglu et al., 2019), curcumin (Guan et al., 2023), tocopherol (Lee et al., 2020), and clove essential oil (Yin et al., 2023).

2.5.1 Stability and Application of Nanoemulsions in Food

Stability is a critical property of nanoemulsions, referring to their ability to resist changes in properties over time (Huck-Iriart et al., 2011). Nanoemulsions formed through high-energy methods such as high-pressure homogenization, microfluidization, and phase-inversion temperature methods are thermodynamically less stable compared to microemulsions (Simonazzi et al., 2018).

Nanoemulsions can become unstable due to environmental factors like thermal and mechanical stress, biological interactions, or physical evolution processes (Leal-Calderon et al., 2007). Common destabilization mechanisms affecting nanoemulsion stability include Ostwald ripening, coalescence, gravitational separation, and flocculation (McClements & Jafari, 2018). These mechanisms become more pronounced

in nanoemulsions with droplet diameters above approximately 180 nm (McClements & Rao, 2011). Nanoemulsions are especially susceptible to Oswald ripening, often followed by creaming, flocculation, and other physical instability (Simonazzi et al., 2018). For nanoemulsions with droplet size below 180 nm, Brownian motion becomes the dominant destabilization mechanism rather than gravitational forces. Macroscopic properties such as stability against sedimentation or creaming, rheology, reactivity, optical transparency, and biological activity change significantly with decreasing droplet size from microemulsion to nanoemulsions, even when produced using the same formulation (McClements, 2011; Solans & Solé, 2012). Extremely small droplet size and adequate use of emulsifying agents can extend the storage stability of nanoemulsions. To counter Ostwald ripening, ripening inhibitors can be added to the oil phase before forming nanoemulsions such as triglyceride (Julian McClements et al., 2012; Lim et al., 2011; Park et al., 2020)

Over the last decade, emulsions have played a crucial role in the texture, rheology, and sensory properties of numerous food products, including salad dressing, cream, desserts, mayonnaise, and beverages (Coupland & Sigfusson, 2005). As consumer demand for nutritious and functional foods continues to rise, the food industry is increasingly fortifying or enriching food products with a variety of micronutrients to enhance their nutritional profiles. Consequently, nanoemulsions have found expanded applications in food products due to their ability to efficiently deliver lipophilic compounds into aqueous food matrices. These compounds include bioactive substances, oil-soluble vitamins, aromas, colour, flavours, and essential oils (Donsì et al., 2013; Jaiswal et al., 2015; Rafiee & Jafari, 2018). The use of encapsulation minimizes alterations in food flavour and appearance, as it shields active compounds from interacting with the food matrix (Donsì & Velikov, 2019). Extensive research has been conducted on encapsulating various micronutrients in nanoemulsions, including conjugated linoleic acid (Fernandez-Avila et al., 2017), fish oil (Walker et al., 2015), vitamin A (Ricaurte et al., 2016), D (Ozturk et al., 2015), E (Ozturk et al., 2014) among others. For lipid-soluble active compounds, a carrier oil such as palm oil, medium-chain triglycerides (MCT), or orange oil has been encapsulated for preservation purposes (Katouzian & Jafari, 2016).

From an industry perspective, nanoemulsions should meet several criteria: the ingredients must be certified as food-grade, preferably all-natural. Nanoemulsions should also effectively disperse payload compounds into the food system to enhance physicochemical stability and minimize adverse effects on food quality. Moreover, nanoemulsions should protect active compounds from degradation due to exposure to heat, light, pH, and chemical reactions with other food ingredients. Additionally, the formation of nanoemulsions should improve payload uptake during consumption and enable the controlled release of compounds in response to specific environmental stimuli (Donsì, 2018; Donsì, Sessa, et al., 2011; McClements et al., 2007).

2.6 Physicochemical Characterization of Nanoemulsions

2.6.1 Zeta Potential

Zeta potential represents the electrical potential at the "shear plane". It quantifies the distance from the droplet surface below which the counter-ions remain strongly attached when the droplet moves in an electrical field (McClements et al., 2007). Practically, the electrical properties of an emulsion droplet are determined by measuring the adsorption of charged counter ions. The electrical characteristics of emulsion droplets depend heavily on the types of emulsifiers used. Small droplet charges are obtained when emulsions are stabilized by nonionic surfactants, like Tweens and Spans. Anionic surfactants (lecithin, fatty acids, diacetyl tartaric acid ester of mono- and diglycerides, citric acid esters of mono and diglycerides and polysaccharide emulsifiers (modified starch, gum Arabic, beet pectin) yield a negative charge, while using protein emulsifiers below their isoelectric point results in a positive charge, and a negative charge is obtained when used above the isoelectric point, for instance, whey protein, casein, and soy proteins (McClements et al., 2007).

2.6.2 Particle Size Distribution (PSD)

Particle Size Distribution (PSD) measures the proportion of particles in different size classes (McClements, 2004). The results are usually presented in tables or plots, displaying particle concentration by volume or number percentage, with droplet size measured in diameter or radius. It assesses central tendency (mean, median, or mode) and distribution width (standard deviation). The PSD of nanoemulsions can be influenced by homogenization conditions such as intensity or duration of energy input. Moreover, changes in system composition, including the type and concentration of emulsifier used, can regulate the PSD of nanoemulsions (McClements et al., 2007). Small droplet sizes are achieved with high homogenization intensity, long duration, or a high emulsifier concentration (Walstra, 1993).

2.6.3 Polydispersity Index (PDI)

The polydispersity index (PDI) gauges particle size distribution and formulation homogeneity. A PDI below 0.2 indicates a narrow droplet size distribution in nanoemulsions (monodispersed), while a PDI nearing 1 signifies very high particle size heterogeneity (polydisperse) (Sail et al., 2018). Some studies have reported that the PDI value of curcumin-loaded Pickering emulsion formed using PPI and dextran ranged between 0.2 to 0.3 (Kim et al., 2024), while emulsions loaded with olive oil produced from PPI-guar gum range from 0.19 to 0.54 (Kamer, 2024). The PDI serves as an emulsion stability indicator. Study found that nanoemulsion of baru seed oil obtained low PDI (< 0.39) stable over 28 days of storage at 25 °C (Paulo et al., 2023). Another study also shows that nanoemulsion with low PDI (< 0.2) obtained good stability at 4 °C in storage conditions and at 37 °C in diluted conditions (Lefebvre et al., 2017).

2.6.4 pH Profile

It was found that pH significantly affects emulsion stability as proteins and polysaccharides emulsifiers have distinct optimum solubility and isoelectric points (Fioramonti et al., 2015). As the pH value approaches the emulsifier's isoelectric point, the net charge approximates zero, increasing the likelihood of aggregation and reducing protein solubility (H. Chen et al., 2014). When the pH value shifts away from the isoelectric point, the net charge of the protein increases, protein molecules repulse each other, which increases the interaction between protein and solvent and the diffusion rate at the interface (Zhang et al., 2023). Therefore, the emulsification properties of the protein are enhanced, resulting in better emulsion stability. Study shows that Pickering emulsion formed by PPI and octenyl succinic anhydrate corn starch exhibited 100% flocculation index under pH 3 to 5 while the particle size of the emulsion were consistent at pH 6 to 7 (Liu et al., 2024). Another study shows that droplet size of emulsion stabilized by pea protein-sodium alginate complex affected by pH. A large droplet size was obtained at pH 6 due to protein aggregation. Small and uniform droplets formed attributed to the strong negative charge at pH 11, which reduces the interfacial tension readily due to electrostatic repulsion (Kim et al., 2022).

2.6.5 Viscosity

Viscosity can be measured using a viscometer equipped with a spindle. The sample is placed in the calibrated spindle, and measurements are taken as the spring deflects due to viscous drag when the spindle moves. The rotary transducer aids in measuring spring deflection (Sail et al., 2018). Dilute emulsions with low viscosity are characterized in terms of apparent shear viscosity. Emulsion shear viscosity is determined by the continuous phase viscosity (ηC), droplet concentration (φ), and the nature of droplet–droplet interactions (w): $\eta = \eta C \times f(\varphi, w)$ (McClements, 2004).

Nanoemulsion viscosity is greatly influenced by the composition, structure of nanoemulsions, oil content, and the type and concentration of added emulsifiers (McClements et al., 2007; Sail et al., 2018). A study by Lim et al. (2024) shows that emulsion stabilized by the PPI-INU complex obtained higher viscosity than PPI alone due to an increase of droplet size. The complex of protein-polysaccharide position readily at the interface with hydrophilic properties contributed by the polysaccharides on the protein molecules. As a result, the complex forms a thick coating layer around the core material, causing larger droplet sizes. Furthermore, the viscosity of emulsion increased with oil content as it reduces turbulence during homogenization, causing a reduction of droplet breakage, hence, resulting in larger droplet size (Kim et al., 2022). Moreover, increasing droplet concentration initially raises emulsion viscosity, which then increases steeply as droplets become densely packed. Emulsions display solid-like behavior, including viscoelasticity and plasticity, at and above a critical droplet concentration (typically around 50% to 60% for a non-flocculated O/W emulsion) (McClements, 2004). A sharp increase in emulsion viscosity depends on the nature of droplet interactions in the system, with strong attractive or repulsive interactions leading to variation (McClements,2005a).

Flocculation often occurs during storage, the emulsion viscosity tends to rise due to increased effective particle concentration within the floc structure. Additionally, flocculation arises in shear-thinning solutions, where increasing shear stresses induce deformation and breakdown of the floc structure (McClements et al., 2007). Therefore, monitoring the viscosity of nanoemulsion systems is crucial for assessing their stability.

2.6.6 Storage Stability

The storage stability of nanoemulsions can be determined by various methods, including thermal stability measurement, centrifugation assay, freeze-thaw cycles, and stability to changes in ionic strength. These studies aim to determine how long nanoemulsion systems can remain stable without physical changes (such as Ostwald ripening, coalescence, creaming, and sedimentation) and chemical changes (like the degradation of active compounds). These investigations provide valuable insights for estimating the shelf life of nanoemulsion systems (Nankar et al., 2016).

2.7 Spray Drying

Spray drying is an economical and effective method known for its high drying rates and short residence times, making it ideal for drying and encapsulating heat-sensitive bioactive compounds (Araujo-Díaz et al., 2017). Encapsulation enhances the stability of bioactive compounds during storage and transportation, thus extending the shelf life of the end products. Moreover, the spray drying of hydrophilic bioactive compounds can enhance their *in vitro* bioaccessibility and bioavailability (Rehman et al., 2021; Timilsena et al., 2017).

The conventional spray-drying method for microencapsulation involves four key steps: emulsion preparation, homogenization, atomization, and dehydration (Shahidi & Han, 1993). During spray drying, the liquid feed material containing bioactive compounds is atomized into a drying chamber. Atomization generates small droplets that facilitate rapid water evaporation when they come into contact with hot air. Subsequently, the spray-dried microcapsules are separated by a cyclone and collected at the outlet (Poozesh et al., 2020). Inlet temperatures typically range from 150 to 200 °C, with outlet temperatures between 70 to 90 °C. Despite the high drying temperatures, the contact time between the hot air and spray-dried microcapsules is very brief (a few seconds), allowing the materials to cool rapidly after spraying (Samborska et al., 2005). This makes spray drying suitable for heat-labile bioactive compounds and food ingredients. However, it is important to note that spray drying has some limitations, including relatively low drying yields (typically 50% to 70%), challenges in controlling particle size and distribution, inability to produce nanoparticles, and the need for optimization (Jafari et al., 2021).

The selection of appropriate wall materials is a crucial aspect of microencapsulation. These materials should possess desirable emulsification properties, a high glass transition temperature, good film-forming characteristics, and efficient drying properties. Wall materials with excellent emulsification properties enhance the stability of feed

emulsions containing hydrophobic ingredients. When dealing with materials high in sugar content, selecting wall materials with a high glass transition temperature is essential to minimize stickiness during spray drying. Effective film-forming properties are crucial for creating a protective capsule around the core material (Jafari et al., 2021). Additionally, wall materials with high water solubility can yield low-viscosity feed solutions, facilitating spraying and pumping during the spray-drying process (Teo et al., 2021). It is also preferable to choose wall materials that have a neutral taste, are non-hygroscopic, cost-effective, readily available, do not interact negatively with the core materials, and have a high atomization drying capacity (Arpagaus, 2019; Wlodarkievicz et al., 2022). In the context of this study, the wall materials used to create microcapsules based on TRF are M, OSS, and INU.

2.7.1 Maltodextrin (M)

Maltodextrin (M) is a product of starch hydrolysis through acid or enzyme processes. Its structure consists of D-glucose polymers linked by α-(1,4) and α-(1,6) linkages (Garnero et al., 2013). It exhibits a dextrose value equivalent ranging from 3 to 20, signifying a mixture of high and low molecular-weight substances (Saavedra-Leos et al., 2015). Maltodextrin has applications in various industries, including food, pharmaceuticals, cosmetics, and agriculture (Xiao et al., 2022). It is one of the most commonly used wall materials for microencapsulation of bioactive compounds due to its low viscosity at high solid concentrations, affordability, colourlessness, neutral taste, and aroma (Da Costa et al., 2013; Fernandes et al., 2014). Maltodextrin also offers good oxidative stability (Gharsallaoui et al., 2007; Jafari et al., 2008), thermal stability, freeze stability (Fioramonti et al., 2017), and stability in low pH conditions (Shepherd et al., 2000). Maltodextrin enhances the solids concentration of emulsion systems, leading to the formation of a protective crust over the dried droplets, safeguarding core materials from oxidation (Zhu et al., 2022). Moreover, maltodextrin can enhance the hygroscopicity and microencapsulation efficiency (MEE) of microcapsules. The residual moisture content (MC) of maltodextrin-based microcapsules typically ranges from 3.3 to 3.9% (Seid Mahdi Jafari et al., 2021). Several studies have demonstrated enhanced encapsulation efficiency by combining maltodextrin with other wall materials to encapsulate hydrophobic core material, such as trehalose (Nguyen et al., 2022; Teo et al., 2021), gum Arabic (Laureanti et al., 2023), and gelatin (Kosasih et al., 2023).

2.7.2 Starch Sodium Octenyl Succinate (OSS)

Starch sodium octenyl succinate (OSS) is a food additive approved by regulatory authorities such as the Food and Drug Administration (FDA), European Food Safety Authority (EFSA), and China Food and Drug Administration (CFDA). It is a modified food starch derived from the esterification of octenyl succinic anhydride (Long et al., 2022). During this esterification process, starch is transformed into an amphiphilic polymer by incorporating both hydrophilic carboxylic acid groups and long-chain oleophilic alkenyl groups simultaneously (Joye & McClements, 2013). It is subsequently neutralized with sodium hydroxide (NaOH) (Song et al., 2006). The OSS possesses both hydrophilic and hydrophobic properties, making it suitable as an emulsifier, thickener, and wall material for microencapsulating bioactive compounds (Liu et al., 2018).

Previous studies have used OSS to produce composite films for the encapsulation of functional active substances in controlled release systems (Łupina et al., 2022). Another study demonstrated that combining OSS with M in the encapsulation of flaxseed oil resulted in higher encapsulation efficiency than the combination of M and whey protein concentrate. Emulsions prepared using M and OSS exhibited lower viscosity compared to those using M and gum Arabic (Carneiro et al., 2013). Furthermore, encapsulation of camellia seed oil using wall material of whey protein concentrate and OSS also demonstrated a higher encapsulation efficiency and oxidative stability over 45 days of storage at 25 °C as compared to whey protein concentrate and M (Song et al., 2022). Therefore, OSS holds promise as a material for encapsulation in both the food and pharmaceutical industries.

2.7.3 Inulin (INU)

Inulin (INU) recognized as GRAS by the FDA, is a fructan-type oligosaccharide naturally occurring in over 36,000 plants, including oats, leeks garlic, and onions. Commercially, INU is primarily obtained from members of the *Asteraceae* family, such as chicory (Afinjuomo et al., 2019). It is a carbohydrate similar to M, consisting of long-chain molecules with a molecular weight exceeding 52 kD (Leyva-Porras et al., 2014). The unique structure comprises D-fructose units linked by β-2,1 glycosidic bonds, allowing it to adopt various structures due to the single atom in the polymer backbone connected to the fructose ring (Beirão-da-Costa et al., 2013). The INU is a dietary fibre that remains undigested in the small intestine but can be partially or completely metabolized by colonic microbiota, providing potential health benefits (Tripodo & Mandracchia, 2019). In addition, consuming INU can enhance calcium bioavailability (Saénz et al., 2009), has immunomodulatory properties (Beirão-da-Costa et al., 2013), and anticancer effect (Korbelik & Cooper, 2007).

In addition to its health-related advantages, INU serves as a wall material for microencapsulation. Its resistance to pH variations and indigestible nature in the stomach and small intestine makes it a suitable candidate for the slow release of drugs in gastrointestinal drug delivery systems (Barclay et al., 2010; Wang et al., 2019). The INU has also been employed in microbially activated drug delivery systems, delivering drugs specifically to the colon, where colonic microbiota metabolize and release the drug (López-Molina et al., 2015). The low hydrolysis capacity of INU is resistant to pH variations (Dima et al., 2016). The INU exhibits low hydrolysis capacity and protects bioactive compounds along the digestive tract until they are released and absorbed by the intestine (Beirão-da-Costa et al., 2013). Additionally, INU offers biodegradability, renewability, non-toxicity, and other favorable properties compared to other polysaccharides (Afinjuomo et al., 2019). Several studies have been conducted using INU to encapsulate food microbes, including *Lactococcus lactis* (Rosolen et al., 2019) and *Lactobacillus acidophilus* (Nunes et al., 2018). One study found that INU, when combined with whey cheese as wall material, effectively protects *Lactococcus lactis* (Rosolen et al., 2019). Encapsulation efficiency was enhanced by incorporation INU with other wall materials such as brea gum (Castel et al., 2018) and Hi-maize (Nunes et al., 2018; Xavier et al., 2019). Another study reported achieving good powder quality by encapsulating corn oil using a combination of INU and brea gum as wall material (Castel et al., 2018).

2.8 Characterization of Microcapsule

2.8.1 Microencapsulation Efficiency (MEE)

Microencapsulation efficiency **(**MEE) is a pivotal parameter for assessing the effectiveness of encapsulating oils within spray-dried microcapsules. It quantifies the amount of surface oil (SO) contained within the microcapsules using a solvent extraction method. To determine MEE, we measure both the amount of SO and the total oil (TO). The SO refers to the oil located on the particle surface, while TO encompasses the TO content, including both the core and SO of the powders (Jafari et al., 2008). Several factors influence the MEE of microcapsules, such as the concentration and molecular weight of the wall material, the solubility of the wall material in the solvent, the ratio of the lipid phase to the aqueous phase, the core-to-wall ratios, and interactions between the core material and the wall material (Jyothi et al., 2010). The choice of the wall material plays a crucial role in microencapsulation, as it determines the ability to encapsulate and seal core materials within the microcapsule during storage and processing. This significantly impacts the integrity and porosity of the microcapsules (Murúa-Pagola et al., 2009).

2.8.2 Moisture Content (MC)

Moisture content (MC) refers to the water content within a food system. Its importance lies in its impact on food stability, as it can lead to lipid oxidation and microbial spoilage (Le Priol et al., 2019). In the food industry, it is generally recommended to maintain the MC of 3 to 4% in powders (Song et al., 2022).

2.8.3 Water Activity (A_w)

Water activity (a_w) measures the free or unbound water present in microcapsules. It assesses the availability of water for biochemical reactions and plays a vital role in evaluating the quality, shelf-life stability, and retention of bioactive compounds in microcapsules. Microcapsules with an a_w ranging from 0.2 to 0.3 demonstrate stability against oxidation (Al Mubarak et al., 2019).

2.8.4 Flowability and Cohesiveness

Flowability refers to the movement of particles relative to neighboring particles or along the container's wall (Kalman, 2021) and is determined by the Carr Index (CI). Cohesiveness, on the other hand, is indicated by the Hausner ratio (HR), which is the ratio of tapped density to bulk density. The low cohesiveness of microcapsules indicates that the attractive forces between adjacent particles or molecules within the same matrix are weak. This is desirable to avoid issues like caking and agglomeration during storage of the microcapsules (Leyva-Porras et al., 2014).

2.8.5 Peroxide Value (PV)

The oxidation of lipids in food products is an unavoidable degradation process that can lead to reduced levels of fat-soluble vitamins, taste issues, the generation of off-flavours, and even the formation of food toxins that can cause food poisoning. To address these problems, Peroxide Value (PV) has become a valuable indicator for assessing the extent of lipid oxidation in fats and oils. The PV quantifies the lipid peroxides that form in the early stage of lipid oxidation (Shantha & Decker, 1994). These peroxides are produced when unsaturated carbon-carbon double bonds break down (Pratt et al., 2011). According to Codex Alimentarius (2001), good oil quality is indicated by a PV below 5 mEq/kg, while rancid oil typically has a PV of above 10 mEq/kg.

2.9 Application of Tocotrienol Microcapsule in Food Matrix

Vitamin E is commonly acquired from daily food intake with the recommended dietary allowance (RDA) of 15 m/day for adolescents, adult men, and non-lactating women (Saini & Keum, 2016). However, vitamin E deficiency is commonly found in 90% of individuals in US who fail to consume the required amount stated by RDA (Saini & Keum, 2016). This is attributed to the consumption of unbalanced diets, excessive workouts, stressful lifestyles, pregnancy, and lactation (Wijekoon et al., 2023). Therefore, to increase the daily intake of vitamin E in the diet, various studies are conducted to fortify these bioactive compounds into food matrixes such as yogurt (Tan et al., 2018), orange juice (Sultana et al., 2023), fresh pork sausages (Georgantelis et al., 2007), infant formula (Zou & Akoh, 2015) and salad dressing (Let et al., 2007). In this study, TRF was fortified into mayonnaise as a food matrix to study the protective effect of microcapsules to extend the oxidative and physicochemical stability of TRF.

2.9.1 Mayonnaise

Mayonnaise, an O/W emulsion, is a creamy, semi-solid dressing with a slightly sour taste. It is typically produced under low pH conditions, around 3.6 to 4.0 (Krishnamurthy & Witte, 1996). Mayonnaise consists of three key components: the dispersed phase, which comprises 65 to 85% vegetable oil; the continuous phase, made up of vinegar and water; and the interface, primarily consisting of egg yolk, which acts as an emulsifier (Abdolmaleki et al., 2019; Li et al., 2014). Mayonnaise is commonly used as a dressing for seasoning and flavouring purposes (Ribes et al., 2019). Currently, consumers are increasingly seeking more nutritious mayonnaise options that offer additional nutritional benefits to their meals. As a result, researchers have explored fortifying mayonnaise with various bioactive compounds, such as natural antioxidants, antimicrobial extracts, and premium oils, to enhance its nutritional value (Miguel et al., 2019; Rabbani et al., 2021; Song & McClements, 2021; Yesiltas et al., 2021). The fortification of natural antioxidants in mayonnaise can provide health-promoting benefits while maintaining a natural appeal, expanding the product's appeal to a broader consumer base (Hermund & Yes, 2015). Furthermore, the addition of natural antioxidants to mayonnaise has the potential to improve the oxidative stability of the oil (Gorji et al., 2016).

2.10 Summary

In this study, pea protein and flaxseed gum were selected to form a complex to stabilize nanoemulsion, which was based on a few criteria. Firstly, pea protein is a protein-rich leguminous plant that contains approximately 20 to 30% protein. The protein fraction is made up of a high content of globulin (65 to 80%) and 10 to 20% albumin. Both protein fractions demonstrate high foaming capacity and emulsifying properties which make it a suitable emulsifier to form nanoemulsion. However, its functionality was limited by its low solubility. To maximize the protein functionality, pH shifting and thermal treatment were applied to modify the protein into a molten conformational state. Secondly, FG acts as an effective emulsion stabilizer in O/W emulsion by enhancing the viscosity of the aqueous phase. FG stabilizing effect was due to its water-soluble nature contributed by the mucilaginous material (soluble gum), which was obtained from the outermost layer of the hull. Additionally, it enhances rheological properties, including emulsification and thickening, along with high water-holding capacity. Thirdly, PPI functions as an emulsifier while FG functions as an emulsion stabilizer. The complexation of PPI and FG by electrostatic interactions works synergistically in producing a more stable TRF-based nanoemulsion. Besides, the high FG portion of the complex exhibited the highest emulsion activity index and emulsion stability index while reducing the creaming index of the nanoemulsion. This is due to a thick and compact coating layer formed around the TRF, thus reducing the phase separation. With the aid of wall material, the complex encapsulated TRF effectively, which helps to reduce thermal degradation during microencapsulation by spray drying. Therefore, it was proposed that the complexation of PPI and FG could contribute to higher emulsion stability and protection.

CHAPTER 3

PREPARATION OF STABLE TOCOTRIENOL-RICH NANOEMULSIONS USING PEA PROTEIN ISOLATE-FLAXSEED GUM COMPLEXES

3.1 Introduction

Emulsifiers are the key ingredients in the formation and stabilization of nanoemulsions. According to the current modern food trend, consumers often look for plant-based and clean-label food products. These lead to an upsurge in demand for plant-based ingredients among food industries to replace the commonly used animal-based or synthetic emulsifiers. Recently, plant proteins have received a lot of attention in the food industry and become good alternatives to animal-based proteins (Burger & Zhang, 2019). When the protein is adsorbed at the oil-water interfaces, the molecules can unfold to maximize the number of hydrophobic groups in contact with the surface (Chen et al., 2023). This allows the hydrophilic groups to rearrange and protrude to the water phase. The amphiphilic properties of a protein are vital as they can reduce the interfacial tension and stabilize the oil-water interface (Burger & Zhang, 2019).

Pea protein has gained popularity in recent years due to its nutritional properties, functionalities, and wide applications. It is an amphiphilic macromolecule, that consists of both polar and non-polar regions, which makes it a potential emulsifier (Jiang et al., 2019). Pea contains 20 to 30% protein, with the major protein fraction consisting of 65 to 80% of globulins and 10 to 20% of albumins (2S; 5 to 80 kDa). Globulins exhibit better emulsification properties. The major globulins present in pea protein are legumin (11S; ~40 kDa), vicilin (7S; ~175 kDa), and convicilin (7 to 8S; ~290 kDa) (Li et al., 2024; Lam et al., 2018). In globulin fraction, vicilin promotes emulsion stability while legumin increases the emulsion capacity, which helps in enhancing the emulsifying properties of the pea protein. However, most of the native pea proteins exhibit low solubility and poor functionalities under neutral pH (7), which limits their applications. A series of pH-shifting treatments or a combination of pH-shifting with thermal treatments are proposed to improve the pea protein solubility in water (Jiang et al., 2014; Yi et al., 2020). These treatments alter the structure of protein and enhance the amphiphilic properties of protein polypeptides, thereby increasing its solubility (Jiang et al., 2014).

Flaxseed gum (FG) is a water-soluble, mucilaginous material obtained from the outermost layer of flaxseed (Liang et al., 2018). It possesses excellent emulsification, thickening, and weak gelling properties as well as strong water-holding capacity. Therefore, it is broadly utilized as an additive in food, cosmeceutical, and pharmaceutical products (Liu, Shim, Shen, et al., 2016). It is reported as an emulsion stabilizer. The protein-polysaccharide complexes are important in interfacial network formations to improve the stability and rheological behaviors of the products (Sun et al., 2023). Numerous studies have reported the synergistic effects of protein and polysaccharide in enhancing emulsion stability through the formation of a thicker interfacial layer via electrostatic interaction (Wang et al., 2023; Berton-Carabin et al., 2014). Protein-

polysaccharide complexes work synergistically whereby the role of protein is to emulsify O/W emulsions while the polysaccharides stabilized by increasing the viscosity to retard collision emulsion. The complexation between protein and polysaccharide at the oil droplet surface can enhance steric stabilization. In the presence of polysaccharides, the droplet size and the rate of creaming may be reduced as bridging flocculation does not occur. Without enzymatic or chemical modifications, the complexation of protein and polysaccharide can lead to improved functionalities (Liu et al., 2010).

Vitamin E derived from palm oil exhibits strong antioxidant properties and beneficial biological activities (Pierpaoli et al., 2010; Sen et al., 2010; Wang et al., 2020) Vitamin E comprises two different classes, namely tocopherols, and tocotrienols. Each class of vitamin E consists of four derivatives which are alpha (α-), beta (β-), gamma (γ-), and delta (δ-) (Ghosh et al., 2020). Both tocopherols and tocotrienols play a vital role in reducing the risk of atherosclerosis, neurodegeneration, cancer, and aging caused by reactive oxygen and nitrogen species (Sen et al., 2010; Pang & Chin, 2019). Tocotrienols possess higher anticancer activity compared to tocopherols (Ghosh et al., 2020). Owing to the nutritional benefits, numerous research has been carried out to incorporate these bioactive compounds into food applications. However, the low aqueous solubility and poor intestinal permeability of both tocopherol and tocotrienol pose great challenges in food product development. Furthermore, the polyunsaturated phytol side chain of tocotrienols is prone to oxidation when exposed to various environmental stresses for instance heat, light, or oxygen (McClements & Xiao, 2012; Sultana et al., 2023).

To overcome the limitations of tocotrienols, one of the promising solutions is fabricating nanoemulsions (Yang & McClements, 2013). The average oil droplet diameters of nanoemulsions range from 10 to 100 nm, which enhances their dispersion in an aqueous system. Moreover, the increased surface area of the droplets improved the bioaccessibility, bioavailability, and control release of the functional compounds (Donsì & Velikov, 2019) Nanoemulsions are easily produced and often exhibit high physicochemical stability. All the advantages have led to the increased popularity of nanoemulsions over conventional emulsions in recent years.

In this study, treated pea protein isolates (TPPI) produced through pH-shifting and thermal treatment were combined with FG at various ratios (3:1, 5:1,7:1, 9:1, and 11:1), as determined by preliminary studies. The turbidity profiles, zeta potential, and optimal working pH of the complexes were investigated. Subsequently, the tocotrienol-rich fraction (TRF)-based nanoemulsions were fabricated using the resulting complexes. The nanoemulsions were characterized in terms of the droplet size, PDI, zeta potential, viscosity, pH, emulsion activity index (EAI), and emulsion stability index (ESI). The optimal nanoemulsion formulation was selected based on a further evaluation under a 7-day short-term stability study at 25 °C. The complexation between TPPI and FG may provide new insight for developing stable formulations to deliver lipophilic bioactive compounds.

3.2 Materials and Methods

3.2.1 Materials

The emulsifiers, PPI, and FG were supplied by Emsland Group Sdn. Bhd (Wietzendorf, Germany) and Qingdao Dehui Halobios Science and Technology Co., Ltd (Qingdao, China), respectively. The palm TRF suspension is provided by ExcelVite Sdn. Bhd. (Chemor, Malaysia) consisted of 38.5 to 42.0% of total tocotrienols, 9.5 to 14.0% of tocopherol, 30.0 to 45.0% of palm olein (monoglyceride, diglyceride, and triglyceride), 1.0 to 3.0% of plant squalene, 0.03 to 0.07% of mixed carotene complex predominantly β-carotene, and 2.0 to 4.0% of sterol complex predominantly β-sitosterol. The active ingredients predominantly of d-α-tocopherol (9.5 to 14.0%), d-γ-tocotrienol (17.5 to 23.0 %), d-α-tocotrienol (12.0 to 16.0%), d-δ-tocotrienol (4.0 to 7.0%), and d-β-tocotrienol (minimum of 1.9%). Furthermore, the Bradford reagent was purchased from Sigma-Aldrich Pty. Ltd (Darmstadt, Germany). Deionized water was used in all sample preparations and analyses.

3.2.2 pH-Shifting and Thermal Treatment of PPI

The PPI was subjected to pH shifting and thermal treatment to maximize its solubility before forming a complex with FG using the method reported by Yi et al., (2021) with minor modifications. The PPI solution (2%, w/w) was adjusted to pH 12.0 ± 0.2 using 1 M NaOH and magnetically stirred overnight to ensure complete hydration of the protein. Next, the PPI solution was thermally treated at 88 ^{o}C for 30 min in a stirring water bath for the protein unfolding and refolding processes. Then, the solution was immediately cooled down to 25 ^{o}C. The pH of the PPI solution was adjusted to pH 6.0 ± 0.2 using 0.25 M hydrochloric acid with continuous stirring at 750 rpm for 10 min. Subsequently, the resulting protein solution was centrifuged at 8610 rpm for 15 min to eliminate the insoluble residues. The supernatant was collected and known as TPPI.

3.2.2.1 Protein Solubility

The protein solubility of PPI and TPPI was evaluated using the method reported by Tomotake et al. (2002) with some minor modifications reported by the Bradford method (Bradford, 1976). The soluble protein concentrations of both 1% (w/w) native PPI and TPPI were compared as a function of pH ranging from 7.0 to 2.0. After the pH adjustment, the PPI and TPPI solutions were stirred for 30 min and centrifuged at 6000 rpm for 20 min. The supernatant which contained the soluble protein was measured using the Bradford method with Cary 60 UV-visible spectrophotometer (Agilent Technologies, California, USA) at 595 nm. Three measurements were performed on each sample as replicates. Bovine serum albumin (BSA) was used as the standard. The soluble protein concentrations in the samples were quantified using the constructed calibration curve with concentrations ranging from 0.05 to 1.6 mg/mL. The protein solubility of the samples was determined using the following equation:

$$\text{Solubility (\%)} = \left[\frac{P_{supernatant} \times 50}{Wt_{sample} \times \left(\frac{P_{sample}}{100}\right)}\right] \times 100\% \quad \text{(Eq.3.1)}$$

where $P_{supernatant}$ represents the protein concentration in the supernatant (mg/mL); Wt_{sample} represents the sample weight (mg); and P_{sample} refers to the protein content in the sample (%); 50 is the dilution factor.

3.2.3 Formation of TPPI-FG Complexes

The solutions containing 2% (w/w) TPPI-FG complexes were prepared using a method modified from Wang et al., (2020). A preliminary study was conducted using TPPI and FG at a ratio of 1:1 to 13:1. However, the complex of TPPI-FG at a ratio of 1:1 was too viscous which restricted the flow of turbulence during the coarse homogenization process. Nanoemulsion formed using TPPI-FG at the ratio of 13:1 experienced phase separation within a few hours after high-pressure homogenization, therefore, this ratio was eliminated in this study. The TPPI was complexed with FG at different ratios (3:1, 5:1,7:1, 9:1, and 11:1). The FG was dissolved in deionized water and stirred overnight at 500 rpm to ensure complete dissolution. Then, complexation was performed by mixing TPPI and FG solutions with continuous stirring at 650 rpm for 30 min. The formation of TPPI-FG complexes was studied by performing turbidimetric and zeta potential measurements.

3.2.3.1 Turbidimetric Measurement

The turbidimetric measurement was performed using the modified method reported by Wang et al. (2020). For turbidimetric measurements, the prepared solutions containing TPPI-FG complexes were further diluted to 0.08% (w/w) to reduce the absorbance values. Then, the pH of the resulting solutions was adjusted to a specific pH (range of pH 2 to 7). The pH-adjusted TPPI-FG complexes were stirred for 30 min before measurement using a UV-visible spectrophotometer (Cary 60, Agilent Technologies, California, USA) at 700 nm. The optical density (OD) of each solution was recorded. Three measurements were performed on each sample as replicates. The critical pH values of the formation of soluble complexes (pH_c), insoluble complexes($pH_{\phi 1}$), optimal complexation (pH_{opt}), and the dissolution of complexes ($pH_{\phi 2}$) which involved in the phase transition of TPPI-FG complexes were determined graphically by the intersection points of two curved tangents.

3.2.4 Preparation of TRF-based Nanoemulsions

The TRF-based o/w nanoemulsions were fabricated using a method modified from Zang et al., (2019). The oil phase of the nanoemulsion consisted of 10% (w/w) palm TRF, while the aqueous phase was composed of 2% (w/w) TPPI-FG soluble complexes formed

at pH 6 using different TPPI-FG ratios (3:1, 5:1, 7:1, 9:1 and 11:1). Before homogenization, the TPPI-FG complexes and TRF were heated to 40 ^{o}C. Next, both oil and aqueous phases were mixed using the high shear homogenizer (Silverson L4R, Silverson Machines Ltd., Chesham, England) at 7500 rpm for 5 min to form a coarse emulsion. Then, the coarse emulsion was further subjected to high-pressure homogenization (Panda 2K, GEA Niro-Soavi, Parma, Italy) at 800 bars for 5 cycles to produce fine nanoemulsions. The fresh nanoemulsions were characterized based on the droplet size, PDI, zeta potential, viscosity, pH, EAI, and ESI. The prepared nanoemulsions were further stored for 7 days at 25 ^{o}C to evaluate the changes in their droplet size distribution, PDI, zeta potential, and CI.

3.2.4.1 Zeta Potential Measurement

The zeta potential values of all solutions containing 0.08% (w/w) TPPI-FG complexes and TRF-based nanoemulsions prepared using different ratios were measured using Zetasizer Nano ZS (Malvern Instruments Ltd., Worcestershire, UK). For nanoemulsion samples, a 100-times dilution was performed before measurement. Three measurements were performed on each sample as replicates.

3.2.4.2 Droplet Size Distribution and Polydispersity Index (PDI)

The droplet size distribution and PDI of the nanoemulsions were measured using Zetasizer Nano ZS (Malvern Instruments Ltd., Worcestershire, UK). Nanoemulsions were diluted 100 times with deionized water before the measurement. The refractive index and temperature for water were set at 1.33 and 25 °C, respectively. Three measurements were performed on each sample as replicates.

3.2.4.3 Viscosity

The viscosity values of the nanoemulsions were measured using a vibrio viscometer (SV-10, A&D Company, Tokyo, Japan) equipped with a tuning fork at 25 °C. Three measurements were performed on each sample as replicates.

3.2.4.4 pH

The pH values of the nanoemulsions were determined using a pH meter (Sartorius Portable pH Meter PT, Goettingen, Germany) at 25 °C. Three measurements were performed on each sample as replicates.

3.2.4.5 Emulsion Activity Index (EAI) and Emulsion Stability Index (ESI)

The EAI and ESI were measured using the method adopted by Guo & Mu (2011), with minor modifications. Ten microliters of nanoemulsion were pipette from the bottom of the test tube right after homogenization. Then, the nanoemulsion was added with 5 mL of 0.1% sodium dodecyl sulfate solution and thoroughly vortexed. A Carry 60 UV-visible spectrophotometer (Agilent Technologies, California, USA) was used to measure the absorbance of the solution at 500 nm. Three measurements were performed on each sample as replicates. The EAI and ESI were quantified using the following equations:

$$\text{EAI } (m^2/g) = \frac{2 \times 2.303 \times A_0 \times \text{dilution factor}}{c \times 1 \times 1 \ (1 - Þ \times 10000)} \quad \text{(Eq.3.2)}$$

$$\text{ESI (min)} = \left(\frac{A_0}{A_0 - A_{10}}\right) \times t \quad \text{(Eq.3.3)}$$

where c denotes the primary protein concentration in complex solution (g/mL); l denotes the optical path (0.01 m); Þ refers to the oil volume fraction of the emulsion; the dilution factor is 250; t is 10 min; and A_0 and A_{10} refer to the absorbance values of the diluted emulsions at 0 and 10 min, respectively.

3.2.4.6 Creaming Index (CI)

The CI values represented the nanoemulsion stability (Chang et al., 2018). Ten millilitres of nanoemulsion were transferred into a 15 mL screw-capped test tube and stored for 7 days at 25 °C. Three measurements were performed on each sample as replicates. The extent of phase separation represented by CI was determined as followed:

$$\text{CI } (\%) = \left(\frac{\text{HS}}{\text{HE}}\right) \times 100\% \quad \text{(Eq. 3.4)}$$

where HS indicates the height of the separated layer (cm) and HE indicates the total emulsion height (cm).

3.2.4.7 Short-term Storage Study

The prepared nanoemulsions were further stored for 7 days at 25 °C to evaluate the changes in their droplet size distribution, PDI, zeta potential, and CI.

3.2.4.8 Transition Electron Microscopy (HR-TEM)

The morphology of the nanoemulsions was investigated using transmission electron microscopy (JEOL-JEMP-2100F, Tokyo, Akishima, Japan). A drop of nanoemulsion was added onto a 400-mesh formvar carbon-coated copper grid (Agar Scientific Ltd., Essex, UK) and left to stand for 5 min. A Whatman filter paper was used to drawn-off the excess nanoemulsion. The grid was stained with a drop of 2% uranyl acetate for 2 min, the excess stain was drawn off with a filter paper and was held for 5 min at room temperature for drying. The nanoemulsions were then analysed under TEM using the operation parameter of 20 kV acceleration voltage and magnification of 25000×.

3.2.5 Statistical Analysis

All measurement data were analyzed using the Minitab statistical software version 17.0 (Minitab Inc., PA, USA). All experiments were replicated and triplicate measurements were performed on each sample. The one-way ANOVA with post-hoc Tukey's test was adopted to determine the significant differences among mean values ($p < 0.05$).

3.3 Results and Discussion

3.3.1 Effect of pH-shifting and Thermal Treatments on PPI Solubility

The protein solubility of both PPI and TPPI were significantly ($p < 0.05$) different at the pH range of 2 to 7, as depicted in Figure 3.1. Generally, the protein solubility of PPI and TPPI decreased by 17% and 55% from pH 7 to 4, respectively; while their solubility increased by 17% and 52%, respectively, as the pH decreased from 4 to 2. One of the main factors which influence protein solubility is the medium's pH value. Pea protein mainly consists of globulins, whereby globulins exhibit minimum solubility when close to the isoelectric point (pI ≈ 4.3-4.9) while they show moderate to high solubility when the pH is far below or above the pI (Barać et al., 2015).

At pH 7, native PPI exhibits low water solubility and poor functional properties which limits its applications. Therefore, pH-shifting and thermal treatments were applied. The treatments were found to be effective in enhancing the PPI's solubility, as shown by the significant ($p < 0.05$) higher solubility of TPPI compared to the native PPI. The findings were similar to those reported by Yi et al. (2021), whereby the PPI was found to exhibit a higher solubility after both pH-shifting and thermal treatments.

The pH-shifting is a chemical treatment whereby PPI is exposed to an extreme alkaline (pH 12). At alkaline conditions, many globular proteins experience significant conformational alteration as they are partially unfolded and refolded when the pH is readjusted back to neutral. These processes lead to a molten globule conformation with unique surface properties (Yi et al., 2021). The proteins' conformational alterations lead

to spectroscopic changes when they are exposed to different pHs. This process is known as the Tanford transition (Tanford et al., 1959). When there is a slight shift in pH (around 2 units), the ligand-binding and releasing efficiency of β-lactoglobulin are altered due to the changes in the protein structure. On the other hand, the surface hydrophobicity of the pea protein is raised by 62% when there is an extreme shift in pH (towards pH 12) (Jiang et al., 2014). The increased surface hydrophobicity is mainly due to the exposure of non-polar amino acid residue side chains. As a result, the treated protein exhibited significantly improved emulsifying properties (Jiang et al., 2009). Jiang et al. (2009) reported the enhanced antioxidant activity and stability of the PPI-based O/W emulsions after using the pH-shifting treated PPI. Besides, this study also suggested the improved functionality of soy protein as the soy globulin structure was modified after the pH-shifting treatment (Jiang et al., 2009).

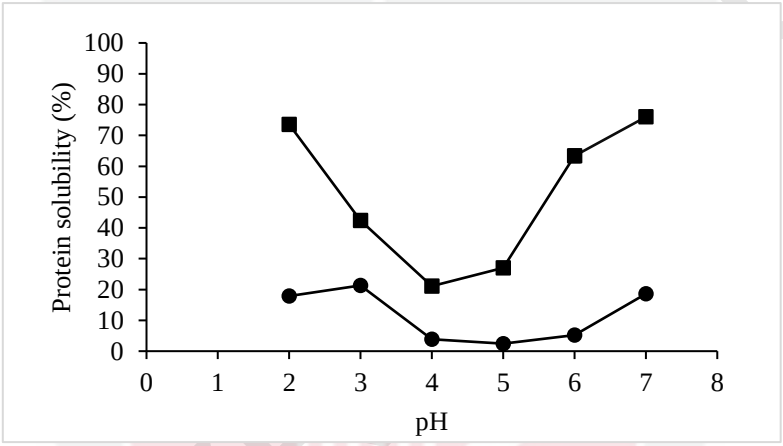

Figure 3.1: Solubility of native (—●—) and treated (—■—) pea protein isolate at different pH.

3.3.2 Characterization of TPPI-FG Complexes

3.3.2.1 Turbidimetric Measurement

The interactions between proteins and polysaccharides during complexation are crucial as they directly influence the resulting complexes' emulsifying capacities. The interactions between protein and polysaccharide were greatly impacted by pH and different biopolymer mixing ratios. In this study, the turbidimetric profile of 0.08% (w/w) TPPI-FG complex solutions prepared using different biopolymer ratios of 3:1, 5:1, 7:1, 9:1, and 11:1 from pH 7.0 to 2.0 was investigated using the pH titration method (Figure 3.2). The critical pH values associated with the structure-forming processes during the complexation of TPPI and FG are shown in Table 3.1. The pure TPPI solution was used as the control. Based on the bell-shaped curve obtained, starting from pH 7, the OD of the complexes started to increase slightly at pH 6.0, which indicated the formation of soluble complexes between both TPPI and FG. The soluble complex was formed

above the isoelectric point of PPI (pI = 4.9), whereby both TPPI and FG exhibited predominantly negative charges. Theoretically, the soluble complex formation could not form at pH 6.0 as negatively charged TPPI and FG repel each other with the repulsive coulombic forces. This has caused the biopolymers to be spatially separated and retain as co-soluble due to the very dilute nature of the system. (Yi et al., 2021). However, it was hypothesized that the carboxyl groups on FG molecules were interacting electrostatically with the positive patches presented on TPPI-TPPI clusters that were associated with hydrophobic interaction. Similar findings were also reported on both lentil protein isolate-carrageenan (Wang et al., 2022) and BSA-FG complexes (Liu et al., 2015). When the complexes were further acidified, the nucleation and growth of primary soluble complexes were initiated to form the quasineutralised insoluble complexes at pH 5.0 to 5.3 ($pH_{\phi 1}$). At this stage, the positively charged TPPI began to attract the negatively charged FG by electrostatic interactions. The OD of TPPI-FG complexes increased as they changed from transparent to cloudy. As the titration proceeded, the OD eventually reached the maximum point (pH_{opt}) at pH 4.0. The formation of insoluble complexes had achieved the maximum at this stage and the electrical equivalences were achieved between both biopolymers. As acidification resumed, the insoluble complexes began to dissociate as protonation of anionic groups (carboxyl groups) of FG occurred. The complexes were largely dissociated at pH 1.7 to 2.1 ($pH_{\phi 2}$), and both TPPI and FG carried similar net charges (Turgeon et al., 2003).

The TPPI and FG mixing ratio is vital to balance the charges between protein and polysaccharide, which influences the degree of complex formation. Generally, the OD of all complex solutions prepared using different biopolymers' ratios was lower than the pure TPPI solution at the determined pH range. This was attributed to the presence of FG which generated electrostatic repulsion to suppress the formation of larger TPPI-TPPI aggregates (Wang et al., 2022). As the TPPI-FG ratio increased from 3:1 to 11:1, the OD also increased. This was due to the reduction of FG in the complex which resulted in a lower degree of electrostatic repulsion, hence more TPPI aggregates were formed and contributed to the higher OD value. Similar trends were observed in the lentil protein isolate-carrageenan complex solutions (Wang et al., 2022). When the TPPI-FG ratio decreased from 3:1 to 1:0, $pH_{\phi 1}$ and $pH_{\phi 2}$ tended to take place at higher pH. However, both the pH_c and pH_{opt} were not significantly ($p > 0.05$) affected by the mixing ratio (Table 3.1). A similar trend was reported by Liu et al. (2015), whereby the pH_c of the BSA-FG complex was not significant as a function of different biopolymers' ratios. At pH_{opt}, the net charges of the complexes were close to zero as TPPI and FG were having opposite charges which neutralized each other. Therefore, the complexes formed exhibited the highest insolubility. In summary, a soluble complex of TPPI-FG was found at pH 6 and was used to form nanoemulsion at difference TPPI-FG ratios (3:1 to 11:1).

Table 3.1: Critical pHs associated with the complexation of treated pea protein isolate-flaxseed gum at different ratios.

TPPI-FG Ratio	pH_c	$pH_{\phi1}$	pH_{opt}	$pH_{\phi2}$
1:0	6.00 ± 0.00^{A}	5.30 ± 0.00^{A}	4.00 ± 0.00^{A}	2.10 ± 0.00^{B}
3:1	6.00 ± 0.00^{A}	4.95 ± 0.21^{C}	4.00 ± 0.00^{A}	1.72 ± 0.23^{C}
5:1	6.00 ± 0.00^{A}	5.08 ± 0.10^{BC}	4.00 ± 0.00^{A}	2.05 ± 0.05^{B}
7:1	6.00 ± 0.00^{A}	5.25 ± 0.05^{AB}	4.00 ± 0.00^{A}	2.62 ± 0.13^{A}
9:1	6.00 ± 0.00^{A}	5.30 ± 0.00^{A}	4.00 ± 0.00^{A}	2.80 ± 0.00^{A}
11:1	6.00 ± 0.00^{A}	5.30 ± 0.00^{A}	4.00 ± 0.00^{A}	2.62 ± 0.24^{A}

Values are expressed as mean ± standard deviation (n = 6). Mean values with different uppercase superscript letters within the same column are significantly different ($p < 0.05$). Abbreviations: Critical pHs corresponding to the formation of soluble complexes (pH_c), insoluble complexes ($pH_{\phi1}$), optimal complexation (pH_{opt}), and the dissolution of complexes ($pH_{\phi2}$).

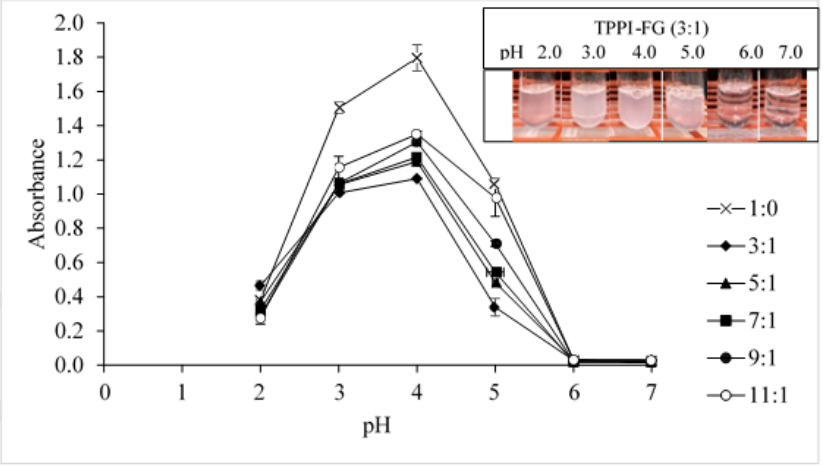

Figure 3.2: Turbidity of Treated Pea Protein Isolate-Flaxseed Gum Complexes with Different Ratios as a Function of pH.

3.3.2.2 Zeta Potential

The main electrostatic interaction involved in protein-polysaccharide complexation is contributed by the oppositely charged biopolymers (Stone & Nickerson, 2012). Due to

this reason, it is vital to obtain information about the electric potentials of the protein-polysaccharide surfaces to form a stable complex. The zeta potential of the TPPI, FG, and TPPI-FG complexes formed using different biopolymer ratios as a function of pH is illustrated in Figure 3.3. When the pure TPPI solution was titrated from pH 7.0 to 2.0, the zeta potential of the solution changed from a negative charge (-30.0 ± 1.5 mV) to a positive charge (24.3 ± 1.6 mV). This phenomenon was due to the amine and carboxy group of TPPI which underwent protonation as they were acidified. On the contrary, the zeta potential of the pure FG solution remained negative (-29.3 ± 1.7 to -3.9 ± 0.3 mV) throughout the whole titration process from pH 7.0 to 2.0. This might be attributed to the low pK_a value of FG molecules; hence, protonation of FG did not occur during the titration. The zeta potential of all the TPPI-FG complexes was lower than the pure TPPI solution when complexation took place at pH above the isoelectric point. The results confirmed that significant charge neutralization took place during complexation between positively charged patches of TPPI and negatively charged FG by electrostatic interaction. In comparison with the pure TPPI, the isoelectric point of the TPPI-FG complexes decreased slightly from pH 4.0 to 3.5.

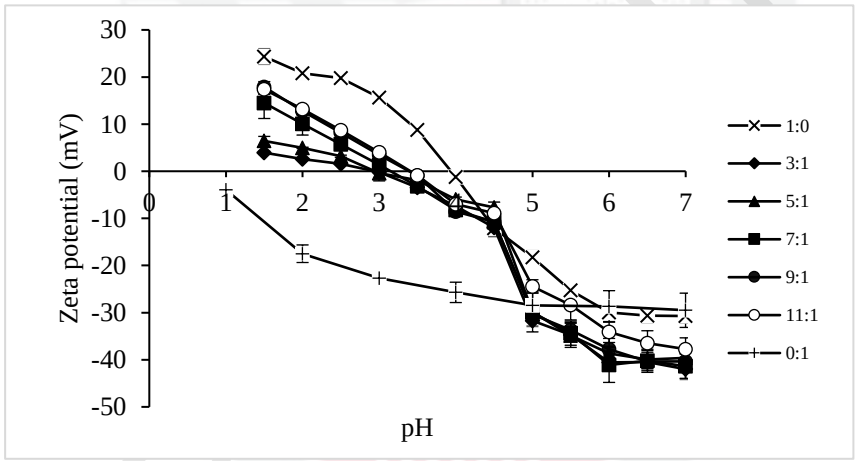

Figure 3.3: Zeta potential of treated pea protein isolate-flaxseed gum complexes with different ratios as a function of pH.

3.3.3 Characterization of Nanoemulsions

3.3.3.1 Droplet Size Distribution and Polydispersity Index (PDI)

Based on a preliminary study, the soluble complexes formed at pH 6 and insoluble complexes formed at pH 4 were utilized to form nanoemulsions. It was found that the nanoemulsion stabilized by insoluble complexes underwent phase separation within a day of storage (results not shown) while the nanoemulsions produced by soluble complexes were more stable. Besides, the protein solubility of TPPI was much higher at pH 6 (63 ± 0.57%) as compared to pH 4 (21 ± 0.24%). Therefore, in the present study,

the nanoemulsions containing 10% TRF were fabricated by incorporating various soluble TPPI-FG complexes formed using different biopolymers' ratios at pH 6.0. At this pH, it was found that the complexation process, which involved electrostatic interaction between the negatively charged carboxyl groups on FG molecules and positively charged patches presence on TPPI was able to stabilize the nanoemulsion (Wang et al., 2022). The full characterization of all nanoemulsion samples is shown in Table 3.2. The nanoemulsions demonstrated a reducing trend in terms of droplet size and PDI value as the proportions of FG were decreased in the formulations. It was suggested that the droplet size was affected by the high molecular weight of FG (1470 kDa) (Qian et al., 2012). The FG mainly consists of arabinoxylans in the neutral fraction and exhibits pseudoplastic flow behavior (Qian et al., 2012). Therefore, when the FG amount decreased, the resulting complexes formed a thinner and less dense coating surrounding the oil droplets, leading to a smaller mean droplet size. Another study also reported the usage reduction of gum Arabic resulted in a smaller droplet size of the nanoemulsion stabilized using a pea protein-gum Arabic complex. It was suggested that the increased polysaccharide proportions would cause an increase in the bridging flocculation of oil droplets due to the interaction of polysaccharides with the positively charged proteins (Carpentier et al., 2022).

On the other hand, PDI measures the width of the droplet size distribution with values ranging from 0 (monodisperse) to 1 (polydisperse). A wide droplet size distribution generally leads to a higher PDI value (> 0.5) (Gibis et al., 2013). With the increasing amount of TPPI incorporated in the TPPI-FG complex, the PDI of the fabricated nanoemulsions decreased significantly ($p < 0.05$) from 0.45 ± 0.02 to 0.31 ± 0.02.

3.3.3.2 Zeta Potential

Table 3.2 shows the zeta potential of TRF-based nanoemulsions produced using TPPI-FG complex formed using different biopolymers' ratios. No significant difference ($p > 0.05$) was observed in the zeta potential values of all nanoemulsions, which ranged from -34.50 ± 2.01 to -37.50 ± 1.94 mV. The zeta potential showed a negative value as the emulsion was having pH above the PPI isoelectric point. A similar result was obtained for soy protein as well (Padial-Domínguez et al., 2020). The stability of the nanoemulsions can be influenced by the electrostatic repulsion between oil droplets (Cuevas-Bernardino et al., 2018). High zeta potential values (more than 30 mV or less than -30 mV) reflected the greater repulsions between oil droplets and reduced aggregations. In other words, the droplet coalescence was minimized which led to enhanced emulsion stability (Chang et al., 2018).

3.3.3.3 Viscosity and pH

The viscosity of emulsion-based food products is also another important quality parameter as it influences the processing steps (mixing, homogenization, and flow rate), textural attributes (mouthfeel), rheological properties (pourability), as well as the emulsion stability (Shao et al., 2019). The viscosity values of the TRF-based nanoemulsions ranged from 4.37 ± 0.31 to 21.40 ± 0.24 mPa.s. With the increasing

amount of FG in the complex, the fabricated nanoemulsions also showed significant ($p < 0.05$) higher viscosity values. The FG is a thickening agent with high molecular weight and intrinsic viscosities (6.63 to 5.13 dLg^{-1}) which provides excellent rheological properties, emulsifying ability, and water-holding capacity (Liu et al., 2016). A medium with enhanced viscosity restricts the movement of molecules and thereby reducing the rate of gravitational separation. No significant ($p > 0.05$) difference was observed in the pH values of all the nanoemulsions fabricated using different TPPI-FG ratios (Table 3.2).

3.3.3.4 Emulsion Activity Index (EAI) and Emulsion Stability Index (ESI)

The EAI and ESI of TRF nanoemulsion stabilized by different TPPI-FG ratios are shown in Table 3.2. The EAI measures the ability of protein and polysaccharides that can be adsorbed on the oil-water interface to form an emulsion layer (Zhang & Li, 2022). Based on the findings of Jiang et al. (2014), the pH-shifting treatment on pea protein has enhanced the coating efficiency of protein on the oil droplet due to its higher emulsifying activity. This is attributed to the formation of a molten protein globular structure after treatment to improve surface activity (Jiang et al., 2009). Besides, the partially unfolded PPI polypeptides can adsorb readily to the oil surface of droplets via hydrophobic interactions to form a thicker protein membrane with multiple layered which can withstand coalescence as compared to pure PPI (Jiang et al., 2014). Another study also reported the improved EAI and ESI of soy protein after the pH-shifting treatment (Jiang et al., 2009). The EAI values of TRF nanoemulsions decreased significantly ($p < 0.05$) by 70.9% with increasing TPPI-FG ratios. The highest EAI was observed in TPPI-FG (3:1) which indicated the highest emulsifying activity as the oil-water interface had more proteins adsorbed to it (Stone et al., 2015). Meanwhile, the ESI expresses the stability of that adsorbed layer in a defined period (Zhang & Li, 2022). Similarly, ESI decreased significantly ($p < 0.05$) by 10.7%. from TPPI-FG ratios of 3:1 to 11:1. The reduction of FG reduced emulsion stability. The stability of the emulsion was enhanced after FG was added due to the increased viscosity of the continuous phase and the decreased interfacial tension. Therefore, it can effectively restrict droplet movement. TPPI-FG (3:1) consists of the highest FG and has obtained the highest ESI which indicates the adsorbed layer was more stable in a defined period (Stone et al., 2015). Similar reducing EAI and ESI trends were found in the study of the coconut protein-pectin system from a ratio of 3:1 to 1:1 (Candraningrum et al., 2022).

Table 3.2: Characterization of fresh nanoemulsions produced using treated pea protein isolate-flaxseed gum complexes with different ratios.

Ratio	Particle size (nm)	Polydispersity index	Zeta potential (mV)	Viscosity (mPa.S)	pH	ESI (min)	EAI (m^2/g)
3:1	541.98 ± 49.05^{A}	0.45 ± 0.02^{A}	-35.42 ± 1.02^{A}	21.40 ± 0.24^{A}	6.20 ± 0.05^{A}	1544.37 ± 11.20^{A}	400.03 ± 32.20^{A}
5:1	497.90 ± 20.62^{B}	0.47 ± 0.03^{AB}	-36.12 ± 0.55^{A}	13.70 ± 0.88^{B}	6.25 ± 0.12^{A}	1458.40 ± 1.06^{B}	272.96 ± 15.10^{B}
7:1	391.87 ± 13.88^{C}	0.43 ± 0.02^{AB}	-34.50 ± 2.01^{A}	8.18 ± 0.04^{C}	6.24 ± 0.03^{A}	1403.98 ± 21.31^{C}	215.50 ± 61.33^{BC}
9:1	363.33 ± 6.64^{CD}	0.42 ± 0.02^{B}	-37.50 ± 1.94^{A}	5.63 ± 0.01^{D}	6.29 ± 0.03^{A}	1384.02 ± 1.11^{D}	193.17 ± 0.15^{C}
11:1	328.03 ± 3.52^{D}	0.31 ± 0.02^{C}	-35.55 ± 2.58^{A}	4.37 ± 0.31^{E}	6.29 ± 0.03^{A}	1379.07 ± 0.90^{D}	116.42 ± 1.62^{D}

Values are expressed as mean ± standard deviation (n = 6). Mean values with different superscript letters within the same column are significant different ($p < 0.05$). Abbreviations: ESI: Emulsion stability index; EAI: Emulsion activity index.

3.3.3.5 Short-term Storage Study

The storage stability of the nanoemulsions stored for 7 days at 25 °C was evaluated by determining the changes in their mean droplet size, PDI, zeta potential, and CI (Figure 3.4a to d). The mean droplet size of the TRF nanoemulsions fabricated using different TPPI-FG ratios increased significantly ($p < 0.05$) throughout the 7-day storage at 25 °C (Figure 3.4a). From day 0 to day 7, the droplet size increased at 25.5%, 37.2%, 18.1%, 17.8%, and 12.5% in all nanoemulsions with the increasing mixed biopolymer ratios. The results showed that the nanoemulsions formed using the TPPI-FG complex at ratios of 7:1, 9:1, and 11:1 was more stable as the increments of the mean droplet size were below 18%. However, the trend was not in line with the ESI, CI, and phase separation findings. Based on the CI, it was noticeable that these ratios obtained a higher degree of coalescence, and phase separation started to occur on day 2. Hence, this might be the reason causing failure in obtaining reliable droplet size (Chang et al., 2018).

Moreover, the PDI of the TRF nanoemulsions with increasing TPPI-FG ratios increased significantly ($p < 0.05$) by 4.4%, 17.8%, 14.0%, 16.7%, and 25.8% respectively throughout the 7-day storage period at 25 °C (Figure 3.4b). The nanoemulsion produced using the TPPI-FG complex at the ratio of 3:1 exhibited the lowest increment in PDI. This might be attributed to the higher polysaccharide proportion, which helped to prevent droplet aggregation during storage.

In the meanwhile, the changes in the zeta potential of the TRF-based nanoemulsions produced using different TPPI-FG ratios during storage were not significant ($p > 0.05$) (Figure 3.4c). The final zeta potential of all nanoemulsions was recorded in a range of -31.47 ± 0.81 to -38.15 ± 0.96 mV. The results indicated that TRF-based nanoemulsions remained stable throughout the storage period.

Moreover, the stability of the TRF-based nanoemulsions stored at 25 °C for 7 days was also determined by monitoring the CI, as depicted in Figure 3.4d. Generally, the CI of the nanoemulsions increased significantly ($p < 0.05$) with the increasing TPPI-FG ratios. In the protein-polysaccharide complex system, a protein normally acts as an emulsifier while polysaccharide plays a role as an emulsion stabilizer. With the higher polysaccharide proportion in the complex, it formed a thicker and denser coating around the oil droplets to provide stronger physical barriers. This slowed down the emulsion phase separation and Ostwald ripening. On day 0, no phase separation was observed in all nanoemulsions. However, the CI started to increase from day 2 for the nanoemulsions produced using TPPI-FG ratios of 7:1 to 11:1. The creaming process occurred at a slower rate in nanoemulsions fabricated with TPPI-FG complex ratios of 3:1 and 5:1, which only started on day 3 of storage. At the end of the storage study, nanoemulsions produced using TPPI-FG complex (3:1) exhibited the lowest CI of 4.5 ± 0.55%, while nanoemulsions fabricated using TPPI-FG complex (11:1) showed the highest CI of 67.5 ± 1.64%. The result indicated that nanoemulsions produced using TPPI-FG complex (3:1) were the most stable nanoemulsion throughout the storage period, as justified by the high ESI (1544.37 ± 11.20 min) and EAI (400.03 ± 32.20 m^2/g). This could be attributed to the highest FG proportion (0.5% w/w) in the complex, which contributed to the highest viscosity (21.40 ± 0.24 mPa.s) towards the medium. This restricted the

mobility of the oil droplets, subsequently reducing the gravitational separation (Perrechil & Cunha, 2010). A study by Kim et al. (2022) also reported the better stability of the pea protein-sodium alginate complex stabilized emulsion with a higher percentage of incorporated polysaccharides, which showed only slight creaming on day 7 of storage. Moreover, the strength of the protein layers could also be enhanced with the addition of polysaccharides when protein and polysaccharides are negatively charged due to the thermodynamic incompatibility which led to greater protein interactions at the oil-water interface (Kim et al., 2022).

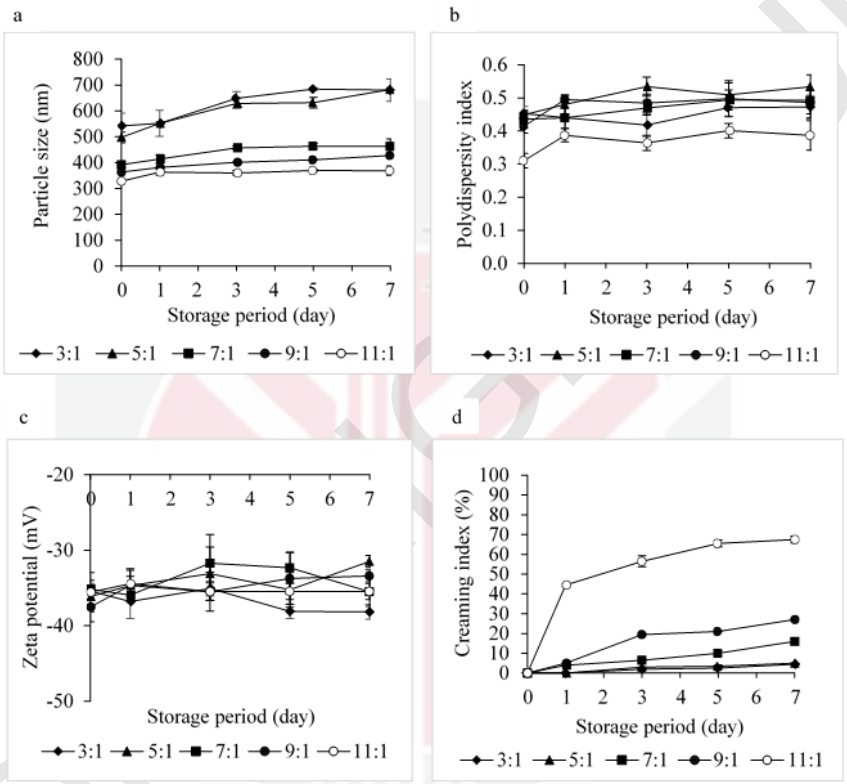

Figure 3.4: (a) Particle size distribution; (b) polydispersity index; (c) zeta potential; and (d) creaming index changes of nanoemulsions produced using treated pea protein isolate-flaxseed gum complexes with different ratios stored for 7 days at 25 °C.

3.3.3.6 Morphology

The morphological structure analysis of the TRF-based nanoemulsions produced using different TPPI-FG ratios was examined by HR-TEM. As shown in Figures 3.5a to e, the black spots represent the dispersion of nano-size oil droplets, while the white background represents the aqueous phase of the nanoemulsion. TPPI-FG (3:1) stabilized nanoemulsion shows the largest initial droplet size among the others and each of the

droplets is separated without coalescence (Figure 3.5a). The TPPI-FG (3:1) complex forms a thicker and denser coating over the oil droplets, which results in a larger initial droplet size. A thicker coating around the oil droplet provides a stronger physical barrier to delay the coalescence from happening. Besides, the absorption of the TPPI-FG (3:1) complex around the oil droplets generated a repulsive force to keep the droplets separated and prevent aggregation with other oil droplets. Additionally, the FG leads to the thickening of nanoemulsion and increased viscosity, this can reduce gravitational separation by restricting the movement of the particles in the medium (Perrechil & Cunha, 2010). Nanoemulsion stabilized by TPPI-FG (5:1) was found to have a small initial droplet size, however, some of the oil droplets started to combine to form large oil droplets (Figure 3.5b). For nanoemulsion produced from TPPI-FG (7:1) to TPPI-FG (11:1), it was observed that the initial droplet size was getting smaller (Figures 3.5c, d, and e). These observations were due to the reduction of FG that decreased the thickness of the coating layer around oil droplets. Meanwhile, the mobility of the oil droplets also increased with the reduction of viscosity. Subsequently, the droplets were getting closer to each other, which led to the formation of large oil droplets and the fastening of the coalescence process. As a result, it caused phase separation to happen over some time.

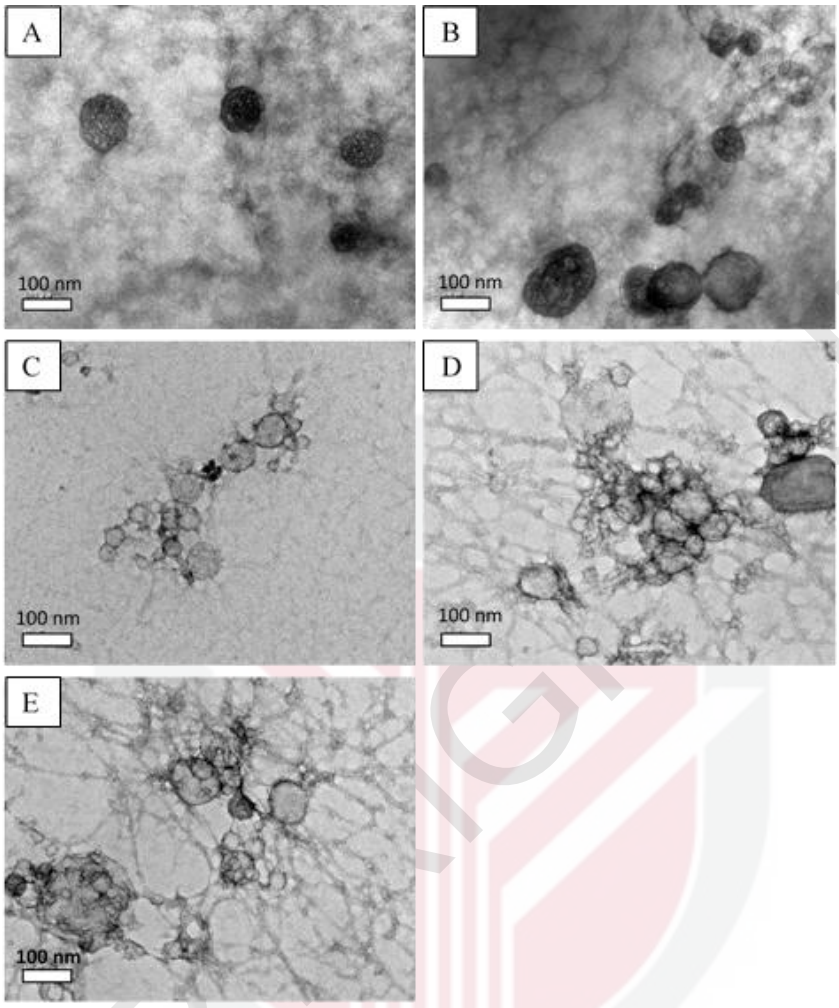

Figure 3.5: TEM micrographs of TRF-based nanoemulsions prepared with different treated pea protein isolate-flaxseed gum complexes ratios (a) 3:1; (b) 5:1; (c) 7:1; (d) 9:1 and (e) 11:1. The scale bar represents 100 nm.

3.4 Conclusion

The poor solubility of PPI at its native state was significantly ($p < 0.05$) improved after the pH-shifting and thermal treatments. Besides, the soluble TPPI-FG complexes were formed through electrostatic interactions at pH 6.0. The TRF-based nanoemulsions (10%, w/w) were successfully fabricated using the assembled TPPI-FG complexes. Among all nanoemulsion samples, TRF-based nanoemulsion stabilized with TPPI-FG (3:1) complex yielded the highest viscosity (21.40 ± 0.24 mPa.s), EAI (400.03 ± 32.20 m^2/g), and ESI (1544.37 ± 11.20 min). Besides, the nanoemulsion also exhibited excellent stability as it demonstrated the smallest changes in CI (4.50 ± 0.55%) and PDI (4.4%) after seven days of storage at 25 °C. Besides, coalescence was not observed in the morphology study of the nanoemulsion produced by the TPPI-FG (3:1) complex. Therefore, nanoemulsion formed using TPPI-FG complex (3:1) was selected in this study due to the highest viscosity, EAI, ESI, while low changes in CI and PDI after storage. The findings evidenced the potential emulsifying activity of the TPPI-FG complex (3:1), thereby enhancing the hydrophobic bioactive compounds' applications, especially in aqueous systems.

CHAPTER 4

OPTIMIZATION AND CHARACTERIZATION OF TOCOTRIENOL-RICH FRACTION-BASED MICROCAPSULES PRODUCE BY SPRAY DRYING USING DIFFERENT CORE-TO-WALL RATIOS, WALL MATERIAL COMPOSITIONS AND MIXING RATIOS

4.1 Introduction

Tocopherols and tocotrienols, lipid-soluble phenolic compounds, are found in four homologs: alpha, beta, gamma, and delta (α-, β-, γ-, and δ-). These compounds naturally occur in palm oil, oilseeds, nuts, and other edible oils (Kornsteiner et al., 2006). Numerous studies have highlighted the health benefits of tocotrienols, including anti-cancer, anti-inflammatory, immune regulation, neuroprotective, and lipid-lowering properties (Meganathan & Fu, 2016). Due to their health benefits, tocotrienols have gained prominence for human consumption. However, their lipophilic nature leads to challenges like low water solubility, limited absorption, and oral bioavailability (Goh et al., 2015).

In response to these challenges, nanoemulsion has emerged as a promising water-soluble delivery system to enhance the solubility of tocotrienols (Fu et al., 2014). Despite its effectiveness, concerns about the shelf-life of lipid nanoemulsions have arisen due to their susceptibility to microbial spoilage upon storage. Additionally, the handling, bulk transport, and application of liquid nanoemulsions in dry food systems are hindered (Teo et al., 2021). Thus, the conversion of liquid nanoemulsion into dry form through microencapsulation has become essential to address these limitations.

The most common method of encapsulation is spray drying, known for its economical, cost-effective, and versatile production of high-quality microcapsules. Spray drying is suitable for encapsulating bioactive compounds such as vitamins, minerals, phenolics, carotenoids, proteins, and essential fatty acids (Jafari et al., 2021). This method effectively transforms nanoemulsion into microcapsules, utilizing intense moisture evaporation from the droplet surface to maintain droplet integrity until achieving a dry state (Fang & Bhandari, 2012). Microencapsulation augments the stability of bioactive compounds during processing, handling, and storage (Teo et al., 2021).

Microencapsulation involves entrapping small particles or droplets with polymer materials to produce microcapsules (Corrêa-Filho et al., 2019). These microcapsules comprise a shell and a core, with the shell serving as a protective barrier against oxygen, light, and water. The wall materials safeguard the bioactive compounds, enhancing their stability under various environmental stresses (Paulo & Santos, 2017).

Maltodextrin (M) is a hydrolyzed starch, commonly used to encapsulate bioactive compounds. Its benefits include high solubility, high solids content with low viscosity,

affordability, minimal taste, and aroma alternation. During spray drying, M forms a crust over dried droplets, providing the necessary solid content to the wall materials (Zhu et al., 2022). In addition, M exhibits stability under high temperatures and low pH conditions (Shepherd et al., 2000). However, its limited emulsifying ability remains a challenge (Xiao et al., 2022), necessitating its combination with other wall materials like OSS and INU to enhance the MEE via spray drying.

Starch sodium octenyl succinate (OSS), derived from tapioca, is a modified starch approved by the FDA and CFDA (Long et al., 2022). Esterification results in amphiphilic molecules with hydrophobic alkenyl groups (Long et al., 2022), making OSS suitable for encapsulating flavours, clouds, vitamins, and spices in the food and pharmaceutical industries. It is a reliable emulsifier and thickener with excellent film-forming properties and low viscosity (Yang et al., 2023).

Inulin (INU), a natural fructan group of carbohydrates, consists of fructose unit chains connected by β-(2-1) glycosidic bonds. Its indigestible nature in the stomach and small intestine positions. The INU acts as a potential transporter for gastrointestinal drug delivery (Wang et al., 2019). The INU also offers health benefits such as improved mineral absorption and reduced colon cancer risk. FDA's GRAS status confirms its safety (Afinjuomo et al., 2019).

Presently, no information exists on the microencapsulation of tocotrienols with a complex of PPI and FG. Furthermore, limited research has explored the impact of core-to-wall ratios, wall material compositions, and mixing ratios on tocotrienol microencapsulation. Therefore, this study's objective is to microcapsules based on TRF using spray drying with various core-to-wall ratios, alongside a combination of M with OSS and INU wall materials at different mixing ratios. The study assesses the physical properties and stability of these TRF-based microcapsules.

4.2 Materials and Methods

4.2.1 Materials

Palm TRF oil was provided by ExcelVite Sdn. Bhd (Chermo, Malaysia). This ingredient consisted of 38.5 to 42.0% total tocotrienols, 9.5 to 14.0% tocopherol, 30.0 to 45.0% palm olein (monoglyceride, diglyceride and triglyceride), 1.0 to 3.0% of plant squalene, 0.03 to 0.07% of mixed carotene complex predominantly β-carotene, and 2.0 to 4.0% of sterol complex predominantly β-sitosterol. The active ingredients predominantly of d-α-tocopherol (9.5 to 14.0%), d-γ-tocotrienol (17.5 to 23.0 %), d-α-tocotrienol (12.0 to 16.0%), d-δ-tocotrienol (4.0 to 7.0%), and d-β-tocotrienol (minimum of 1.9%). The plant-based emulsifiers, PPI, and FG were sourced from EMSland Group Sdn. Bhd (Wietzendorf, Germany) and Qingdao Dehui Halobios Science and Technology Co., Ltd (Qingdao, China), respectively. Wall materials of INU were purchased from V.I.S. Foodtech Ingredient Supplies Sdn. Bhd. (Kepong, Malaysia), while M and OSS were purchased from Ingredion Incorporated (Westchester, United States). High-performance

liquid chromatography (HPLC) grade standards of tocopherols and tocotrienols mixtures (α-, β-, γ-, and δ-) were acquired from ChromaDex (Los Angeles, United States). The HPLC-grade hexane and 1,4-dioxane were obtained from Fisher Scientific (Pittsburgh, United States). Deionized water was utilized in all sample preparation and analyses.

4.2.2 Preparation of TPPI-FG Complex

Based on the previous chapter, TPPI-FG at a ratio of 3:1 has obtained better emulsification properties, which will be further studied in this chapter. The TPPI was prepared using a pH-shifting and thermal treatment method, adapted from Yi et al. (2021). The PPI solution containing 1.5% w/w PPI was adjusted to pH 12.0 ± 0.2 using 1 M NaOH and stirred overnight to ensure complete protein hydration. The solution was thermally treated at 88 ºC for 30 min in a water bath for protein unfolding and refolding. After cooling to 25 ºC, the pH was adjusted to pH 6.0 ± 0.2 using 0.25 M hydrochloric acid with continuous stirring at 750 rpm for 10 min. The resulting solution was centrifuged to eliminate the insoluble residues using a Centrifuge machine X1 (Thermo Scientific, Waltham, USA) at 8610 rpm for 15 min. The supernatant was collected and known as TPPI. A 0.5% w/w of FG was dissolved in deionized water and stirred overnight at 500 rpm to ensure full dissolution. A TPPI-FG complex (2% w/w) was formed by stirring TPPI and FG at a ratio of 3:1 at 650 rpm for 30 min.

4.2.3 Preparation of TRF-based Microcapsules

TRF-based microcapsules were produced by homogenizing the lipid with the aqueous phase at a ratio of 1:9. The lipid phase consisted of 10% palm TRF-oil, while the aqueous phase comprised 2% w/w of TPPI-FG (3:1) complex and wall materials. A preliminary study was conducted using a core-to-wall ratio from 1:1 to 1:4, it was found that a ratio of 1:1 obtained very low MEE, which indicates insufficient wall material to encapsulate the core material. Therefore, core-to-wall ratios of 1:2, 1:3, and 1:4 were used in this study. The wall materials were initially prepared with M at different core-to-wall material ratios to assess MEE. The 1:4 core-to-wall ratio, which achieved the highest MEE, was selected to combine M with OSS and INU at varying mixing ratios (M:OSS and M:INU in ratios of 9:1 and 8:2 respectively). The microcapsules are shown in Table 4.1. The TPPI-FG complexes and TRF were heated to 40 ºC before homogenization. A high-shear homogenizer (Silverson L4R, Silverson Machines Ltd., Chesham, England) operated at 7500 rpm for 5 min was used to create a coarse emulsion. Subsequently, a high-pressure homogenizer (Panda 2K, GEA Niro-Soavi, Parma, Italy) was employed to form nanoemulsions at 80 MPa homogenization pressure and 5 cycles.

Table 4.1: Formulations of TRF-based microcapsules produced by spray-drying using different core-to-wall ratios, wall material compositions, and mixing ratios.

Formulations	Core-to-wall ratios	Wall material mixing ratios	Wall materials (%)		
			M	OSS	INU
1:2 M	1:2	1:0	18.0	-	-
1:3 M	1:3	1:0	28.0	-	-
1:4 M	1:4	1:0	38.0	-	-
1:4 M:OSS (9:1)	1:4	9:1	34.2	3.8	-
1:4 M:OSS (8:2)	1:4	8:2	30.4	7.6	-
1:4 M:INU (9:1)	1:4	9:1	34.2	-	3.8
1:4 M:INU (8:2)	1:4	8:2	30.4	-	7.6

Abbreviations: M: Maltodextrin; OSS: Starch sodium octenyl succinate; INU: Inulin.

4.2.4 Spray-drying

A pilot-scale spray dryer (GEA Niro A/S, Mobile Minor 2000, Denmark) was utilized to spray dry the homogenized nanoemulsions, with inlet and outlet temperatures of 170 °C and 90 °C, respectively, to produce microcapsules. The pump rate ranged from 10 to 12 mL/min, and the aspiration rate remained at 100%. The resulting powders were sealed in an air-tight amber glass bottle and stored at room temperature for subsequent analysis.

4.2.4.1 Microencapsulation Efficiency (MEE)

The MEE of TRF-based microcapsule was determined using a method adapted from Bae & Lee (2008). To ascertain the TO, 1 g of powder was dispersed in 6 mL of boiling water and vortexed for 60 s in a centrifuge tube. The mixture was then cooled to room temperature (25 °C). Subsequently, 1 mL of 25% ammonia solution and 7.5 mL of methanol were added, followed by vortexing for 2 min. Next, 17 mL of diethyl ether and 17 mL of petroleum ether were introduced. The resulting mixture was manually agitated before centrifuging at 10000 rpm for 10 min. The upper layer of the supernatant was pipetted out and evaporated using a rotary evaporator (EyeLa, NY, USA).

For the quantification of SO, 1 g of microcapsule was dispersed in 15 mL of hexane in a centrifuge tube. After vortexing for 2 min at room temperature (25 °C) to release the free oil, the mixture was filtered using Whatman filter paper number 1. The microcapsules collected on the filter were rinsed three times with 20 mL of hexane. The solvent was

removed using a rotary evaporator (EyeLa, NY, USA) at 60 °C, followed by drying at 105 °C for 1 hr. SO refers to the oil located on the particle surface, calculating by subtracting the mass of an empty flask from the flask containing the extracted oil (Jafari et al., 2008). TO represents the total oil content, encompassing the core and SO content of the powders. Three measurements were performed on each sample as replicates. The calculation for MEE was as follows:

$$\text{MEE}\ (\%) = \left(\frac{\text{TO} - \text{SO}}{\text{TO}}\right) \times 100 \qquad \text{(Eq.4.1)}$$

where TO is the total oil content (g) and SO is the surface oil content (g).

4.2.4.2 Moisture Content (MC)

Moisture content (MC) of the microcapsules, calculated on a dry basis, was assessed using a method adapted from Ishwarya & Anandharamakrishnan (2015). A quantity of one gram of TRF-based microcapsules was introduced into a hot air oven (MMM-Group, Semmelweisstra, Germany) set at 105 °C. The sample weight was monitored until consistent measurements were obtained across three replicates. The MC was determined through the following equation:

$$\text{MC}\ (\%) = \frac{\text{W}_\text{m}}{\text{W}_\text{d}} \times 100 \qquad \text{(Eq.4.2)}$$

where W_m is the mass of water in the sample (g), and W_d mass of dry solids (g).

4.2.4.3 Water Activity (A_w)

The a_w of 1 g microcapsule was determined by an Aqua Lab CX-2 (Aqua Lab, Pullman WA. U.S.A.). The a_w of the microcapsules was performed in triplicate.

4.2.4.4 Flowability and Cohesiveness

Bulk density represents the volume of 2 g microcapsule measured in a 25 mL graduated cylinder without tapping. Subsequently, the graduated cylinder containing the microcapsule was tapped 10 times on thick fabric with a height of 15 cm to determine the tapped density. The final volume was recorded (Asokapandian et al., 2016). Bulk and tapped densities were calculated as follows:

$$\text{Bulk density } (g/cm^3) = \frac{M_p}{V_p} \quad \text{(Eq.4.3)}$$

$$\text{Tap Density } (g/cm^3) = \frac{M_p}{V_T} \quad \text{(Eq.4.4)}$$

where M_p is the mass of powder (g), V_p is the volume of powder (cm^3) and V_T is the final tapped volume (cm^3). Three measurements were performed on each sample as replicates.

The flowability of the TRF-based microcapsule was determined using the CI and the HR, following a method derived from Caparino et al. (2012). The calculated values were the. classified according to Table 4.2.

$$CI\ (\%) = \frac{\rho_T - \rho_B}{\rho_T} \times 100 \quad \text{(Eq.4.5)}$$

$$HR = \frac{\rho_T}{\rho_B} \quad \text{(Eq.4.6)}$$

where ρ_B is bulk density (g/cm^3) and ρ_T is tapped density (g/cm^3).

Table 4.2: Classification of microcapsules flowability based on the Carr Index (1965) and Hausner ratio (1967).

Flowability	Carr Index (%)	Cohesiveness	Hausner ratio
Very good	0-14	Low	0-1.2
Good	15-20	Intermediate	1.2–1.4
Fair	20-35	High	>1.4
Bad	35-45		
Very bad	>45		

4.2.4.5 Water Solubility Index (WSI) and Water Absorption Index (WAI)

The water solubility index (WSI) and water absorption index (WAI) of the TRF-based microcapsules were measured using a method adapted from Caparino et al. (2012) with slight modifications. Around 2.5 g of microcapsule was dissolved in 30 mL of distilled water at 40 °C. The mixture was stirred for 30 min at room temperature (25 °C) and then centrifuged for 10 min at 10,000 rpm. The supernatant was carefully transferred to an evaporating dish and dried overnight at 105 °C in a hot air oven. WSI represents the

weight of dried solids after centrifugation over the weight of the initial dry sample, while WAI indicates the weight of remaining wet solids after centrifugation over the dry weight of the initial sample (dimensionless). The WSI and WAI were determined as follows:

$$\text{WSI } (\%) = \left(\frac{W_d}{W_i}\right) \times 100 \quad \text{(Eq.4.7)}$$

$$\text{WAI } = \frac{W_w}{W_i} \quad \text{(Eq.4.8)}$$

where W_d is the weight of dry solids after centrifugation (g), W_i is the weight of the initial dry sample (g) and W_w is the weight of wet solids remaining after centrifugation (g).

4.2.4.6 Colour

The colour of the spray-dried microcapsules was directly measured using a Chroma meter CR-410 (Konica Minolta, Osaka, Japan). All the measurements were conducted in triplicate.

4.2.4.7 Tocopherol and Tocotrienol Content Analysis

The method for TRF extraction and analysis was adapted from Tan et al., (2000) with slight modifications. Two grams of spray-dried TRF-based microcapsules were continuously stirred in 5 mL deionized water for 30 min. The mixture was then combined with 2 mL isopropanol and vortexed for 1 min. Subsequently, 10 mL of hexane was vigorously vortex-mixed for another 2 min. Centrifugation was conducted at 10,000 rpm for 10 min to collect the supernatant layer in a scintillation vial. The extraction steps were repeated with isopropanol and hexane, followed by centrifugation. The collected supernatant was purged using nitrogen gas. About 1.5 mg of TRF extracts were reconstituted with 7.5 mL of hexane and vortex-mixed for 1 min. The resulting solution was filtered using a 0.45 µm polytetrafluoroethylene syringe filter, and the filtrate was collected in an autosampler vial for analysis.

The method of tocopherol and tocotrienol content analysis was slightly modified from Tan et al. (2000). Tocopherol and tocotrienol peaks were evaluated using the HPLC system from Shimadzu, connected to a fluorescence detector (Shimadzu, Prominence LC-20AD), and a C18 column (250 × 4.6 mm, 5 µm, Phenomenex, Torrance, CA, USA). An isocratic mobile phase consisting of n-hexane: dioxane: isopropanol (97.5%:2%: 0.5 v/v/v) was employed with a flow rate of 1 mL/min, and the analysis lasted for 30 min. An injection volume of 15 µL was used, and the column temperature was set at 30 °C. The fluorescence detector was adjusted to 295 nm.

The α-tocopherol, α-, β-, γ-, and δ-tocotrienols in the TRF-based microcapsules were quantified using external calibration curves ($R^2 \geq 0.99$) established for the mixture isomers using the reference standard mixture. Standard solutions were prepared at concentrations of 0.3 to 50 ppm with n-hexane through serial dilution. These solutions were injected in triplicates to determine tocopherol and tocotrienol content by referring to the calibration curves. The retention of tocopherol and tocotrienol was calculated as follows:

$$\text{Percentage of retention } (\%) = \left(\frac{T_m}{T_o}\right) \times 100 \quad \text{(Eq.4.9)}$$

where T_m is the tocopherol and tocotrienol in the microcapsule, T_o is the tocopherol and tocotrienol in the TRF bulk-oil.

4.2.4.8 Scanning Electron Microscopy (SEM)

The microstructure of the TRF-based microcapsules was observed under a field scanning electron microscope (SEM), JOEL JSM-IT100 (Tokyo, Japan), at 5 kV. The microcapsules were first fixed on metallic stubs and then coated with a layer of platinum. The observation was conducted at a magnification of 1000×.

4.2.5 Statistical Analysis

Minitab statistical software version 17.0 (Minitab Inc., PA, USA) was used to analyse all the measurement data. All experiments were replicated, and triplicate measurements were taken for each sample. The one-way ANOVA with post-hoc Tukey's test was applied to determine significant differences among mean values ($p < 0.05$).

4.3 Results and Discussion

4.3.1 Microencapsulation Efficiency (MEE)

Microencapsulation efficiency (MEE) stands as a pivotal parameter in evaluating the encapsulation efficacy of oils within spray-dried microcapsules. It quantified the amount of SO contained within microcapsules using a solvent extraction method. The evaluation of SO was performed indirectly, gauging the quantity of encapsulated oil present within the microcapsule matrix (Jafari et al., 2008). Initially, MEE was determined for TRF-based microcapsules fabricated with M at core-to-wall ratios of 1:2, 1:3, and 1:4. Notably, as the core-to-wall ratios increased the MEE exhibited a significant rise ($p < 0.05$), escalating from 19.05 ± 0.66 to 93.40 ± 0.51% (Table 4.3).

At the core-to-wall ratio of 1:4, microcapsules manifested a significant MEE augmentation ($p < 0.05$) compared to M (93.40 ± 0.51%), with M:INU (93.68 ± 0.01 to

95.54 ± 1.04%) and M:OSS (95.53 ± 0.53 to 97.28 ± 0.16%). A previous study noted that M has modest emulsification capability. This shortcoming was addressed by integrating alternative wall materials (Xiao et al., 2022). Results indicated that M:OSS microcapsules exhibited superior MEE in comparison to M:INU, possibly owing to OSS's amphiphilic attributes, which enhanced emulsification (Long et al., 2022). Previous study also highlighted that succinylated starches exhibited better retention and emulsion stability (Jafari et al., 2008).

Furthermore, microcapsules produced with 8:2 mixing ratio displayed significantly higher MEE ($p < 0.05$) than the 9:1 ratio. This enhancement could be attributed to the elevated OSS content, contributing to a more robust emulsion due to OSS's thickening and film-forming properties (Yang et al., 2023). A more stable emulsion corresponded to a higher MEE. Moreover, augmenting OSS content was associated with increased film thickness, as documented elsewhere (Long et al., 2022). The additional OSS contributed to heightened viscosity in the wall materials, creating a denser coating around the core material. This robust barrier limited solvent penetration into the microcapsule core, reducing extracted oil content.

4.3.2 Moisture Content (MC)

Moisture content (MC) refers to the water constituent within a food system. Its significance lies in its influence on food stability, as it can prompt lipid oxidation and microbial spoilage. In the food industry, powder is typically recommended to maintain an MC of 3 to 4% (Song et al., 2022). Table 4.3 illustrates MC within the range of 3.15 ± 0.13 to 3.93 ± 0.79% for all microcapsules, aligning with industry specifications. Notably, the MC remained unaffected ($p > 0.05$) by the variations in wall material compositions.

4.3.3 Water Activity (A_w)

The a_w gauges the availability of free water engaged in biochemical reactions. It plays an important role in the evaluation of microcapsule quality, shelf-life stability, and retention of bioactive compounds. Microcapsules boasting an a_w range of 0.2 to 0.3 demonstrate stability against oxidation (Al Mubarak et al., 2019). As shown in Table 4.3, all TRF-based microcapsules exhibited low a_w values, spanning from 0.26 ± 0.03 to 0.32 ± 0.05. Core-to-wall material mixing ratios. Ratios did not significantly alter a_w ($p > 0.05$).

4.3.4 Flowability and Cohesiveness

Desirable microcapsule attributes include the capacity to flow freely, facilitating homogeneous bottling and decanting (Rautenberg & Lamprecht, 2022). The flowability and cohesiveness of the TRF-based microcapsules are shown in Table 4.3. Flowability, denoted by CI values, refers to the movement of particles relative to neighboring particles or along the container's wall (Kalman, 2021). Cohesiveness, determined by HR values,

arises from inter-particle forces like van der Waal force and mechanical interlocking (Geldart et al., 2009). With rising core-to-wall ratios, microcapsule flowability significantly improved ($p < 0.05$), shifting from fair to good CI values (26.14 ± 1.31 to 18.8 ± 0.00%). Concurrently, microcapsules displayed intermediate cohesiveness, with a significant decrease ($p < 0.05$) in HR values (1.36 ± 0.02 to 1.22 ± 0.00).

Flowability and cohesiveness were affected by MEE results. Elevated ratios increased, correlated with greater solid content in microcapsules, inducing thicker coating layers that limited SO leakage. Consequently, microcapsules exhibited favourable flowability, minimal agglomeration, and low cohesiveness. Contrastingly, a low core-to-wall ratio resulted in diminished bulk density, prompting agglomeration and poor flowability. Low density also indicates a higher amount of air trapped in the spaces between particles, which can promote lipid oxidation (Carneiro et al., 2013).

At a 1:4 core-to-wall ratio, microcapsules displayed significantly distinct CI and HR values ($p < 0.05$) among various wall material compositions. Remarkably, M:OSS microcapsules exhibited very good flowability (CI = 12.5 ± 0.00%), while M and M:INU microcapsules demonstrated good flowability (CI = 14.29 ± 0.00 to 18.18 ± 0.00%). Flowability hinged on particle morphology, size, and surface roughness, along with bulk density (Beakawi Al-Hashemi & Baghabra Al-Amoudi, 2018).

Microcapsules' morphology (Figure 4.1a and b) indicated M:OSS's higher sphericity, smoother surface, and lower bulk density, resulting in improved flowability. Wall material composition also influenced flowability. INU microcapsules were noted for poor flowability due to surface plasticization, arising from INU's hydrophilic nature, impeding water transfer during spray drying (Beirão-da-Costa et al., 2013). However, in this study, combining INU with M enhanced flowability. Cohesiveness remained low across microcapsules (HR = 1.14 ± 0.00 to 1.20 ± 0.00). Furthermore, mixing ratios significantly impacted ($p < 0.05$) CI and HR values for M:INU microcapsules, with higher INU content at 8:2 mixing ratio promoting poorer flowability and greater agglomeration. In contrast, M:OSS microcapsules displayed no significant ($p > 0.05$) CI and HR effects.

4.3.5 Water solubility index (WSI) and water absorption index (WAI)

The WSI and WAI of the TRF-based microcapsules are shown in Table 4.3. WSI reflects microcapsule's wettability and dispersibility in aqueous solutions. Significantly heightened WSI values ($p < 0.05$) accompanying increasing core-to-wall ratios, attributed to increased M content. M is widely favoured for spray drying due to its exceptional water solubility (Zhu et al., 2022). Conversely, WAI measured by the volume expansion of microcapsules upon immersion in excess water (Yousf et al., 2017), demonstrated that the 1:2 M microcapsule yielded significantly higher WAI ($p < 0.05$) compared to 1:3 M and 1:4 M.

In general, at the 1:4 core-to-wall ratio, wall material compositions do not significantly affect the WSI ($p > 0.05$), except for M:OSS (8:2) microcapsules (78.45 ± 0.80%) and M:INU (8:2) microcapsules (83.12 ± 3.04%). Overall, WSI values range from 74.75 ± 2.25 to 83.12 ± 3.04%, indicating sufficient water solubility of the microcapsules. At 8:2 mixing ratios, the proportion of OSS and INU is higher. OSS, a modified starch undergoing esterification of starch hydroxyl groups and octenyl succinic anhydride in a 1:1 ratio under alkaline conditions (Borrmann et al., 2013), mainly consists of amylopectin, rendering it highly soluble. Furthermore, INU, a hydrophilic carbohydrate (Beirão-da-Costa et al., 2013), contributes to increased WSI when used as wall material due to its high-solubility nature. Of all wall material compositions and mixing ratios, microcapsules of M:INU (9:1) achieve the highest WAI ($p < 0.05$). INU's high hygroscopicity, stemming from its branched structure facilitating hydrogen bonding (Akalin & Erişir, 2008), results in enhanced water retention during reconstitution, thereby leading to increased WAI.

4.3.6 Colour

Colour assessment for TRF-based microcapsules is detailed in Table 4.3. The L* value, on the CIE scale, signifies microcapsule brightness, ranging from 0 (black) to 100 (white). The a* and b* values indicate greenness (-a*) and redness (+a*), as well as blueness (-b*) and yellowness (+b*), respectively. No significant differences ($p > 0.05$) were observed in L* (ranging from 77.28 ± 2.23 to 79.82 ± 0.77), a* (ranging from 8.67 ± 0.92 to 10.30 ± 1.35), and b* values (ranging from 69.98 ± 1.18 to 72.10 ± 0.07) among microcapsules produced at various core-to-wall ratios, wall material compositions, and mixing ratios. Positive a* and b* values indicated red and yellow hues in all microcapsules. A study also reported that carrier type insignificantly impacts spray-dried powder colour (Bednarska & Janiszewska-Turak, 2020).

Table 4.3: Characterization of treated pea protein isolate-flaxseed gum complex stabilized TRF-based microcapsules produced by spray-drying core-to-wall ratios, wall material compositions and mixing ratios.

Formulation	MEE (%)	MC (%)	A_w	WSI (%)	WAI	Flowability	CI (%)	Cohesiveness	HR	Colour		
										L*	a*	b*
1:2 M	19.05 ± 0.66^{E}	3.15 ± 0.13^{A}	0.32 ± 0.05^{A}	69.81 ± 1.83^{D}	0.76 ± 0.06^{A}	Fair	26.14 ± 1.31^{A}	Intermediate	1.36 ± 0.02^{A}	79.25 ± 0.77^{A}	9.27 ± 0.78^{A}	69.99 ± 1.91^{A}
1:3 M	74.38 ± 0.76^{D}	3.20 ± 0.08^{A}	0.29 ± 0.01^{A}	72.77 ± 1.32^{CD}	0.50 ± 0.04^{B}	Fair	22.22 ± 0.00^{B}	Intermediate	1.29 ± 0.00^{B}	79.82 ± 0.05^{A}	9.69 ± 0.33^{A}	72.10 ± 0.07^{A}
1:4 M	93.40 ± 0.51^{C}	3.23 ± 0.32^{A}	0.26 ± 0.05^{A}	74.75 ± 2.25^{BC}	0.47 ± 0.02^{B}	Good	18.18 ± 0.00^{C}	Intermediate	1.22 ± 0.00^{C}	79.62 ± 1.04^{A}	8.67 ± 0.92^{A}	69.98 ± 1.18^{A}
1:4 M:OSS (9:1)	95.53 ± 0.53^{B}	3.93 ± 0.79^{A}	0.27 ± 0.00^{A}	76.91 ± 1.83^{BC}	0.50 ± 0.05^{B}	Very good	12.50 ± 0.00^{F}	Low	1.14 ± 0.00^{E}	78.14 ± 0.21^{A}	9.49 ± 0.87^{A}	70.48 ± 1.56^{A}
1:4 M:OSS (8:2)	97.28 ± 0.16^{A}	3.78 ± 0.33^{A}	0.27 ± 0.04^{A}	78.45 ± 0.80^{B}	0.48 ± 0.02^{B}	Very good	12.50 ± 0.00^{F}	Low	1.14 ± 0.00^{E}	78.17 ± 0.97^{A}	10.30 ± 1.35^{A}	71.05 ± 2.58^{A}
1:4 M:INU (9:1)	93.68 ± 0.01^{C}	3.28 ± 0.22^{A}	0.28 ± 003^{A}	76.53 ± 1.85^{BC}	0.67 ± 0.06^{A}	Good	14.29 ± 0.00^{E}	Low	1.20 ± 0.00^{C}	79.76 ± 0.96^{A}	9. 37 ± 0.60^{A}	70.54 ± 0.88^{A}
1:4 M:INU (8:2)	95.54 ± 1.04^{B}	3.11 ± 0.01^{A}	0.26 ± 0.03^{A}	83.12 ± 3.04^{A}	0.53 ± 0.03^{B}	Good	16.67 ± 0.00^{D}	Low	1.17 ± 0.02^{D}	77.28 ± 2.23^{A}	9.70 ± 0.00^{A}	70.64 ± 0.20^{A}

Values are expressed as mean ± standard deviation (n = 6). Mean values with different superscript letters within the same column are significantly different ($p < 0.05$). Abbreviations: TRF: Tocotrienol-rich fraction; M: Maltodextrin; OSS: Starch sodium octenyl succinate; INU: Inulin; MEE: Microencapsulation efficiency; MC: Moisture content; Aw: Water activity; WSI: Water solubility index; WAI: Water absorption index; CI: Carr Index; HR: Hausner ratio.

4.3.7 Tocopherol and Tocotrienol Content Retention

Comparative analysis of tocopherol and tocotrienol content in TRF-based microcapsules and TRF oil is illustrated in Table 4.4. Retention percentages ranged from 79.77 ± 0.32 to 99.72 ± 0.26%. No significant differences ($p > 0.05$) were found to be observed among the four tocopherol and four tocotrienol isomers (α-, β-, γ-, and δ-). Enhanced core-to-wall ratios yielded higher retention percentages ($p < 0.05$). Elevated wall material density, facilitated by solid content, promoted efficient core material encapsulation, reducing diffusion and migration to the wall and resulting in superior embedding (Yu et al., 2022). Consequently, higher core-to-wall ratio, correlated with augmented MEE (93.40 ± 0.51%) and tocopherol/tocotrienols retention (84.01 ± 0.36 to 87.70 ± 0.84%).

Overall, the percentage of tocopherol and tocotrienol retention significantly increased ($p < 0.05$) in the following order: microcapsules of M > M:INU > M:OSS. The combination of M and INU contributed to higher retention percentages compared to M alone. A previous study suggested that INU has the ability to entrap δ-tocotrienol within the encapsulating matrix (Silva et al., 2016), providing protection against degradation during spray drying. Moreover, the M:OSS microcapsules exhibited the highest retention percentages, indicating that M:OSS formed the most effective barrier to safeguard the core material. These results align with the MEE outcomes mentioned earlier. Additionally, the morphology of M:OSS microcapsules displayed a smooth and spherical external structure, signifying extensive coverage of the core by the wall materials. This coverage is crucial for ensuring core material protection and retention (Carneiro et al., 2013).

Another study elucidated that a higher M portion could lead to incomplete emulsification of components in the emulsion, resulting in an unstable emulsion and less dense film formation on the microcapsule surface (Yu et al., 2022). This situation permits the infiltration of oxygen and moisture into the core materials, accelerating lipid oxidation and causing lower retention of bioactive compounds. In contrast, a lower M portion (mixing ratio of 8:2) yielded significantly higher ($p < 0.05$) percentages of tocopherol and tocotrienol retention. Furthermore, microcapsules at the 8:2 mixing ratio exhibited denser external structures, as evident in Figure 4.1b. This denser structure hinders the ingress of oxygen and moisture, effectively delaying the degradation of tocopherol and tocotrienol during high-temperature spray drying.

Table 4.4: Tocopherol and tocotrienol content analysis of TRF-based microcapsules produced by spray-drying using different core-to-wall ratios, wall material compositions, and mixing ratios.

Formulations	Percentage of retention (%)				
	α-tocopherol	α-tocotrienol	β-tocotrienol	γ-tocotrienol	δ-tocotrienol
1:2 M	80.56 ± 0.46^{aD}	79.77 ± 0.32^{aD}	84.05 ± 0.25^{aC}	81.44 ± 0.66^{aC}	80.94 ± 0.33^{aC}
1:3 M	82.08 ± 3.89^{aCD}	81.90 ± 0.29^{aCD}	82.80 ± 4.75^{aC}	82.73 ± 4.61^{aC}	80.63 ± 5.54^{aC}
1:4 M	84.01 ± 0.36^{aBCD}	84.55 ± 0.50^{aBCD}	87.70 ± 0.84^{aBC}	84.15 ± 0.70^{aBC}	83.47 ± 1.28^{aBC}
1:4 M:OSS (9:1)	94.59 ± 6.32^{aAB}	94.72 ± 7.34^{aAB}	94.93 ± 3.29^{aAB}	94.68 ± 4.87^{aA}	94.61 ± 4.85^{aAB}
1:4 M:OSS (8:2)	97.69 ± 1.93^{aA}	99.72 ± 0.26^{aA}	98.07 ± 1.16^{aA}	98.10 ± 0.03^{aA}	98.28 ± 0.34^{aA}
1:4 M:INU (9:1)	92.60 ± 0.18^{aABC}	92.12 ± 1.39^{aABC}	97.01 ± 0.09^{aA}	93.46 ± 0.42^{aAB}	92.82 ± 0.20^{aAB}
1:4 M:INU (8:2)	95.40 ± 0.28^{aAB}	94.77 ± 0.12^{aAB}	98.85 ± 0.71^{aA}	96.83 ± 0.06^{aA}	97.47 ± 1.50^{aA}

Values are expressed as mean ± standard deviation (n = 6). Mean values with different uppercase superscript capital letters within the same column are significantly different ($p < 0.05$). Mean values with different lowercase superscript letters between columns are significantly different ($p < 0.05$)
Abbreviations: TRF: Tocotrienol-rich fraction; M: Maltodextrin; OSS: Starch sodium octenyl succinate; INU: Inulin.

4.3.8 Scanning Electron Microscopy (SEM)

The external structure of the TRF-based microcapsules produced using the same core-to-wall ratios of 1:4 was observed under SEM at × 1000 magnification (Figure 4.1). Overall, microcapsules comprised of varying wall material compositions and mixing ratios displayed similar rounded shapes, albeit with slightly distinct external morphologies. The composition of the feed material stands as one of the important factors influencing microcapsule morphology (Seid Mahdi Jafari et al., 2021).

Among the various wall material compositions, the microcapsules of M:OSS (Figures 4.1a and b) exhibited the highest sphericity with a smooth surface, although some areas displayed minor roughness. The acquisition of the lowest CI value and excellent flowability underscored the presence of smooth spherical particles of the M:OSS microcapsules. Such a smooth microcapsule surface is particularly desirable in food applications, as it contributes to optimal flow properties. Furthermore, the smooth and spherical structure indicates substantial coverage of the core by the wall materials, a critical factor ensuring the protection and retention of core materials (Carneiro et al., 2013). Notably, no crack was found on the surface of these M:OSS microcapsules, affirming their higher MEE compared to other wall materials, as previously mentioned. An ideal wall material is required to have the ability to hold and seal the core materials within the microcapsule when it is stored and processed. This can be determined by the degree of integrity and porosity of the microcapsules (Murúa-Pagola et al., 2009). When comparing mixing ratios, the M:OSS (8:2) microcapsule exhibited greater compactness and reduced porous than the M:OSS (9:1) microcapsule. This outcome can be attributed to a higher proportion of OSS, which possesses rapid film-forming properties (Łupina et al., 2022). During spray drying, a film rapidly forms around the droplet surface, preventing deflation and shrinkage of the microcapsules, thereby resulting in smooth surfaces with minimal superficial imperfections (Seid Mahdi Jafari et al., 2008).

Conversely, microcapsules of M:INU (Figures 4.1c and d) displayed an uneven and slightly rough external surface with some visible cracks. The formation of uneven and rough surfaces is undesirable, contributing to higher CI values and reduced flowability. The presence of cracks on the microcapsule's external surface has resulted to lower MEE. These cracks facilitate the increased penetration of the extraction solvent into the microcapsules, leading to greater oil extraction and subsequently lower MEE (Teo et al., 2021). In cases of higher mixing ratios, the M:INU (8:2) microcapsule exhibited a more compact, spherical and smoother external surface. The use of a higher proportion of INU led to an enhanced microstructure. Similarly, microcapsule M (Figure 4.1e) exhibited an uneven and rough external surface, accompanied by some cracks. Therefore, as evident from the results, M microcapsules exhibited the lowest MEE, highest CI value and poorest flowability when compared to M:INU and M:OSS at the same core-to-wall ratios (1:4).

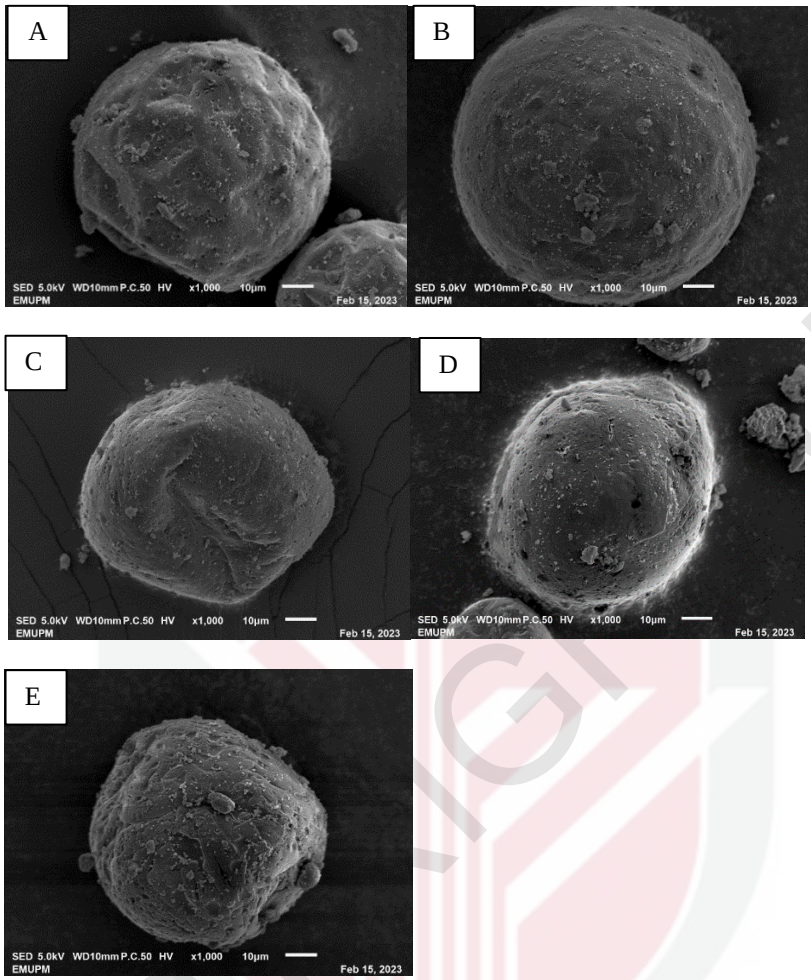

Figure 4.1: SEM micrographs of TRF-based microcapsules prepared at 1:4 core-to-wall ratio with different wall material compositions and mixing ratios (a) M:OSS (9:1); (b) M:OSS (8:2); (c) M:INU (9:1); (d) M:INU (8:2) and (e) M. Scale bar represent 10 µm.

4.4 Conclusions

The present study has unveiled the effects of core-to-wall ratios, wall material compositions, and mixing ratios on the physical properties and stability of tocopherol and tocotrienol in TRF-based microcapsules. Initially, microcapsules were synthesized using M across various core-to-wall ratios (1:2, 1:3, 1:4). Among these ratios, microcapsules produced with a core-to-wall ratio of 1:4 exhibited superior characteristics, including higher MEE (93.40 ± 0.51%), enhanced WSI (74.75 ± 2.25%), increased retention of tocopherol and tocotrienol (83.01 ± 1.28 to 87.70 ± 0.84%), good flowability (CI = 18.18 ± 0.00%), and intermediate cohesiveness (HR = 1.22 ± 0.00).

Consequently, the investigation focused on the effect of wall material compositions and mixing ratios, employing the core-to-wall ratio of 1:4.

Based on the results, it became evident that microcapsules consisting of M:OSS, with a mixing ratio of 8:2, showcased the highest MEE (97.28 ± 0.16%), excellent flowability (CI = 12.50 ± 0.00%), and low cohesiveness (HR = 1.14 ± 0.00). Furthermore, M:OSS (8:2) microcapsules demonstrated the highest retention levels for α-tocopherol (97.69 ± 1.93%), α-tocotrienol (99.72 ± 0.26%), β-tocotrienol (98.07 ± 1.16%), γ-tocotrienol (98.10 ± 0.03%), and δ-tocotrienol (98.28 ± 0.34%). Notably, these microcapsules exhibited optimal sphericity, a smooth and dense external surface, and an absence of cracks. These findings underscore the potential encapsulating capacity of the combined M and OSS wall material, particularly in a mixing ratio of 8:2, in bolstering the viability and stability of applications involving bioactive compounds, particularly within microcapsule formulations.

CHAPTER 5

DETERMINATION OF THE STORAGE STABILITY, RELEASE CHARACTERISTICS, AND BIOACCESSIBILITY OF THE TOCOTRIENOL-RICH FRACTION ENCAPSULATED IN MALTODEXTRIN-STARCH SODIUM OCTENYL SUCCINATE MICROCAPSULES

5.1 Introduction

Tocotrienols have gained widespread attention in recent years due to their exceptional antioxidant properties and bioactivity. Palm oil, known as a tocotrienol-rich fraction (TRF), is abundant in these compounds. Extensive research has been conducted on the health benefits of tocotrienols, particularly their anticancer, anti-inflammatory, and neuroprotective properties (Sun et al., 2022; Wong et al., 2017). Given these health advantages, there has been a growing interest in incorporating tocotrienols into food products (Tan et al., 2018). However, the hydrophobic nature of tocotrienols poses challenges as they exhibit low aqueous solubility and limited intestinal permeability when ingested orally. Additionally, during storage, polyunsaturated tocotrienol is prone to degradation due to lipid oxidation triggered by environmental stressors such as oxygen, heat, or light (Goh et al., 2015).

Microencapsulation has emerged as a promising approach to improve the delivery and stability of tocotrienol. This process involves enclosing an active ingredient within micro-sized carrier matrices to shield the core material from the external environment (Gibbs et al., 1999). The resulting microencapsulated active compound is transformed into a powder through spray drying, further enhancing its stability during storage. Spray drying is a highly effective and widely employed method for producing microparticulate powders used in active compound delivery systems. Research has shown that the oral bioavailability of hydrophobic active compounds can be significantly improved through the process of spray drying (Hu et al., 2018).

The selection of appropriate wall materials is critical for the production of spray-dried microcapsules to safeguard tocotrienols from adverse external environmental conditions. These wall materials must possess the capability to create a protective shell around the microcapsule, serving as a physical barrier against light, oxygen, and water. In this study, the wall material for the TRF-based microcapsule consisted of a blend of M and OSS. M is a polysaccharide composed of $_D$-glucose monomers linked by α (1,4) and α (1,6)-glycosidic bonds. It is characterized by a slight sweetness, odourlessness, colourlessness, high water solubility, and low viscosity at high solid content. Furthermore, M is stable under thermal and acidic conditions. However, it is worth noting that M has limited emulsifying ability (Saavedra-Leos et al., 2022), necessitating its combination with OSS to create a more robust wall material. OSS, on the other hand, is a modified food starch resulting from the esterification of octenyl succinic anhydride (Long et al., 2022). OSS exhibits both hydrophilic and hydrophobic properties and is commonly applied as an emulsifier, thickener, and wall material in the microencapsulation of bioactive compounds (Liu et al., 2018).

Over time, tocotrienols undergo lipid oxidation, which is influenced by factors such as elevated MC, a_w, storage temperature, and exposure to light and oxygen (de Camargo et al., 2019). Consequently, it is imperative to investigate the storage stability of microencapsulated tocotrienols. Moreover, preserving the bioactivity of tocotrienols as they traverse the gastrointestinal tract, from consumption to metabolism, is crucial (Altin et al., 2018). This ensures that a substantial amount of tocotrienol remains accessible for absorption following digestion. This can be assessed by measuring the bioaccessibility and release of tocotrienols after undergoing *in vitro* digestion. Bioaccessibility refers to the portion of ingested nutraceuticals that is available for absorption through the intestinal epithelial membrane (Jafari & McClements, 2017). Consequently, the study examined the bioaccessibility of encapsulated tocotrienols to discern their impact on adsorption and metabolization.

In summary, the study aimed to investigate the impact of storage on the physical and oxidative stability of microencapsulated TRF using the M:OSS wall material. The release characteristics of the TRF-based microcapsule were assessed under different ionic strengths and pH conditions. Additionally, bioaccessibility and release of TRF from the bulk oil and microcapsule following *in vitro* digestion were determined.

5.2 Materials and Methods

5.2.1 Materials

Palm TRF was generously provided by ExcelVite Sdn. Bhd (Chermo, Malaysia). It comprised 38.5 to 42.0% of total tocotrienols, 9.5 to 14.0% of tocopherol, 30.0 to 45.0% of palm olein (monoglyceride, diglyceride and triglyceride), 1.0 to 3.0% of plant squalene, 0.03 to 0.07% of mixed carotene complex predominantly β-carotene, and 2.0 to 4.0% of sterol complex predominantly β-sitosterol. The active ingredients predominantly of d-α-tocopherol (9.5 to 14.0%), d-γ-tocotrienol (17.5 to 23.0 %), d-α-tocotrienol (12.0 to 16.0%), d-δ-tocotrienol (4.0 to 7.0%), and d-β-tocotrienol (minimum of 1.9%). The PPI and FG were sourced from Emsland Group Sdn. Bhd (Wietzendorf, Germany) and Qingdao Dehui Halobios Science and Technology Co., Ltd (Qingdao, China), respectively. The wall materials, M, and OSS were purchased from Ingredion Incorporated (Westchester, United States). The HPLC-grade standards of tocotrienol (d-α-, β-, γ- and δ-) and tocopherol (d-α-, β-, γ- and δ-) mixture were purchased from ChromaDex (Los Angeles, United States). HPLC-grade n-hexane and 1,4-dioxane were purchased from Fisher Scientific (Pittsburgh, United States). For the in vitro digestion model, α-amylase (20000 units/mL) was obtained from Sigma-Aldrich (St Louis, United States), pepsin (3000 - 3500 units/g), and pancreatin (> 4000 units/g) from Beijing Solarbio Science & Technology Co., Ltd. (Beijing, China), and bile salt from R & M Chemicals (Semeyih, Malaysia). All reagents and solvents used were of analytical grade, and deionized water was employed for all sample preparation and analyses.

5.2.2 Preparation of TPPI-FG Complex

Based on the previous chapter, TPPI-FG at a ratio of 3:1 has obtained excellent emulsification properties. Thus, the emulsifier of the TPPI-FG (3:1) complex was prepared as described in Section 4.2.2.

5.2.3 Preparation of TRF-based Microcapsule

According to previous findings, the wall material of M:OSS (8:2) has exhibited the highest encapsulation efficiency. Therefore, it will be further studied in this chapter. The TRF-based microcapsule was prepared using the method described in Section 4.2.3.

5.2.4 Spray Drying

Refer to Section 4.2.4.

5.2.5 Storage Stability

The TRF-based microcapsule was vacuum-packed and stored in a 40 °C incubator for 13 weeks. The storage stability of the microcapsule was assessed by measuring MEE, MC, a_w, flowability and cohesiveness, colour, reconstitution properties, PV, as well as tocopherol and tocotrienol content analysis. Analysis was conducted in weeks 0, 1, 2, 3,4 and 13. Three measurements were performed on each sample as replicates.

5.2.5.1 Microencapsulation Efficiency (MEE)

Refer to Section 4.2.4.1.

5.2.5.2 Moisture Content (MC)

Refer to Section 4.2.4.2.

5.2.5.3 Water Activity (A_w)

Refer to Section 4.2.4.3.

5.2.5.4 Flowability and Cohesiveness

Refer to Section 4.2.4.4.

5.2.5.5 Colour

The colour of the TRF-based microcapsule was measured as described in Section 4.2.4.6. Three measurements were performed on each sample as replicates. The total colour difference (ΔE) was calculated using the following formula:

$$\Delta E = \sqrt{(L_o^* - L_t^*)^2 + (a_o^* - a_t^*)^2 + (b_o^* - b_t^*)^2} \quad \text{(Eq.5.1)}$$

Chroma (C) was determined as the following equation:

$$C = \sqrt{a^{*2} + b^{*2}} \quad \text{(Eq.5.2)}$$

Where L* is the brightness, ranging from white to black (100 to 0), a* is the green (-a*) and red (+a*), and b* is the blue (-b*) and yellow (+b*) colour.

5.2.5.6 Reconstitution Properties

The TRF-based microcapsules were reconstituted with deionized water, and their reconstitution properties were evaluated (Chang et al., 2018). A 0.5 g of microcapsules were dissolved in 150 mL of deionized water at room temperature (25 °C) under continuous stirring at 400 rpm for 30 mins. The refractive index of TRF was 1.45. The mean droplet size and span index of the reconstituted dispersions were measured at 25 °C using a Mastersizer MS 2000 (Malvern, Worcestershire, UK). Three measurements were performed on each sample as replicates.

5.2.5.7 Peroxide Value (PV)

The extraction of oil for PV was performed following the method adapted from Chang et al. (2018). 0.5 g of the microcapsule was suspended with 2.5 mL of deionized water and stirred at 300 rpm for 30 min to ensure dissolution. Then, 300 µL of the suspension was added to 1.5 mL of an iso-octane/isopropanol (2:1) mixture and vortexed for 10 s, repeated three times to extract the oil. The resultant solution was centrifuged at 1000 *g* for 4 min. The extraction was repeated three times. The PV of extracted oil was measured spectrophotometrically based on IDF standard 74A:1991. The resultant solution (400 μL) was combined with 9.6 mL of chloroform/methanol (7:3) mixture. To induce colour

formation, 50 μL of iron (II) chloride solution was added and vortexed for 5 seconds. Subsequently, 50 μL of ammonium thiocyanate solution was added and vortexed for another 5 seconds. The resultant solution was allowed to react for 5 min in the dark, and then the absorbance was measured using a UV-VIS spectrophotometer (Agilent Technologies, CARY 60 UV-VIS, California, USA) at 500 nm in triplicates in subdued light within 10 min. Three measurements were performed on each sample as replicates. PV was calculated using the Fe (III) calibration curve with the following equation:

$$\text{PV (mEq /kg oil)} = \frac{(Abs_{sample} - Abs_{blank})}{(\text{S} \times 55.84 \times 2 \times \text{W})} \quad \text{(Eq.5.3)}$$

Where Abs is the absorbance of the solution, S is the slope of the Fe (III) standard curve, 55.84 is the atomic weight of Fe (III), 2 is the unit conversion factor, and W is the sample weight.

5.2.5.8 Tocopherol and Tocotrienol Content Analysis

The extraction and HPLC analysis methods were carried out as described in Section 4.2.4.7. The degradation of tocopherol and tocotrienol during storage (3 months) was calculated as follows:

$$\text{Degradation (\%)} = \frac{(T_0 - T_n)}{T_0} \times 100 \quad \text{(Eq.5.4)}$$

Where T_0 is the tocopherol and tocotrienol content in the microcapsule in week 0, T_n is the tocopherol and tocotrienol content in the microcapsule in subsequent weeks.

5.2.6 Release Characteristics

5.2.6.1 Effect of Ionic Strength

To examine the release behaviour of TRF in response to changes in ionic strength, a method was adapted from Chang et al. (2018). TRF-based microcapsules weighing 0.5 grams were dispersed in 5 mL of NaCl solution at various concentrations (0, 50, 100, 150, and 200 mM). The mixture was stirred for 1 hr. Subsequently, 40 mL of hexane was added followed by gentle hand-shaking for 2 min to extract the released TRF from the emulsion. The mixture was then centrifuged at 10000 rpm for 10 min. The hexane layer containing TRF was collected in a round-bottom flask and evaporated using a rotary evaporator in a 60 °C water bath. The flask, now containing the released oil, was further dried in a 105 °C hot air oven for 1 h. Three measurements were performed on each sample as replicates. TRF release was calculated using the formula:

TRF release (%) = $\frac{(W_f - W_i)}{W_p} \times 100$ (Eq.5.5)

Where W_f is the mass of round bottom flask containing TRF (g), W_i is the mass of empty round bottom flask (g), and W_p is the mass of powder (g).

5.2.6.2 Effect of pH

The release behavior of TRF as a function of pH was determined using a method adapted from Chang et al. (2018). In this procedure, 0.5 g of TRF-based microcapsules were dispersed into 5 mL of deionized water at different pH conditions (3, 5, 7, and 9) and stirred for 1 h. Afterward, approximately 40 mL of hexane was added, and gentle hand-shaking for 2 min was performed to extract the released TRF from the emulsion. The mixture was then centrifuged at 10,000 rpm for 10 min. The hexane layer containing TRF was collected in a round-bottom flask and evaporated using a rotary evaporator in a 60 °C water bath. The flask, now containing the released TRF, was further dried in a 105 °C hot air oven for 1 hr. Three measurements were performed on each sample as replicates. TRF release was calculated using the same formula as mentioned above.

5.2.7 *In Vitro* Digestion

The INFOGEST *in vitro* digestion model by Brodkorb et al. (2019) was employed in this study. Enzyme concentrations were determined to mimic the conditions of the mouth, stomach, and small intestine, simulated saliva fluids (SSF), simulated gastric fluids (SGF), and simulated intestinal fluids (SIF) according to the INFOGEST method. To achieve this, 0.5 grams of TRF-based microcapsules were reconstituted with 50 mL of deionized water at room temperature, with continuous stirring at 500 rpm for 30 min.

For the mouth phase, reconstituted microcapsules (5 g) were mixed with 4 mL of SSF (pH 7), 0.5 mL of amylase, 25 µL of 0.3 M calcium chloride, and topped up to 5 mL with deionized water. The mixture was then incubated at 37 °C for 2 min.

For the stomach phase, the sample from the mouth phase (10 mL) was added with 8.6 mL of SGF and adjusted to pH 3 using a hydrochloric acid solution. Subsequently, 1 mL of pepsin solution and 0.4 mL of deionized water were added to reach a total volume of 20 mL. The pepsin solution was stored in an ice box before use. The mixture was placed in a shaking incubator at 37 °C for 2 hr at 100 rpm.

For the small intestine phase, the sample from the stomach phase (20 mL) was combined with 8 mL of SIF and adjusted to pH 7 using NaOH solution. Approximately 3 mL of bile salt solution (10 mM), 40 µL of calcium chloride solution (0.3 M), 5 mL of pancreatin/lipase solution (2000 U/mL), and 4 mL of deionized water were added to

reach a total volume of 40 mL. SIF was used to dissolve enzymes and bile salts before being added.

5.2.7.1 Bio-Accessibility and Percentage of Release

Tocotrienol bioaccessibility and the percentage of release were determined using a method adapted from Tan et al. (2018). After 2 h of digestion, digesta was collected from the small intestine phase solution. The digesta (15 mL) underwent centrifugation at 18,000 rpm, 4 °C for 50 min to obtain the micelle phase (middle clear phase). Subsequently, tocotrienol in 0.5 mL of digesta or micelle phase was extracted using 1.2 mL of organic solvent (hexane/isopropanol: v/v = 2/3). The resultant solution was centrifuged at 6,000 rpm for 2 min, and the upper clear layer was collected and analyzed using a UV-VIS Spectrophotometer (Agilent Technologies, CARY 60 UV-VIS, California, USA) at 450 nm. Three measurements were performed on each sample as replicates.

$$Release\ (\%) = \frac{(C_{micelle} + C_{sediment})}{C_{digesta}} \times 100 \quad \text{(Eq.5.11)}$$

$$Bioaccessbility\ (\%) = \frac{C_{micelle}}{C_{initial}} \times 100 \quad \text{(Eq.5.12)}$$

Where $C_{micelle}$ is tocotrienol concentration in micelle phase, $C_{sediment}$ is tocotrienol concentration in the sediment phase, $C_{digesta}$ is tocotrienol concentration in digesta phase, $C_{initial}$ is tocotrienol concentration in the initial phase.

5.2.8 Statistical Analysis

All analyses were conducted in triplicates on duplicate samples. The results underwent statistical analysis using Minitab statistical software version 17.0 (Minitab Inc., PA, USA). The one-way ANOVA with post-hoc Tukey's test was employed to identify significant differences among mean values ($p < 0.05$).

5.3 Results and Discussion

5.3.1 Storage Stability

The TRF-based microcapsule was stored at 40 °C for 13 weeks. To assess its stability, various physical and oxidative parameters were examined, including MEE, MC, a_w, flowability and cohesiveness, colour, and reconstitute properties whereas the oxidative stability was determined by the PV, tocopherol and tocotrienol content analysis.

5.3.1.1 Microencapsulation Efficiency (MEE)

Table 5.1 presents the MEE values of TRF-based microcapsules, ranging from 91.49 ± 0.81 to 94.63 ± 2.56%. These high MEE values suggest successful TRF encapsulation with minimal SO on the particles, indicating effective core material retention. Importantly, MEE values remained stable ($p > 0.05$), decreasing insignificantly by 3.32% over the storage period. This stability can be attributed to the protective layer formed by the TPPI-FG (3:1) complex during emulsification and the barrier provided by the M:OSS (8:2) wall material against the extraction solvent during MEE analysis.

5.3.1.2 Moisture Content (MC)

Moisture content (MC) measures the total amount of water present within particles and serves as an indicator of food powder stability (Priol et al., 2019). The MC of the TRF-based microcapsule significantly increased ($p < 0.05$) by 36.13% during storage (Table 5.1). The MC ranged from 3.93 ± 0.19 to 5.35 ± 0.19%, slightly surpassing the targeted MC for food powder (3 to 4%) (Song et al., 2022). The increase may be due to moisture absorption from the surrounding environment, potentially affecting TRF's oxidative stability. However, this concern can be addressed by incorporating moisture absorbers, such as silica gel, in sachet form.

5.3.1.3 Water Activity (A_w)

The a_w measures free or non-chemically bonded water in microcapsules. Over the storage period, aw increased ($p < 0.05$) from 0.32 ± 0.02 to 0.46 ± 0.00, representing a 43.75% increase (Table 5.1). These results showed a positive correlation with MC, as the microcapsule absorbed moisture from its environment during storage. While elevated a_w can favour microbial growth and contribute to degradation through enzymatic and non-enzymatic reactions, it's worth noting that the overall a_w of the microcapsule remained below 0.6, a level considered microbiologically stable (Quek et al., 2007).

5.3.1.4 Flowability and Cohesiveness

Table 5.1 provides data on the flowability and cohesiveness of the TRF-based microcapsule over the 13-week storage period at 40 °C. Flowability, denoted by the CI, characterizes particle movement relative to neighbouring particles or container walls (Kalman, 2021). At the end of the storage period, CI exhibited a significant increase ($p < 0.05$) of 40.58%, indicating reduced flowability. This decrease in flowability is correlated with the rise in MC, as the thicker liquid layer on particle surfaces increased the strength of liquid bridges between particles (Kalman, 2021). Meanwhile, cohesiveness, indicated by the HR, also exhibited a significant increase ($p < 0.05$) from 1.12 ± 0.00 to 1.18 ± 0.00 at week 13. Despite this increase, the microcapsule still maintained low cohesiveness, signifying minimal attractive forces between adjacent particles or molecules of the same matrix. This property is desirable, as it can help

mitigate issues related to caking and agglomeration during storage (Leyva-Porras et al., 2014).

5.3.1.5 Colour

Table 5.1 shows the colour changes (L*, a*, b*, ΔE, and C) of TRF-based microcapsules throughout the storage period. It was observed that the L* value of the microcapsule increased slightly ($p < 0.05$) by 4.04%, indicating a lightening of colour during storage. Notably, at week 13, both the positive a* value (indicating redness) and the positive b* value (indicating yellowness) decreased significantly ($p < 0.05$) by 48.58% and 19.62%, respectively, along with the C value, which decreased by 18.6%. A similar trend was reported in another study on the microencapsulation of red palm oil by spray drying, where L* values increased, while a*, b*, and C values decreased with increased storage time and temperature (Lee et al., 2020). The final ΔE value for the microcapsule was recorded as 13.63 ± 0.23, signifying a significant colour change, as it exceeded the threshold of 6 (Wibowo et al., 2015). This slight degradation in colour could be related to TRF degradation triggered by the MC and storage temperature.

5.3.1.6 Reconstitution Properties

Reconstitution properties were evaluated by measuring the particle size and span value of the dispersed microcapsule. Particle size is an important parameter as it affects water solubility, hygroscopicity, and wettability (Lacerda et al., 2016). Throughout storage, the particle size of the microcapsule increased significantly ($p < 0.05$) by 25.9% rising from 3.32 ± 0.27 to 4.18 ± 0.10 µm (Table 5.1). Simultaneously, the span value of the microcapsule exhibited a rising trend, increasing significantly ($p < 0.05$) by 48.68% from 1.89 ± 0.18 to 2.81 ± 0.09. These increases in particle size and span value were attributed to MC, which caused slight agglomeration between microcapsules during storage. Another study explained that the droplets experienced mechanical damage during spray drying, which caused agglomeration in emulsion, thus the small droplets merged to form large droplets (Guo et al., 2023).

Table 5.1: Physical stability of TRF-based microcapsule produced by wall material of M:OSS (8:2) stored at 40 °C for 13 weeks.

Weeks	MEE (%)	MC (%)	A_w	Colour					Flowability	CI (%)	Cohesiveness	HR	PS (μm)	Span
				L*	a*	b*	ΔE	Chroma						
0	94.63 ± 2.56^{A}	3.93 ± 0.19^{C}	0.32 ± 0.02^{B}	78.78 ± 0.07^{C}	8.44 ± 0.07^{B}	70.43 ± 0.16^{A}	0.00 ± 0.00^{E}	69.72 ± 0.69^{B}	Very good	10.00 ± 0.00^{B}	Low	1.11 ± 0.00^{B}	3.32 ± 0.27^{C}	1.89 ± 0.18^{D}
1	93.65 ± 2.32^{A}	4.70 ± 0.18^{B}	0.34 ± 0.02^{B}	78.73 ± 0.11^{C}	8.83 ± 0.24^{A}	69.21 ± 0.70^{B}	1.29 ± 0.20^{D}	70.98 ± 0.18^{A}	Very good	10.00 ± 0.00^{B}	Low	1.11 ± 0.00^{B}	3.78 ± 0.14^{BC}	1.95 ± 0.03^{CD}
2	94.85 ± 3.05^{A}	5.15 ± 0.10^{A}	0.43 ± 0.01^{A}	79.83 ± 0.44^{B}	7.92 ± 0.07^{C}	68.84 ± 0.70^{BC}	1.42 ± 0.13^{D}	69.29 ± 0.70^{BC}	Very good	9.28 ± 2.49^{B}	Low	1.10 ± 0.03^{B}	4.03 ± 0.05^{AB}	1.96 ± 0.11^{CD}
3	92.86 ± 2.63^{A}	5.23 ± 0.22^{A}	0.45 ± 0.03^{A}	80.20 ± 0.36^{B}	7.41 ± 0.07^{D}	67.99 ± 0.13^{C}	2.16 ± 0.20^{C}	68.39 ± 0.12^{C}	Very good	10.42 ± 1.39^{B}	Low	1.12 ± 0.02^{B}	4.03 ± 0.12^{AB}	2.22 ± 0.01^{BC}
4	92.28 ± 2.07^{A}	5.13 ± 0.10^{A}	0.46 ± 0.02^{A}	80.19 ± 0.11^{B}	7.04 ± 0.06^{E}	66.43 ± 0.07^{D}	3.42 ± 0.02^{B}	66.80 ± 0.07^{D}	Very good	10.67 ± 0.29^{B}	Low	1.12 ± 0.00^{B}	4.43 ± 0.53^{A}	2.23 ± 0.14^{B}
13	91.49 ± 0.81^{A}	5.35 ± 0.19^{A}	0.46 ± 0.00^{A}	81.96 ± 0.44^{A}	4.34 ± 0.61^{F}	56.61 ± 0.15^{E}	13.63 ± 0.23^{A}	56.78 ± 0.15^{E}	good	15.00 ± 0.00^{A}	Low	1.18 ± 0.00^{A}	4.18 ± 0.10^{AB}	2.81 ± 0.09^{A}

Values are expressed as mean ± standard deviation (n = 6). Mean values with different superscript letters within the same column are significantly different ($p < 0.05$). Abbreviations: TRF: Tocotrienol-rich fraction; M: Maltodextrin; OSS: Starch sodium octenyl succinate; MEE: Microencapsulation efficiency; MC: Moisture content; A_w: Water activity; L*: Lightness; a*: (+) red/(−) green; b*: (+) yellow/(−) blue; ΔE: Total colour difference; CI: Carr index; HR: Hausner ratio; PS: Particle size.

5.3.1.7 Peroxide Value (PV)

PV serves as an indicator of TRF's oxidative stability, measuring the formation of hydroperoxide during the early stages of lipid oxidation, a process initiated by the breakdown of unsaturated carbon-carbon double bonds (Pratt et al., 2011). PV measurements were taken for the TRF-based microcapsule during different storage weeks at 40 °C (Table 5.2). The results revealed a slight increase ($p < 0.05$) in PV from 1.05 ± 0.06 to 5.40 ± 0.00 mEq/kg during storage. According to Codex Alimentarius (2001), good-quality oil should have a PV below 5 mEq/kg, while rancid oil typically exhibits a PV above 10 mEq/kg. Although the PV of the encapsulated TRF exceeded the requirement for good-quality oil, the increase was minimal, suggesting that the TRF remained relatively stable against oxidation during storage.

The slight increase in the PV of the microcapsule may be attributed to MC and the storage temperature of 40 °C, which promoted the formation of various lipid oxidation products. The specific mechanism of lipid oxidation in the presence of water is not entirely clear, but water tends to interact with more hydrophilic lipid oxidation products and mobilize pro-oxidative reactants, as suggested by (Labuza & Dugan, 1971). These interactions collectively contribute to lipid oxidation.

However, it's noteworthy that the PV increment was relatively low, indicating that the TRF remains relatively stable against oxidative degradation during storage. The stability of the core material against oxidation is primarily influenced by the thickness of the interfacial layer, as discussed by Berton-Carabin et al. (2013). In the present study, the TPPI-FG (3:1) complex acted as an emulsifier, forming a dense interfacial layer around the oil droplet due to the high molecular weight of FG (1470 kDa). Additionally, the inclusion of M:OSS (8:2) further augmented the thickness of the interfacial layer by increasing the viscosity and solid content of the wall material. During the spray drying process, this resulted in the formation of a compact and thick microcapsule, which serves as a robust barrier against pro-oxidants, thus minimizing oxidative degradation of the TRF.

5.3.1.8 Tocopherol and Tocotrienol Content Analysis

The TRF-based microcapsule was vacuum-sealed in a nylon bag and stored in darkness at 40 °C for 13 weeks. Subsequently, the degradation of tocopherol and tocotrienol in the microcapsule was assessed (Table 5.2). At the end of the storage, there was a slight degradation ($p < 0.05$) in α-tocopherol, α-, β-, γ-, and δ-tocotrienols, with degradation percentages of 17.33 ± 0.99%, 16.45 ± 1.79%, 20.89 ± 1.20%, and 18.12 ± 1.63%, respectively. The degradation of vitamin E compounds occurred during both processing and storage, consistent with previous reports indicating that vitamin E can degrade even at temperatures as low as 40 °C (Sabliov et al., 2009). This degradation is typically attributed to oxidation, which primarily affects the polyunsaturated phytyl side chain in tocotrienol isomers (Chaiyasit et al., 2007). Notably, these results align with the earlier PV findings, which showed that TRF in the microcapsule experienced slight oxidation. However, the degradation of these isomers was minimized due to the effective barrier

created over the TRF by the TPPI-FG complex and the M:OSS (8:2) wall material, as explained previously. Another study also reported that encapsulated tocotrienol and tocopherol experienced minimal degradation when stored in the dark at 40 °C without exposure to ambient air (Surjit et al., 2022).

Upon closer examination of the tocopherol and tocotrienol isomers, it was evident that β-tocotrienol exhibited the highest degradation throughout the storage period, indicating its sensitivity to degradation. This observation aligns with the results of Surjit et al. (2022). Besides, the findings of Tan et al. (2018) reported that β-tocotrienol in the microcapsule were more prone to oxidation upon storage, due to high initial loss which summed up to 94.9 ± 0.1% at the final storage stage. Additionally, β-tocotrienol is highly susceptible to degradation, it could be explained by a lower initial amount of β-tocotrienol (~1.9%) in the TRF feedstock compared to other isomers. Another study also reported that β-tocotrienol was not found in deep-fat fried French fries due to very low initial concentration of β-tocotrienol in the crude palm oil (Mba et al., 2018). In general, the degradation order of tocopherol and tocotrienol isomers in the microcapsule was as follows: β-tocotrienol > δ-tocotrienol > α-tocotrienol > α-tocopherol > γ-tocotrienol (Table 5.2).

Table 5.2: Oxidative stability of TRF-based microcapsule produced by wall material of M:OSS (8:2) stored at 40 °C for 13 weeks.

Weeks	Peroxide Value (mEq/kg)	Percentage of degradation (%)				
		α-tocopherol	α-tocotrienol	β-tocotrienol	γ-tocotrienol	δ-tocotrienol
0	1.05 ± 0.06^{D}	0.00 ± 0.00^{C}	0.00 ± 0.00^{D}	0.00 ± 0.00^{E}	0.00 ± 0.00^{D}	0.00 ± 0.00^{D}
1	3.80 ± 0.12^{C}	4.89 ± 0.20^{E}	3.94 ± 0.14^{C}	8.34 ± 0.64^{D}	4.44 ± 0.45^{C}	5.73 ± 0.02^{C}
2	4.60 ± 0.47^{B}	7.20 ± 0.13^{D}	6.40 ± 0.51^{B}	11.30 ± 0.04^{CD}	7.86 ± 0.16^{B}	8.50 ± 0.69^{BC}
3	5.60 ± 0.34^{A}	9.50 ± 0.29^{C}	7.44 ± 0.52^{B}	12.07 ± 0.40^{C}	9.63 ± 0.67^{B}	10.15 ± 0.80^{B}
4	5.50 ± 0.00^{A}	14.47 ± 0.28^{B}	16.50 ± 0.3^{A}	17.22 ± 1.32^{B}	10.78 ± 0.16^{B}	10.48 ± 0.09^{B}
13	5.40 ± 0.00^{A}	17.33 ± 0.99^{A}	17.84 ± 1.19^{A}	20.89 ± 1.20^{A}	16.45 ± 1.79^{A}	18.12 ± 1.63^{A}

Values are expressed as mean ± standard deviation (n = 6). Mean values with different superscript letters within the same column are significantly different ($p < 0.05$). Abbreviations: TRF: Tocotrienol-rich fraction; M: Maltodextrin; OSS: Sodium octenyl succinate.

5.3.2 Release Characteristics

The TRF-based microcapsule may encounter diverse environmental conditions when applied to various food or pharmaceutical systems. Therefore, the influence of environmental factors, such as pH and ionic strength, on the release characteristic of the microcapsule were investigated.

5.3.2.1 Effect of Ionic Strength

The release characteristic of the freshly spray-dried microcapsules was evaluated under various ionic strengths, as presented in Table 5.3. As the ionic strength increased, there was a slight increase ($p < 0.05$) in TRF release, ranging from 2.67 ± 0.34 to $5.97 \pm 0.12\%$. This increase can be attributed to the presence of electrostatic screening and ion-binding effects. Counter-ions such as Na+ and Cl- accumulated around the droplet's surface, diminishing electrostatic repulsion between droplets and causing droplet aggregation, consistent with prior research by Ozturk et al. (2014). It's noteworthy, however, that the overall percentage of TRF released remained relatively low (ranging from 2.67% to 5.97%) compared to the release percentages of fish oil (ranging from 2.27% to 21.74%) observed under similar NaCl concentrations in a separate study (Chang et al., 2018). These results indicate that the TPPI-FG (3:1) complex effectively stabilizes the emulsion by strengthening electrostatic interactions between droplets, thus reducing aggregation as NaCl concentrations rise. The interaction between TPPI and FG results in a robust and thicker complex enveloping the droplets, preventing nanoemulsion destabilization with increasing ionic strength. Additionally, the droplets gain further stability from the M:OSS (8:2) wall material, which forms an additional protective layer around them. This protective layer prevents direct contact between the complex and counterions, thereby reducing the electrostatic free energy of the complex, as elucidated by Chang et al. (2018). Consequently, the protein solubility of TPPI is only minimally affected, resulting in a low percentage of TRF release across the range of NaCl concentrations.

5.3.2.2 Effect of pH

The freshly prepared TRF-based microcapsules were exposed to different pH environments (3, 5, 7 and 9) to assess their release characteristic (Table 5.3). The percentage of TRF released was found to be statistically insignificant ($p > 0.05$) across the pH range, except at pH 7, where the highest TRF release was observed ($4.35 \pm 0.19\%$). Overall, the TRF release remained relatively low, ranging from $3.37 \pm 0.28\%$ to $4.35 \pm 0.19\%$. It is worth noting that the performance of protein emulsifiers is often influenced by pH, with biopolymers losing their surface-active properties near their isoelectric point (Jafari et al., 2008). Consequently, nanoemulsions become unstable, resulting in high oil released.

However, it is noteworthy that the TRF released remained low at pH 3, which is close to the isoelectric point of TPPI-FG complex (pI = 3.5). This suggests that the TPPI-FG (3:1) complex maintains effective emulsion stabilization even at its isoelectric point.

Furthermore, the high MEE of 97.28% achieved by the microcapsules demonstrates the effectiveness of the M:OSS (8:2) wall material in TRF encapsulation. The thick and compact wall material also shields the tocotrienols by binding the compounds within the hydrocolloid network (Tan et al., 2018), to avoid direct exposure to varying pH environments that could disrupt the system. A study reported that succinylated starches used as wall materials exhibited high retention and emulsion stability (Jafari et al., 2008). In summary, these results confirm the stability of TRF-based microcapsules when exposed to diverse pH conditions.

Table 5.3: Release characteristic of spray-dried TRF-based microcapsule as a function of ionic strength and pH.

Concentration of sodium chloride (mM)	Percentage of TRF release (%)	pH	Percentage of TRF release (%)
0	2.67 ± 0.34^{C}	3	3.37 ± 0.28^{B}
50	3.97 ± 0.20^{B}	5	3.59 ± 0.37^{B}
100	4.61 ± 0.25^{B}	7	4.35 ± 0.19^{A}
150	5.56 ± 0.60^{A}	9	3.73 ± 0.34^{AB}
200	5.97 ± 0.12^{A}		

Values are expressed as mean ± standard deviation (n = 6). Mean values with different superscript letters within the same column are significantly different ($p < 0.05$). Abbreviations: TRF: Tocotrienol-rich fraction.

5.3.3 Percentage of TRF Release and Bioaccessibility after *In Vitro* Digestion

Understanding the digestion behaviour of TRF-based microcapsules is crucial for their application in food. To investigate the potential oral delivery of TRF in both bulk oil and microcapsules, the INFOGEST *in vitro* digestion method was employed. Both bulk oil and microcapsules underwent SSF, SGF, and SIF conditions to mimic the mouth, stomach, and small intestine environments. Subsequently, we compared the percentage of TRF released and its bioaccessibility.

The percentage of TRF released was determined by analysing the presence of TRF in the micelle and sediment phases relative to the digesta phase. The microcapsules released 85.77 ± 1.43% of TRF, while bulk oil released only 34.57 ± 0.02% (Figure 5.1). Notably, TRF release from the microcapsules was significantly higher ($p < 0.05$) than from bulk oil, with a difference of 51.20%. A similar trend was obtained by *in vitro* digestion of walnut oil encapsulated using soy protein isolate and konjac glucomannan (Hu et al., 2024). A high percentage of TRF released is desirable as it indicates more TRF will be released in the gastrointestinal tract after digestion. The results also show that the wall materials did not impair the *in vitro* digestibility of TRF. This is attributed to the presence

of the M:OSS (8:2) wall material, which effectively minimized TRF degradation under the harsh conditions of the digestion process. Moreover, minimal TRF release was observed when the microcapsules were subjected to varying pH conditions, further substantiating the protective role of the wall material.

During the digestion, the hydrolytic enzymes broke down the interaction between M:OSS (8:2) and the TPPI-FG (3:1) complex, leading to the formation of large pores in the wall matrix and subsequent TRF release (Karaca et al., 2013). In contrast, bulk oil was more susceptible to degradation as it lacked a protective layer and was directly exposed to acidic gastric conditions during digestion, resulting in low TRF release by the end of the process. Similar findings were reported by Tan et al. (2018), indicating that acidic conditions lead to the immediate oxidation of non-encapsulated tocotrienol.

It is worth noting that TRF release from the microcapsules was not complete (unable to release 100% of TRF) at the final stage of in vitro digestion. This suggests that a small amount of TRF remained binding within the matrix (Tan et al., 2018), possibly due to the thick and compact coating layers of the wall material. The protective effect of the M:OSS (8:2) wall material can be attributed to the 97.28% MEE obtained, as explained in previous findings. This wall material restricts enzyme access during digestion, as observed in another study where chitosan wall material limited enzyme access, resulting in incomplete fish oil release (Chang et al., 2018). Additionally, hydrophobic TRF may have deposited within the core of the emulsion droplets (Alayoubi et al., 2013). Nonetheless, this limitation is minimal. In summary, the wall material has proven highly effective in stabilizing and protecting TRF.

Bioaccessibility refers to the amount of active compounds released into the gastrointestinal tract and available for absorption (Xu et al., 2018). Bioaccessibility of TRF was significantly higher ($p < 0.05$) in the microcapsules ($40.81 \pm 0.68\%$) compared to bulk oil ($19.49 \pm 0.01\%$), as shown in Figure 5.1. TRF is known to have poor digestibility and bioaccessibility when ingested orally due to its lipophilic properties (Goh et al., 2015). However, the results of this study demonstrate that microencapsulation enhances the bioaccessibility of TRF.

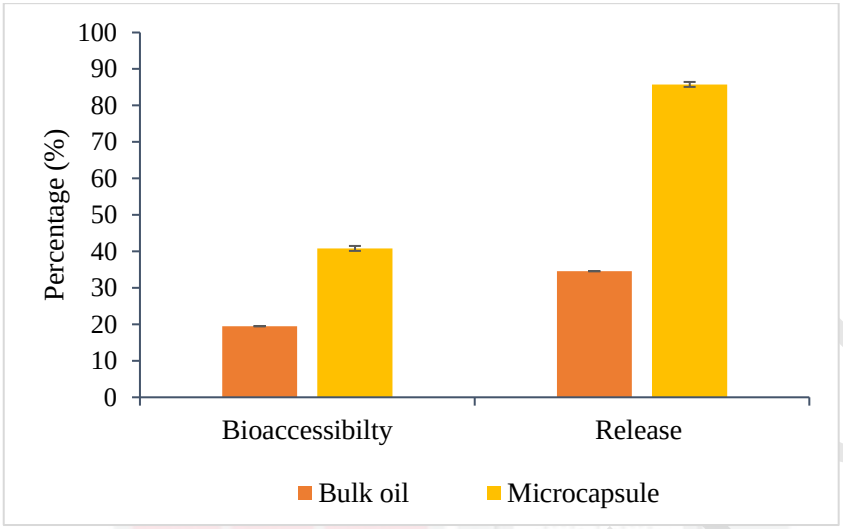

Figure 5.1: Bioaccessibility and release of tocotrienol-rich fraction (TRF) from bulk oil and microcapsule after *in vitro* digestion.

5.4 Conclusions

This study has shed light on the physical and oxidative stability of TRF-based microcapsules following 13 weeks of storage at 40 °C. At the end of the storage period, the microcapsule exhibited a slight increase in cohesiveness (5.36%) and L* value (4.04%), alongside a minor decrease in MEE (3.32%), b* (19.62%) and C values (18.56%). Conversely, the stored microcapsules displayed a notable increase in MC by 36.13%, a_w by 43.75%, and flowability by 50%, but experienced a significant decrease in a* value by 48.85%. The particle size and span value of the reconstituted microcapsules at week 13 measured 4.18 µm and 2.81, respectively. By the end of the storage period, the microcapsules showed a low PV value of 5.40 mEq/kg, slightly surpassing the threshold for good quality oil (PV < 5 mEq/kg). In the analysis of tocopherol and tocotrienol content, it was observed that α-tocopherol (17.33%), α-tocotrienols (17.84%), β-tocotrienols (16.45%), γ-tocotrienols (20.89%), and δ-tocotrienols (18.12%) experienced increased degradation throughout the storage period. Additionally, we investigated the influence of ionic strength and pH on the release of TRF from microcapsules. The highest TRF release was achieved at an ionic strength of 200 mM and pH 7, with percentages of 5.97% and 4.35%, respectively. Following *in vitro* digestion, TRF microcapsules exhibited significantly higher bioaccessibility (40.81%) and TRF release (85.77%) compared to bulk oil. These findings underscore the physical and oxidative stability of microencapsulated TRF during storage, as well as provide insights into release characteristics, bioaccessibility, and TRF release following *in vitro* digestion.

CHAPTER 6

THE EFFECT OF STORAGE STABILITY OF TOCOTRIENOL-RICH FRACTION (TRF) ENCAPSULATED IN MALTODEXTRIN-STARCH SODIUM OCTENYL SUCCINATE MICROCAPSULES ON MAYONNAISE MATRIX

6.1 Introduction

Mayonnaise is a widely consumed dressing known for its creamy white appearance and slightly tangy flavour. It is traditionally prepared as an O/W emulsion, containing a significant oil content (typically 65% to 85%), and is crafted under acidic conditions with a pH ranging from 3.7 to 4.2 (Akhtar & Masoodi, 2022). The essential ingredients of mayonnaise encompass vegetable oil, water egg yolk, mustard, vinegar or lemon juice, salt, and seasoning ingredients (Abdolmaleki et al., 2019). Within the structure of mayonnaise, these components exist in three phases: vegetable oil as the dispersed phase, vinegar, and water as the continuous phase, and egg yolk serving as the emulsifier at the interface (Li et al., 2014).

Over time, traditional mayonnaise has faced challenges aligning with the preferences of nutrition-demanding consumers. Consequently, several studies have explored enriching mayonnaise with natural antioxidants such as resveratrol, tocopherol, rosemary essential oil, and *Ferulago angulata* extract (Abdolmaleki et al., 2019; Rabbani et al., 2021). The addition of natural antioxidants has the potential to improve the oxidative stability of the oil (Gorji et al., 2016), and confer health benefits, appealing to a broader consumer base (Hermund & Yes, 2015).

Recently, tocotrienols have gained prominence due to their exceptional antioxidative properties, comparable to tocopherol. Both components of Vitamin E have been widely recognized for their role in preventing various diseases associated with oxidative stress, such as atherosclerosis, neurodegeneration, cancer, and aging (Park et al., 2010; Sen et al., 2010). It is concerning that over 90% of individuals in the United States fail to meet the recommended dietary allowances (RDAs) for vitamin E intake, which is 15 mg (22.5 IU) per day for adolescents, adult men, and non-lactating women (Saini & Keum, 2016). Consequently, fortifying tocotrienol-rich fraction (TRF) into food products like mayonnaise is encouraged to boost vitamin E consumption.

A significant challenge in fortifying food products with pure polyunsaturated tocotrienols is their susceptibility to lipid oxidation, especially when exposed to environmental stressors such as heat, light, oxygen, moisture, and extreme pH levels. Furthermore, interactions between bioactive compounds and other food matrix ingredients can lead to the degradation of these bioactive compounds (Dima et al., 2020). This can result in reduced tocotrienol bioactivity and the formation of undesirable reaction products (Ko et al., 2010). Moreover, hydrophobic tocotrienols have low water solubility and intestinal permeability when ingested orally, making it challenging to

incorporate pure tocotrienol into food products (Alayoubi et al., 2013). Additionally, the incorporation of tocotrienols can adversely affect the sensory properties of food products due to their highly perishable nature, unfavourable aroma, and unpleasant taste (Maqsoudlou et al., 2020).

To address these challenges, microencapsulation has emerged as a solution to enhance the stability of tocotrienols, preventing their degradation during storage or exposure to environmental stressors (Tan et al., 2018). In this study, a TPPI was created through pH-shifting and thermal treatments to form a complex with FG, resulting in a TPPI:FG (3:1) complex. This complex acts as an emulsifier, stabilizing TRF in the form of Pickering nanoemulsion. This approach is suitable for producing natural and vegan food products as it relies on a fully plant-based emulsifier, eliminating the need for synthetic or animal-based emulsifiers. The TRF-based microcapsule was produced using M:OSS (8:2). M, chosen for its low viscosity, high water solubility, and stability under thermal and acidic conditions, forms a robust, compact, and thick protective layer around the TRF, safeguarding it against lipid oxidation (Liu et al., 2018a; Saavedra-Leos et al., 2022).

In light of these considerations, this study involved fortifying mayonnaise with TRF in the form of microcapsules and bulk oil, respectively, and assessed the physicochemical properties and oxidative stability of TRF-fortified mayonnaise during one month of storage at 4°C. Additionally, sensory properties, including colour, aroma, taste, creaminess, sourness, and overall acceptability, were evaluated using a 9-point hedonic scale.

6.2 Materials and Methods

6.2.1 Materials

The raw materials necessary for mayonnaise preparation, including soybean oil, egg yolk, vinegar, cheese powder, mustards, and salt were purchased from a local supermarket in Ampang, Selangor, Malaysia. Palm TRF was kindly provided by ExcelVite Sdn. Bhd (Chermo, Malaysia). This material comprised 38.5 to 42.0% of total tocotrienols, 9.5 to 14.0% of tocopherol, 30.0 to 45.0% of palm olein (monoglyceride, diglyceride, and triglyceride), 1.0 to 3.0% of plant squalene, 0.03 to 0.07% of mixed carotene complex predominantly β-carotene, and 2.0 to 4.0% of sterol complex predominantly β-sitosterol. The active ingredients predominantly of d-α-tocopherol (9.5 to 14.0%), d-γ-tocotrienol (17.5 to 23.0 %), d-α-tocotrienol (12.0 to 16.0%), d-δ-tocotrienol (4.0 to 7.0%), and d-β-tocotrienol (minimum of 1.9%). The PPI and FG were obtained from Emsland Group Sdn. Bhd (Wietzendorf, Germany) and Qingdao Dehui Halobios Science and Technology Co., Ltd (Qingdao, China), respectively. The wall materials M and OSS were purchased from Ingredion Incorporated (Westchester, United States). HPLC-grade standards for (d-α-, β-, γ- and δ-) tocopherol and (d-α-, β-, γ- and δ-) tocotrienol mixtures were purchased from ChromaDex (Los Angeles, United States). HPLC grade n-hexane and 1,4-dioxane were purchased from Fisher Scientific (Pittsburgh, United States).

6.2.2 Preparation of TRF-based microcapsule

Spray-dried TRF-based microcapsule was prepared as described in sections 5.2.2, 5.2.4, and 5.2.5**.**

6.2.3 Preparation of TRF-fortified Mayonnaise

The mayonnaise samples were prepared using a method modified by Ribes et al. (2019). The formulations for control (C-mayo), and TRF-fortified mayonnaise from microcapsule (M-mayo) and bulk oil (O-mayo) are detailed in Table 6.1. In 100 g of TRF-fortified mayonnaises, the quantity of pure TRF was fixed at 30 mg, equivalent to approximately 12.15 mg of tocotrienol isomers, for both M-mayo and O-mayo. Initially, a small amount of water was used to create the mustard paste. The egg yolk was added into the mixing bowl and blended at medium speed for 30 s. The mustard paste was introduced into the mixing bowl and blended at medium speed for 2 min using a wire whip. During the next 15 min, soybean oil was slowly added at high speed, with approximately 10% of the soybean oil and TRF bulk oil (for O-mayo only) added during the first 5 min. This involved gradually adding a small amount of soybean oil, followed by a 30-second interval between each addition. In the subsequent 5 min, approximately 50% of the soybean oil was added, and during the final 5 min, the remaining soybean oil was incorporated into the mixing bowl. Subsequently, the dissolved salt, cheese powder, TRF-based microcapsule (for M-mayo only), vinegar, and the remaining water were stirred until fully dissolved. The mixture was blended at medium speed for 2 min, followed by an additional 1 min at low speed. The resulting mayonnaise was stored at 4 °C for further analysis.

Table 6.1: Formulations of TRF-fortified mayonnaises.

	Percentage (%)		
Ingredients	C-mayo	O-mayo	M-mayo
Soybean oil	75.0	74.4	72.0
Egg yolk	8.0	8.0	8.0
Vinegar	6.0	6.0	6.0
Water	5.0	5.0	5.0
Cheese powder	4.5	4.5	4.5
Mustard	1.0	1.0	1.0
Salt	0.5	0.5	0.5
TRF-based microcapsule	-	-	3.0
TRF bulk oil	-	0.60	-

Abbreviations: TRF: Tocotrienol-rich fraction; C-mayo: Control mayonnaise; O-mayo: Mayonnaise containing TRF bulk oil; M-mayo: Mayonnaise containing TRF-based microcapsule.

6.2.4 Storage Stability

The mayonnaise samples (C-mayo, M-mayo, and O-mayo) were stored at 4°C for 1 month with weekly sampling intervals. The physico-chemical properties of the mayonnaise samples were evaluated based on colour, pH, viscosity, and texture, while the oxidative stability was determined by PV and the tocopherol and tocotrienol content.

6.2.4.1 Colour

Refer to section 4.2.4.6.

6.2.4.2 pH

Refer to section 3.2.4.4.

6.2.4.3 Viscosity

The viscosity of the mayonnaise samples was determined using a rheometer (RheolabQC, Anton Paar GmbH, Graz, Austria) equipped with a concentric cylinder measuring system. The cylindrical cup was filled with cheese-flavoured mayonnaise up to the filling level mark. Viscosity was measured at a temperature of 4 ± 2 °C, employing a shear rate of $100s^{1}$. Three measurements were performed on each sample as replicates.

6.2.4.4 Texture

The texture of the mayonnaise samples was measured using a TA-XT2i texture analyzer (Stable Micro System, Massachusetts, USA) equipped with an SMSP/0.5 probe. The texture profile analyzer operated at a test speed of 2 mm/s and a test distance of 10 mm. The mayonnaises were characterized based on firmness, consistency, and cohesiveness. Three measurements were performed on each sample as replicates.

6.2.4.5 Peroxide Value (PV)

Refer to Section 5.3.1.7.

6.2.4.6 Tocopherol and Tocotrienol Content Analysis

The TRF extraction method was adapted from Tan et al., (2000) with slight modifications. Two grams of M-mayo and O-mayo were vortexed mixed with 5 mL of methanol for 2 min. The mixture was held at room temperature for 2 min. Then, the mixture was added with 10 mL of n-hexane and vortexed for 1 min. Next, 5 mL of deionized water was added to the mixture and vortexed for 1 min. The resultant mixture was centrifuged at 10,000 rpm for 5 min. The supernatant layer was collected in a scintillation vial and purged with nitrogen gas. About 24 mg of TRF extract was reconstituted with 1 mL of n-hexane and vortex-mixed for 1 min. The resultant solution was filtered using a 0.45 µm polytetrafluoroethylene syringe filter. The filtrate was collected in an autosampler HPLC vial for analysis. The HPLC analysis method was carried out as described in Section 4.2.4.7. The mayonnaise samples (C-mayo, M-mayo, and O-mayo) were stored at 4°C for 1 month with weekly sampling intervals calculated as follows:

$$\text{Degradation (\%)} = \frac{(T_0 - T_n)}{T_0} \times 100 \qquad \text{(Eq.6.1)}$$

Where T_0 is the tocotrienol content in the mayonnaise in week 0, T_n is the tocotrienol content in the mayonnaise in the subsequent weeks.

6.2.5 Sensory Evaluation

A sensory evaluation (Approved NO. JKEUPM-2023-814) of the TRF-fortified mayonnaise samples was conducted with the participation of 60 panelists. These panelists were selected according to the general guidelines of UNE-ISO 8586 (2012). Various preparatory sessions were held to familiarize the panelists with the sensory analysis process, enabling them to recognize and score the quality attributes associated with each sample. The assessments were carried out using a structured 9-point hedonic scale (ranging from 1: "dislike extremely" to 9: "like extremely"), as outlined in UNE-ISO 4121 (2003). This scale was employed to evaluate the colour, aroma, taste, creaminess, sourness, and overall acceptability of the mayonnaise.

The panelists were presented with three distinct mayonnaise samples for assessment: i) C-mayo (control); ii) O-mayo (mayonnaise containing TRF bulk oil); iii) M-mayo (mayonnaise containing TRF-based microcapsule**)**. The sensory analysis took place within 1 h of sample preparation, with the samples stored at 4 °C in sealed glass jars during this time. Each sample was served to the panelists in transparent plastic glass, labelled with three arbitrary digits. To prevent aftertaste, the panellists were instructed to consume an unsalted cracker and drink water between samples, following the protocol outlined by Ribes et al. (2017).

6.2.6 Statistical Analysis

All analyses were performed in triplicates on duplicate samples. The results were analyzed using Minitab statistical software version 17.0 (Minitab Inc., PA, USA). To determine significant differences among mean values ($p < 0.05$), a one-way ANOVA with post-hoc Tukey's test was employed.

6.3 Results and Discussion

6.3.1 Storage Stability

6.3.1.1 Colour

Measurement of the colour of TRF-fortified mayonnaises is essential, as it significantly influences consumer preference. As indicated in Table 6.2, all fresh mayonnaise samples exhibited a light colour with a tendency towards red (positive a* value) and yellow (positive b* value). The yellowness of the mayonnaise samples primarily stemmed from the addition of cheese powder and TRF. Notably, fresh M-mayo displayed significantly lower L* values and higher a* and b* values compared to fresh O-mayo and C-mayo. As depicted in Figure 6.1, M-mayo had the deepest yellow colour, primarily influenced by the TRF-based microcapsule's wall material, which altered the light-scattering properties within the mayonnaise.

Over the storage period, the L*, a*, and b* values of all mayonnaise samples increased significantly ($p < 0.05$). However, the changes in L*, a*, and b* values for M-mayo (1.19%, 7.50%, and 9.11%) were lower than those for O-mayo (2.65%, 27.18%, and 21.24%). This suggests that the encapsulated TRF was more stable during storage. The TRF was effectively protected within the TPPI-FG (3:1) complex and maintained stable within the M:OSS (8:2) wall materials, minimizing deterioration under acidic conditions. In contrast, TRF in O-mayo was unprotected, making it more susceptible to lipid oxidation, resulting in more pronounced colour changes. These results demonstrate that encapsulated TRF better preserves the colour of mayonnaise during prolonged storage.

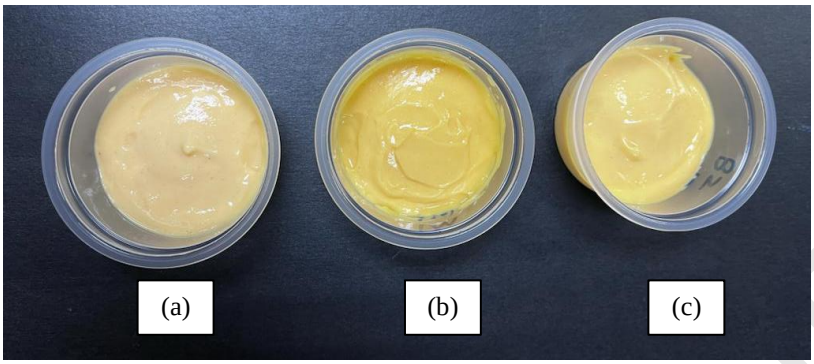

Figure 6.1: Fresh mayonnaise samples prepared from different formulations: (a) Control mayonnaise (C-mayo); (b) Mayonnaise containing TRF-based microcapsule (M-mayo); (c) Mayonnaise containing TRF bulk oil (O-mayo).

6.3.1.2 pH

Table 6.2 presents the pH values of the mayonnaise samples after storage. The pH remained similar across all types of mayonnaise, indicating that the addition of TRF had no significant impact on the pH of the mayonnaise. However, the pH of all mayonnaise samples exhibited a slight increase during storage. This pH increase can be attributed to the addition of oil and mustard, which contributed to higher pH levels in the mayonnaises. The final pH values ranged between 4.25 and 4.28, falling within the microbiological safety pH range (pH 3.6 to 4.2) for mayonnaise (Hill et al., 2020).

Table 6.2: The effect of storage on the pH and colour of different mayonnaise samples.

Properties	Samples	Week 0	Week 1	Week 2	Week 3	Week 4
pH	C-mayo	4.18 ± 0.08^{bA}	4.25 ± 0.02^{abA}	4.24 ± 0.01^{abA}	4.25 ± 0.02^{abA}	4.28 ± 0.01^{aA}
	O-mayo	4.18 ± 0.02^{cA}	4.26 ± 0.01^{bA}	4.25 ± 0.01^{bA}	4.25 ± 0.01^{abA}	4.25 ± 0.01^{aA}
	M-mayo	4.17 ± 0.04^{bA}	4.25 ± 0.01^{aA}	4.25 ± 0.01^{aA}	4.25 ± 0.02^{aA}	4.28 ± 0.01^{aA}
Colour L*	C-mayo	77.61 ± 0.29^{cA}	77.80 ± 0.12^{cA}	78.29 ± 0.20^{bcA}	79.34 ± 0.33^{bA}	81.90 ± 1.04^{aA}
	O-mayo	75.23 ± 0.49^{dB}	76.53 ± 0.36^{dB}	75.65 ± 0.11^{cB}	76.21 ± 0.21^{bC}	77.22 ± 0.17^{aC}
	M-mayo	74.81 ± 0.18^{cB}	74.34 ± 0.18^{cC}	75.33 ± 0.34^{cB}	75.66 ± 0.28^{abB}	75.70 ± 0.17^{aB}
a*	C-mayo	8.61 ± 0.12^{cC}	9.28 ± 0.37^{bB}	9.60 ± 0.17^{bB}	10.28 ± 0.09^{aA}	10.58 ± 0.07^{aA}
	O-mayo	9.31 ± 0.04^{dB}	9.64 ± 0.25^{cB}	9.95 ± 0.67^{bA}	9.93 ± 0.03^{bA}	11.84 ± 0.06^{aA}
	M-mayo	10.80 ± 0.08^{bA}	10.54 ± 0.37^{abA}	10.05 ± 0.07^{abA}	11.00 ± 1.19^{abA}	11.61 ± 0.13^{aB}
b*	C-mayo	37.76 ± 0.53^{bC}	39.41 ± 0.53^{aB}	39.44 ± 0.47^{aB}	39.85 ± 0.73^{aB}	40.30 ± 0.67^{aC}
	O-mayo	43.27 ± 0.60^{cB}	47.59 ± 0.50^{bA}	47.58 ± 0.25^{bA}	48.15 ± 2.12^{bA}	52.46 ± 0.15^{aA}
	M-mayo	46.12 ± 0.54^{eA}	47.35 ± 0.13^{dA}	48.31 ± 0.47^{cA}	49.44 ± 0.23^{bA}	50.32 ± 0.35^{aB}

Values are expressed as mean ± standard deviation (n = 6). Mean values with different uppercase superscript letters within the same column are significantly different ($p < 0.05$). Mean values with different lowercase superscript letters within the same row are significantly different ($p < 0.05$). Abbreviations: C-mayo: Control mayonnaise; O-mayo: Mayonnaise containing TRF bulk oil; M-mayo: Mayonnaise containing TRF-based microcapsule; L*: Lightness; a*: (+) red/(−) green; b*: (+) yellow/(−) blue.

6.3.1.3 Viscosity

The viscosity of the mayonnaise samples is summarized in Table 6.3. According to the findings, M-mayo exhibited the highest viscosity, followed by C-mayo and O-mayo. This higher viscosity in M-mayo resulted from the addition of TRF-based microcapsules produced from TPPI-FG (3:1) complex and M:OSS (8:2) wall materials. The FG contributed thickening properties, while both M and OSS possessed hydrophobic properties, collectively increasing the viscosity of M-mayo by thickening the mayonnaise network. This thickening effect is desirable as it limits oil release by restricting the movement of droplets within limited thermodynamic entropy (Akhtar & Masoodi, 2022). Conversely, O-mayo, which directly incorporated TRF from bulk oil, exhibited lower viscosity. After 1 month of storage, the viscosity of M-mayo increased by a smaller margin (21.29%) compared to O-mayo (33.27%). Viscosity was correlated with the diameter of oil droplets (Katsaros et al., 2020), with smaller droplet diameter resulting in less pronounced viscosity increase. Therefore, it can be concluded that the oil droplets in M-mayo remained more stable due to the thickening effect following the addition of the microcapsule.

6.3.1.4 Texture

In this section, the textural properties (firmness, consistency, and cohesiveness) of the mayonnaises were evaluated, which were affected by TRF incorporation and storage duration. Generally, O-mayo exhibited textural properties more similar to C-mayo. Firmness measures the force required to reach the maximum depth, while cohesiveness gauges the degree of deformation before fracture, representing the force needed to pull the probe from the sample (Gutiérrez et al., 2016). According to Table 6.3, M-mayo displayed the highest firmness, consistency, and cohesiveness among O-mayo and C-mayo. As previously explained, the ingredients of the TRF-based microcapsule induced a thickening effect on the mayonnaise, resulting in a more viscous and firmer texture for M-mayo. Additionally, the higher firmness in M-mayo was attributed to the formation of a complex between TPPI and FG, increasing the stiffness of the gel matrix. Consequently, M-mayo exhibited greater mechanical stability against rupture. Moreover, mayonnaises are water-in-oil emulsions that are predominantly composed of oil. The inclusion of microcapsules increased the solid content of the mayonnaises, resulting in enhanced consistency and cohesiveness. As the storage time increased, all textural values for the mayonnaise samples increased significantly ($p < 0.05$), likely due to water loss from the mayonnaise matrix during storage.

Table 6.3: The effect of storage on the texture and viscosity of different mayonnaise samples.

Properties	Samples	Week 0	Week 1	Week 2	Week 3	Week 4
Firmness (g)	C-mayo	16.94 ± 0.28^{dB}	27.50 ± 2.38^{cB}	28.73 ± 0.20^{bcB}	31.08 ± 0.64^{abB}	33.49 ± 1.08^{aB}
	O-mayo	18.38 ± 0.31^{dB}	27.07 ± 0.91^{cB}	28.87 ± 1.45^{bcB}	29.45 ± 0.57^{abB}	31.27 ± 1.02^{aB}
	M-mayo	31.75 ± 2.21^{bA}	33.30 ± 2.18^{bA}	34.74 ± 1.03^{bA}	43.45 ± 1.3^{abA}	45.98 ± 2.25^{aA}
Consistency (g.s)	C-mayo	29.09 ± 0.99^{cC}	96.21 ± 1.73^{bC}	98.52 ± 2.26^{bB}	103.33 ± 1.98^{aB}	103.72 ± 1.71^{aB}
	O-mayo	32.75 ± 1.38^{dB}	78.06 ± 1.20^{cB}	97.47 ± 1.54^{bB}	103.14 ± 0.50^{aB}	105.61 ± 3.79^{aB}
	M-mayo	46.51 ± 1.61^{dA}	126.58 ± 3.05^{cA}	142.80 ± 1.98^{bA}	146.26 ± 4.12^{abA}	151.89 ± 1.67^{aA}
Cohesiveness (g)	C-mayo	-9.49 ± 0.15^{cA}	-15.64 ± 0.54^{cA}	-15.80 ± 0.71^{bA}	-17.54 ± 0.36^{bA}	-17.67 ± 0.71^{aA}
	O-mayo	-10.86 ± 0.59^{dB}	-14.47 ± 0.35^{cB}	-16.58 ± 0.35^{cA}	-17.13 ± 0.37^{bA}	-18.19 ± 0.42^{aA}
	M-mayo	-15.69 ± 0.60^{dC}	-22.33 ± 0.39^{dC}	-24.18 ± 0.40^{cB}	-25.61 ± 0.26^{bB}	-25.61 ± 0.22^{aB}
Viscosity (mPa.s)	C-mayo	1856.30 ± 23.80^{cB}	1861.40 ± 21.40^{cB}	1875.36 ± 15.99^{bcB}	1921.4 ± 45.40^{bB}	2021.13 ± 7.89^{aB}
	O-mayo	1439.79 ± 13.28^{cC}	1779.90 ± 91.20^{bB}	1812.80 ± 2.31^{abC}	1914.70 ± 61.30^{aB}	1920.20 ± 35.70^{aC}
	M-mayo	2510.30 ± 55.70^{dA}	2799.30 ± 58.90^{cA}	2807.55 ± 10.10^{cA}	2899.60 ± 22.90^{bA}	3044.75 ± 6.87^{aA}

Values are expressed as mean ± standard deviation (n = 6). Mean values with different uppercase superscript letters within the same column are significantly different ($p < 0.05$). Mean values with different lowercase superscript letters within the same row are significantly different ($p < 0.05$). Abbreviations: C-mayo: Control mayonnaise; O-mayo: Mayonnaise containing TRF bulk oil; M-mayo: Mayonnaise containing TRF-based microcapsule.

6.3.1.5 Peroxide Value (PV)

The evaluation of primary oxidation product formation involved measuring the PV of TRF-fortified mayonnaises (O-mayo and M-mayo) over a 1-month storage period (Table 6.4). M-mayo consistently displayed lower PV values ($p < 0.05$) compared to O-mayo from week 0 to week 4, indicating superior oxidative stability due to encapsulated TRF. This aligns with previous research (Tan et al., 2018), which demonstrated that microencapsulated tocotrienol exhibited better stability against lipid oxidation compared to unencapsulated tocotrienol when incorporated into yogurt.

However, it's worth noting that the PV of M-mayo gradually increased during storage. This indicates that the TRF in M-mayo still underwent oxidation, albeit at a slower rate, despite being encapsulated within the wall materials. This phenomenon might be attributed to alterations in the properties of the wall material due to prolonged storage in mayonnaise. Over time, the oil tends to diffuse from the core to the surface of the microcapsule through molecular diffusion (Ferreira et al., 2016). Consequently, the SO becomes exposed to pro-oxidants, making it susceptible to oxidation (Kha et al., 2015), leading to a gradual increase in the PV. In contrast, the TRF in O-mayo was highly susceptible to lipid oxidation as it was directly exposed to harsh environmental conditions, resulting in a higher increment in PV. According to the Codex Alimentarius (2001), oil with a PV below 5 mEq/kg is classified as good quality oil, while a PV exceeding 10 mEq/kg is categorized as rancid oil. In this study, the final PVs for both M-mayo and O-mayo were 2.66 ± 0.00 and 8.62 ± 0.00 mEq/kg, respectively. The former can be considered good quality oil, whereas the latter is close to being categorized as rancid.

6.3.1.6 Degradation of Tocopherol and Tocotrieno

HPLC analysis detected one tocopherol and four tocotrienol isomers in the TRF-fortified mayonnaise (O-mayo and M-mayo). The degradation of these compounds over a four-week storage period is summarized in Table 6.4. As expected, the degradation of all the isomers was significantly less distinct ($p < 0.05$) in M-mayo (ranging from 11.86 ± 0.48 to $30.76 \pm 0.64\%$) compared to O-mayo (ranging from 29.23 ± 0.07 to $34.15 \pm 3.62\%$). These results are consistent with the finding of Tan et al. (2018), who reported that the degradation of tocotrienol isomers was lower when microencapsulated TRF was fortified into yogurt compared to bulk oil. The protective effect of the M:OSS (8:2) wall material, which encapsulated the TRF, limits the contact between the isomers and pro-oxidants in the mayonnaise. Additionally, the lower PV value observed in M-mayo further supports the idea that the degradation of the isomers was reduced compared to O-mayo. The degradation order of tocopherol and tocotrienol isomers in both mayonnaise samples was as follows: β-tocotrienol > δ-tocotrienol > α-tocotrienol > α-tocopherol > γ-tocotrienol. This order aligns with other studies that also reported β-tocotrienol as the most susceptible to degradation compared to other isomers (Surjit Singh et al., 2022; Tan et al., 2018). This susceptibility is due to the lower initial concentration of β-tocotrienol in the TRF feedstock (~1.9%) as compared to other isomers.

Table 6.4: The effect of storage on the peroxide value and degradation of tocopherol and tocotrienol on different mayonnaise samples.

Properties	Samples	Week 0	Week 1	Week 2	Week 3	Week 4
Peroxide value (mEq/kg)	O-mayo	0.70 ± 0.01^{eA}	3.97 ± 0.01^{dA}	4.33 ± 0.01^{cA}	7.27 ± 0.01^{bA}	8.62 ± 0.00^{aA}
	M-mayo	0.36 ± 0.01^{dB}	0.42 ± 0.00^{dB}	1.34 ± 0.09^{cB}	1.84 ± 0.02^{bB}	2.66 ± 0.00^{aB}
α-tocopherol (%)	O-mayo	0.00 ± 0.00^{dA}	20.52 ± 0.00^{cA}	23.30 ± 1.92^{bcA}	26.28 ± 0.63^{abA}	27.98 ± 0.30^{aA}
	M-mayo	0.00 ± 0.00^{eA}	5.17 ± 0.00^{dB}	9.33 ± 0.00^{cB}	13.89 ± 0.37^{bB}	18.74 ± 0.05^{aB}
α-tocotrienol (%)	O-mayo	0.00 ± 0.00^{cA}	22.60 ± 0.00^{bA}	24.45 ± 2.31^{abA}	27.35 ± 0.90^{aA}	28.77 ± 0.47^{aA}
	M-mayo	0.00 ± 0.00^{dA}	7.99 ± 0.00^{cB}	8.85 ± 0.33^{cB}	14.62 ± 2.07^{bB}	19.39 ± 1.09^{aB}
β-tocotrienol (%)	O-mayo	0.00 ± 0.00^{cA}	25.10 ± 0.00^{bA}	28.78 ± 0.00^{abA}	29.89 ± 1.49^{abA}	34.15 ± 3.62^{aA}
	M-mayo	0.00 ± 0.00^{dA}	17.99 ± 2.35^{cA}	24.52 ± 1.83^{bA}	27.33 ± 0.34^{abA}	30.76 ± 0.64^{aA}
γ-tocotrienol (%)	O-mayo	0.00 ± 0.00^{cA}	14.00 ± 1.72^{bA}	17.38 ± 2.05^{abA}	20.81 ± 0.57^{aA}	22.23 ± 0.21^{aA}
	M-mayo	0.00 ± 0.00^{dA}	3.92 ± 0.00^{cB}	4.37 ± 0.05^{cB}	7.36 ± 0.26^{bB}	11.86 ± 0.48^{aB}
δ-tocotrienol (%)	O-mayo	0.00 ± 0.00^{eA}	17.65 ± 0.14^{dA}	20.40 ± 0.00^{cA}	21.76 ± 0.00^{bA}	29.23 ± 0.07^{aA}
	M-mayo	0.00 ± 0.00^{dA}	6.35 ± 0.00^{cB}	12.50 ± 0.61^{bB}	13.29 ± 0.46^{bB}	19.38 ± 1g.13^{aB}

Values are expressed as mean ± standard deviation (n = 6). Mean values with different uppercase superscript letters within the same column are significantly different ($p < 0.05$). Mean values with different lowercase superscript letters within the same row are significantly different ($p < 0.05$). Abbreviations: O-mayo: Mayonnaise containing TRF bulk oil; M-mayo: Mayonnaise containing TRF-based microcapsule.

6.3.2 Sensory Evaluation

Sixty panellists participated in sensory evaluations of three different mayonnaise samples (C-mayo, O-mayo, and M-mayo) based on various sensory attributes, including colour, aroma, taste, creaminess, sourness, and overall acceptability (Table 6.5). The average score for colour was highest for M-mayo (7.60 ± 1.34), followed by O-mayo (7.52 ± 1.37) and C-mayo (6.98 ± 1.47). This indicates that most panellists preferred the mayonnaise with a darker yellow colour, finding it more attractive and flavourful. Aroma, taste, creaminess, and sourness showed no significant differences ($p > 0.05$) among the three samples. This suggests that panellists had similar preferences for these sensory attributes across all mayonnaise samples. The average scores for these attributes fell within the range of 6.45 to 7.29, indicating that most panellists liked them moderately. The addition of cheese powder as a flavouring agent likely contributed to the pleasant cheesy and creamy taste of the mayonnaise, effectively masking the TRF's unpleasant aroma and taste. As a result, panellists could not distinguish between the fortified and unfortified mayonnaises, leading to similar average ratings for all the samples.

In terms of overall acceptability, M-mayo received the highest rating (7.29 ± 1.31), followed by C-mayo (7.27 ± 1.26) and O-mayo (7.27 ± 1.31), with no significant difference ($p > 0.05$) between them. This suggests that M-mayo was preferred by panellists in terms of colour, sourness, and overall acceptability. The study indicates that TRF-fortified mayonnaises were well-received by the panellists, even though the TRF's unpleasant aroma and taste did not significantly impact consumer preference.

Table 6.5: Sensory attributes of TRF-fortified mayonnaise samples based on hedonic ratings (n = 60)*.

Samples	Colour	Aroma	Taste	Creaminess	Sourness	Overall acceptability
C-mayo	6.98 ± 1.47^{B}	6.97 ± 1.43^{A}	7.07 ± 1.45^{A}	7.10 ± 1.30^{A}	6.77 ± 1.53^{A}	7.27 ± 1.26^{A}
O-mayo	7.52 ± 1.37^{AB}	7.02 ± 1.31^{A}	7.17 ± 1.46^{A}	7.28 ± 1.20^{A}	6.45 ± 2.14^{A}	7.27 ± 1.31^{A}
M-mayo	7.60 ± 1.34^{A}	6.98 ± 1.46^{A}	7.08 ± 1.36^{A}	6.93 ± 1.49^{A}	6.83 ± 1.62^{A}	7.29 ± 1.31^{A}

Values are expressed as mean ± standard deviation (n = 6). Mean values with different uppercase superscript letters within the same column are significantly different ($p < 0.05$). Abbreviations: C-mayo: Control mayonnaise; O-mayo: Mayonnaise containing TRF bulk oil; M-mayo: Mayonnaise containing TRF-based microcapsule.

6.4 Conclusions

The addition of TRF-base microcapsules had significant effects on the colour, texture, and viscosity of fresh mayonnaise. The overall results indicate that fortifying mayonnaise with encapsulated TRF was more stable than using bulk oil when stored at 4°C for four weeks. Based on the findings, M-mayo showed smaller increases in lightness (1.19%), redness (7.50%), yellowness (9.11%), firmness (44.82%), consistency (63.22%), and viscosity (21.29%) compared to the other samples. Additionally, the M:OSS (8:2) microcapsules offered distinct protection to TRF against oxidation for two weeks of storage. This was evident in M-mayo, which had a significantly lower PV value (2.66 mEq/kg) and lower degradation of tocopherol and tocotrienol isomers (ranging from 11.86% to 30.76%). Among all tocopherols and tocotrienol isomers, β-tocotrienol was found to be the most unstable compound, with the highest percentage of degradation (ranging from 30.76 ± 0.64 to 34.15 ± 3.62%) in both mayonnaise samples during storage. Regarding sensory evaluation, M-mayo received the highest sensory rating for colour, while other sensory attributes received similar levels of preference. This suggests that panellists had a comparable liking for these sensory attributes across all mayonnaise samples. This study shows the impact of storage and the mayonnaise matrix on the stability of TRF encapsulated in M:OSS microcapsules. However, it was observed that the degradation of encapsulated TRF could not be eliminated, completely as oxidation persisted during extended mayonnaise storage. Therefore, further research can explore methods to enhance the stability of active compounds by adjusting the preparation and processing parameters of the microcapsules.

CHAPTER 7

SUMMARY, CONCLUSIONS AND FUTURE RECOMMENDATIONS

In this study, TRF-based nanoemulsions were successfully developed, utilizing fully plant-based emulsifiers in combination with TPPI-FG complexes. Tocotrienol, a member of the vitamin E family known for its potent antioxidant properties and various health benefits, was the central focus. In this study, the TPPI solubility was enhanced through pH-shifting and thermal treatments. The resulting soluble complexes, formed at varying TPPI to FG ratios (3:1, 5:1, 7:1, 9:1, and 11:1), were employed as emulsifiers for TRF-based O/W nanoemulsions. The study revealed that the TPPI-FG (3:1) stabilized nanoemulsion exhibited the highest viscosity, EAI, and ESI. Over a 7-day storage period, this nanoemulsion maintained remarkable stability, with minimal changes in droplet size, PDI, and creaming index, and no observed coalescence. Then, TRF-based microcapsules were optimized using spray-drying with various core-to-wall ratios, wall material compositions, and mixing ratios. The core-to-wall ratio of 1:4 was identified as optimal, resulting in microcapsules with superior characteristics, including high MEE, improved Water Solubility Index (WSI), enhanced retention of tocopherol and tocotrienol, good flowability, and moderate cohesiveness. Subsequently, the research explored wall material compositions and mixing ratios, revealing that a combination of M:OSS (8:2) offered the highest MEE, low cohesiveness, and excellent retention of tocotrienol and tocopherol. These microcapsules exhibited optimal sphericity, smooth surfaces, and no cracks. Subsequently, the storage stability, release behavior, and bioaccessibility of tocotrienol within the optimized TRF-based microcapsules were evaluated. Over a 13-week storage period at 40 °C, the microcapsules showed slight increases in cohesiveness and lightness, alongside minimal reductions in MEE, yellowness, and chroma. The reconstituted microcapsules maintained consistent particle size and span value. Additionally, the microcapsules demonstrated oxidative stability and low release under varying ionic strengths and pH conditions. After *in vitro* digestion, the microcapsules exhibited higher bioaccessibility compared to bulk oil. Lastly, the optimized TRF-based microcapsules were fortified into mayonnaises (M-mayo), which were then stored at 4 °C for one month. The M-mayo showed stability during storage, as evidenced by minor changes in attributes like lightness, redness, yellowness, firmness, consistency, and viscosity. Moreover, the oxidative stability of M-mayo was maintained, with only slight changes observed in the PV, tocotrienol and tocopherol isomers. Sensory evaluation revealed that M-mayo received the highest rating for colour, with similar ratings for other attributes like aroma, taste, creaminess, sourness, and overall acceptability compared to the original mayonnaise. This indicated that the fortification of TRF-based microcapsules did not negatively impact panelists' preferences, maintaining a similar degree of liking as the original mayonnaise.

In this study, a TRF-based nanoemulsion stabilized by fully plant-based emulsifiers, utilizing the TPPI-FG (3:1) complex, was successfully developed. Furthermore, successful encapsulation of TRF within wall materials comprising M:OSS (8:2) was achieved, demonstrating excellent stability during storage and high in vitro bioaccessibility. The TRF-fortified mayonnaise also exhibited remarkable stability and received a high degree of liking from sensory evaluation.

Future research approaches may involve exploring the potential of complexing TPPI with other types of polysaccharides, such as guar gum, to investigate their emulsifying properties. Additionally, comparing the encapsulation efficiency of TRF-based microcapsules produced using alternative drying techniques like the supercritical drying method and employing different types of wall materials, such as proteins or gums, could be pursued. As the oxidative stability of TRF can vary in different food matrices, especially those with high moisture content, fortifying TRF into these food matrices to study its release behavior and stability is important. Moreover, conducting i*n vivo* studies in animal models could provide valuable insights into the delivery of TRF.

REFERENCES

Abd Rashed, A., Md Noh, M. F., Khalid, N. M., Ab Rahman, N. Ì., Tasirin, A., Omar, W. S. W., Nawi, M. N. M., Jamilan, M. A., & Selamat, R. (2017). The nutritional composition of mayonnaise and salad dressing in the Malaysian market. *Sains Malaysiana*, *46*(1), 139–147. https://doi.org/10.17576/jsm-2017-4601-18

Abdolmaleki, K., Nayebzadeh, K., & Shahin, R. (2019). Effects of tocopherol, rosemary essential oil and Ferulago angulata extract on oxidative stability of mayonnaise during its shelf life: A comparative study. *Food Chemistry*, *19*, 46–52. https://doi.org/10.1016/j.foodchem.2019.01.028

Abi-Melhem, R., & Hassoun, Y. (2023). Is pea our hidden allergen? An American pediatric case series. *Journal of Allergy and Clinical Immunology: Global*, *2*(2), 100090. https://doi.org/10.1016/J.JACIG.2023.100090

Abu-Fayyad, A., Kamal, M. M., Carroll, J. L., Dragoi, A. M., Cody, R., Cardelli, J., & Nazzal, S. (2018). Development and in-vitro characterization of nanoemulsions loaded with paclitaxel/γ-tocotrienol lipid conjugates. *International Journal of Pharmaceutics*, *536*(1), 146–157. https://doi.org/10.1016/j.ijpharm.2017.11.062

Afinjuomo, F., Barclay, T. G., Song, Y., Parikh, A., Petrovsky, N., & Garg, S. (2019). Synthesis and characterization of a novel inulin hydrogel crosslinked with pyromellitic dianhydride. *Reactive and Functional Polymers*, *134*, 104–111. https://doi.org/10.1016/j.reactfunctpolym.2018.10.014

Aggarwal, B. B., Sundaram, C., Prasad, S., & Kannappan, R. (2010). Tocotrienols, the vitamin E of the 21st century: Its potential against cancer and other chronic diseases. *Biochemical Pharmacology*, *80*(11), 1613–1631. https://doi.org/10.1016/j.bcp.2010.07.043

Akalin, A. S., & Erişir, D. (2008). Effects of inulin and oligofructose on the rheological characteristics and probiotic culture survival in low-fat probiotic ice cream. *Journal of Food Science*, *73*(4), 184–188. https://doi.org/10.1111/j.1750-3841.2008.00728.x

Akhtar, G., & Masoodi, F. A. (2022). Structuring functional mayonnaise incorporated with Himalayan walnut oil Pickering emulsions by ultrasound assisted emulsification. *Ultrasonics Sonochemistry*, *86*(11), 106022. https://doi.org/10.1016/j.ultsonch.2022.106022

Al Mubarak, A., Hamid, N., Kam, R., & Chan, H. (2019). The Effects of Spray Drying Conditions on the Physical and Bioactive Properties of New Zealand Tamarillo (Solanum betaceum) Powder. *Acta Scientific Nutritional Health*, *3*(12), 121–131. https://doi.org/10.31080/asnh.2019.03.0545

Alayoubi, A., Kanthala, S., Satyanarayanajois, S. D., Anderson, J. F., Sylvester, P. W., & Nazzal, S. (2013). Stability and in vitro antiproliferative activity of bioactive " Vitamin E" fortified parenteral lipid emulsions. *Colloids and Surfaces B: Biointerfaces*, *103*, 23–30. https://doi.org/10.1016/j.colsurfb.2012.10.003

Alayoubi, A. Y., Anderson, J. F., Satyanarayanajois, S. D., Sylvester, P. W., & Nazzal, S. (2013). Concurrent delivery of tocotrienols and simvastatin by lipid nanoemulsions potentiates their antitumor activity against human mammary adenocarcenoma cells. *European Journal of Pharmaceutical Sciences*, *48*(3), 385–392. https://doi.org/10.1016/j.ejps.2012.12.011

Almajwal, A. M., Abulmeaty, M. M. A., Feng, H., Alruwaili, N. W., Dominguez-Uscanga, A., Andrade, J. E., Razak, S., & Elsadek, M. F. (2019). Stabilization of vitamin D in pea protein isolate nanoemulsions increases its bioefficacy in rats. *Nutrients*, *11*(1). https://doi.org/10.3390/nu11010075

Altin, G., Gültekin-Özgüven, M., & Ozcelik, B. (2018). Chitosan coated liposome dispersions loaded with cacao hull waste extract: Effect of spray drying on physico-chemical stability and in vitro bioaccessibility. *Journal of Food Engineering*, *223*, 91–98. https://doi.org/10.1016/j.jfoodeng.2017.12.005

Amine, C., Dreher, J., Helgason, T., & Tadros, T. (2014). Investigation of emulsifying properties and emulsion stability of plant and milk proteins using interfacial tension and interfacial elasticity. *Food Hydrocolloids*, *39*, 180–186. https://doi.org/10.1016/j.foodhyd.2014.01.001

Arancibia, C., Riquelme, N., Zúñiga, R., & Matiacevich, S. (2017). Comparing the effectiveness of natural and synthetic emulsifiers on oxidative and physical stability of avocado oil-based nanoemulsions. *Innovative Food Science and Emerging Technologies*, *44*, 159–166. https://doi.org/10.1016/j.ifset.2017.06.009

Araujo-Díaz, S. B., Leyva-Porras, C., Aguirre-Bañuelos, P., Álvarez-Salas, C., & Saavedra-Leos, Z. (2017). Evaluation of the physical properties and conservation of the antioxidants content, employing inulin and maltodextrin in the spray drying of blueberry juice. *Carbohydrate Polymers*, *167*, 317–325. https://doi.org/10.1016/j.carbpol.2017.03.065

Arpagaus, C. (2019). Production of food bioactive-loaded nanoparticles by nano spray drying. In *Nanoencapsulation of Food Ingredients by Specialized Equipment: Volume 3 in the Nanoencapsulation in the Food Industry series*. *3*, 151-211. https://doi.org/10.1016/B978-0-12-815671-1.00004-4

Asokapandian, S., Venkatachalam, S., Swamy, G. J., & Kuppusamy, K. (2016). Optimization of Foaming Properties and Foam Mat Drying of Muskmelon Using Soy Protein. *Journal of Food Process Engineering*, *39*(6), 692–701. https://doi.org/10.1111/jfpe.12261

Bae, E. K., & Lee, S. J. (2008). Microencapsulation of avocado oil by spray drying using whey protein and maltodextrin. *Journal of Microencapsulation*, *25*(8), 549–560. https://doi.org/10.1080/02652040802075682

Bai, L., Huan, S., Gu, J., & McClements, D. J. (2016). Fabrication of oil-in-water nanoemulsions by dual-channel microfluidization using natural emulsifiers: Saponins, phospholipids, proteins, and polysaccharides. *Food Hydrocolloids*, *61*, 703–711. https://doi.org/10.1016/j.foodhyd.2016.06.035

Barać, M. B., Pešić, M. B., Stanojević, S. P., Kostić, A. Z., & Čabrilo, S. B. (2015). Techno-functional properties of pea (Pisum sativum) protein isolates-a review. *Acta Periodica Technologica*, *46*, 1–18. https://doi.org/10.2298/APT1546001B

Barclay, T., Ginic-Markovic, M., Cooper, P., & Petrovsky, N. (2010). Inulin - A versatile polysaccharide with multiple pharmaceutical and food chemical uses. *Journal of Excipients and Food Chemicals*, *1*(3), 27–50.

Beakawi Al-Hashemi, H. M., & Baghabra Al-Amoudi, O. S. (2018). A review on the angle of repose of granular materials. *Powder Technology*, *330*, 397–417. https://doi.org/10.1016/j.powtec.2018.02.003

Bednarska, M. A., & Janiszewska-Turak, E. (2020). The influence of spray drying parameters and carrier material on the physico-chemical properties and quality of chokeberry juice powder. *Journal of Food Science and Technology*, *57*(2), 564–577. https://doi.org/10.1007/s13197-019-04088-8

Beirão-da-Costa, S., Duarte, C., Bourbon, A. I., Pinheiro, A. C., Januário, M. I. N., Vicente, A. A., Beirão-da-Costa, M. L., & Delgadillo, I. (2013). Inulin potential for encapsulation and controlled delivery of Oregano essential oil. *Food Hydrocolloids*, *33*(2), 199–206. https://doi.org/10.1016/j.foodhyd.2013.03.009

Benichou, A., Aserin, A., & Garti, N. (2002). Protein-polysaccharide interactions for stabilization of food emulsions. *Journal of Dispersion Science and Technology*, *23*(1–3), 93–123. https://doi.org/10.1081/DIS-120003307

Berton-Carabin, C. C., Ropers, M. H., & Genot, C. (2014). Lipid Oxidation in Oil-in-Water Emulsions: Involvement of the Interfacial Layer. *Comprehensive Reviews in Food Science and Food Safety*, *13*(5), 945–977. https://doi.org/10.1111/1541-4337.12097

Berton-Carabin, C., Genot, C., Gaillard, C., Guibert, D., & Ropers, M. H. (2013). Design of interfacial films to control lipid oxidation in oil-in-water emulsions. *Food Hydrocolloids*, *33*(1), 99–105. https://doi.org/10.1016/j.foodhyd.2013.02.021

Bisten, A., & Schuchmann, H. P. (2016). Optical measuring methods for the investigation of high-pressure homogenisation. *Processes*, *4*(4), 6–9. https://doi.org/10.3390/pr4040041

Borrmann, D., Pierucci, A. P. T. R., Leite, S. G. F., & Leão, M. H. M. D. R. (2013). Microencapsulation of passion fruit (Passiflora) juice with n-octenylsuccinate-derivatised starch using spray-drying. *Food and Bioproducts Processing*, *91*(1), 23–27. https://doi.org/10.1016/j.fbp.2012.08.001

Brodkorb, A., Egger, L., Alminger, M., Alvito, P., Assunção, R., Ballance, S., Bohn, T., Bourlieu-Lacanal, C., Boutrou, R., Carrière, F., Clemente, A., Corredig, M., Dupont, D., Dufour, C., Edwards, C., Golding, M., Karakaya, S., Kirkhus, B., Le Feunteun, S., Recio, I. (2019). INFOGEST static in vitro simulation of gastrointestinal food digestion. *Nature Protocols*, *14*(4), 991–1014. https://doi.org/10.1038/s41596-018-0119-1

Bryant, C. J. (2022). Plant-based animal product alternatives are healthier and more environmentally sustainable than animal products. *Future Foods*, *6*, 100174. https://doi.org/10.1016/J.FUFO.2022.100174

Budin, S. B., Othman, F., Louis, S. R., Bakar, M. A., Das, S., & Mohamed, J. (2009). The effects of palm oil tocotrienol-rich fraction supplementation on biochemical parameters, oxidative stress and the vascular wall of streptozotocin-induced diabetic rats. *Clinics (São Paulo, Brazil)*, *64*(3), 235–244. https://doi.org/10.1590/s1807-59322009000300015

Bueno, A. S., Pereira, C. M., Menegassi, B., Arêas, J. A. G., & Castro, I. A. (2009). Effect of extrusion on the emulsifying properties of soybean proteins and pectin mixtures modelled by response surface methodology. *Journal of Food Engineering*, *90*(4), 504–510. https://doi.org/10.1016/j.jfoodeng.2008.07.028

Burger, T. G., & Zhang, Y. (2019). Recent progress in the utilization of pea protein as an emulsifier for food applications. *Trends in Food Science and Technology*, *86*, 25–33. https://doi.org/10.1016/j.tifs.2019.02.007

Cabanillas, B., Jappe, U., & Novak, N. (2018). Allergy to Peanut, Soybean, and Other Legumes: Recent Advances in Allergen Characterization, Stability to Processing and IgE Cross-Reactivity. *Molecular Nutrition and Food Research*, *62*(1), 1–40. https://doi.org/10.1002/mnfr.201700446

Cameron, D. R., Weber, M. E., Neufeld, R. J., Cooper, D. G., Cameron, D. R., & Idziak, E. S. (1991). Determination of interfacial areas in emulsions using turbidimetric and droplet size data: Correction of the formula for emulsifying activity index. *Journal of Agricultural and Food Chemistry*, *39*(4), 655–659. https://doi.org/10.1021/jf00004a005

Candraningrum, R. G. S., Setiowati, A. D., & Hidayat, C. (2022). Electrostatic-Maillard formation of coconut protein Concentrate-Pectin conjugate for Oil-in-Water Emulsion: Effects of Ratio, Temperature, and pH. *Journal of the Saudi Society of Agricultural Sciences*, *xxxx*, 0–6. https://doi.org/10.1016/j.jssas.2022.05.004

Caparino, O. A., Tang, J., Nindo, C. I., Sablani, S. S., Powers, J. R., & Fellman, J. K. (2012). Effect of drying methods on the physical properties and microstructures of mango (Philippine "Carabao" var.) powder. *Journal of Food Engineering*, *111*(1), 135–148. https://doi.org/10.1016/j.jfoodeng.2012.01.010

Carneiro, H. C. F., Tonon, R. V., Grosso, C. R. F., & Hubinger, M. D. (2013). Encapsulation efficiency and oxidative stability of flaxseed oil microencapsulated by spray drying using different combinations of wall materials. *Journal of Food Engineering*, *115*(4), 443–451. https://doi.org/10.1016/j.jfoodeng.2012.03.033

Carpentier, J., Conforto, E., Chaigneau, C., Vendeville, J. E., & Maugard, T. (2022). Microencapsulation and controlled release of α-tocopherol by complex coacervation between pea protein and tragacanth gum: A comparative study with arabic and tara gums. *Innovative Food Science and Emerging Technologies*, *77*, 102951. https://doi.org/10.1016/j.ifset.2022.102951

Castel, V., Rubiolo, A. C., & Carrara, C. R. (2018). Brea gum as wall material in the microencapsulation of corn oil by spray drying: Effect of inulin addition. *Food Research International*, *103*, 76–83. https://doi.org/10.1016/J.FOODRES.2017.10.036

Chaiyasit, W., Elias, R. J., McClements, D. J., & Decker, E. A. (2007). Role of physical structures in bulk oils on lipid oxidation. *Critical Reviews in Food Science and Nutrition*, *47*(3), 299–317. https://doi.org/10.1080/10408390600754248

Chang, H. W., Tan, T. B., Tan, P. Y., Abas, F., Lai, O. M., Wang, Y., Wang, Y., Nehdi, I. A., & Tan, C. P. (2018). Microencapsulation of fish oil using thiol-modified β-lactoglobulin fibrils/chitosan complex: A study on the storage stability and in vitro release. *Food Hydrocolloids*, *80*, 186–194. https://doi.org/10.1016/j.foodhyd.2018.02.002

Chen, H., Jin, Y., Ding, X., Wu, F., Bashari, M., Chen, F., Cui, Z., & Xu, X. (2014). Improved the emulsion stability of phosvitin from hen egg yolk against different pH by the covalent attachment with dextran. *Food Hydrocolloids*, *39*, 104–112. https://doi.org/10.1016/j.foodhyd.2013.12.031

Chen, Y., Chen, Y., Jiang, L., Yang, Z., Fang, Y., & Zhang, W. (2023). Shear emulsification condition strategy impact high internal phase Pickering emulsions stabilized by coconut globulin-tannic acid: Structure of protein at the oil-water interface. *LWT*, *187*, 115283. https://doi.org/10.1016/J.LWT.2023.115283

Corrêa-Filho, L. C., Moldão-Martins, M., & Alves, V. D. (2019). Advances in the application of microcapsules as carriers of functional compounds for food products. *Applied Sciences (Switzerland)*, *9*(3), 571. https://doi.org/10.3390/app9030571

Coupland, J. N., & Sigfusson, H. (2005). Food emulsions. In *Handbook of Food Science, Technology, and Engineering - 4 Volume Set*. https://doi.org/10.1201/9781420029581.ch9

Cuevas-Bernardino, J. C., Leyva-Gutierrez, F. M. A., Vernon-Carter, E. J., Lobato-Calleros, C., Román-Guerrero, A., & Davidov-Pardo, G. (2018). Formation of biopolymer complexes composed of pea protein and mesquite gum – Impact of quercetin addition on their physical and chemical stability. *Food Hydrocolloids*, *77*, 736–745. https://doi.org/10.1016/j.foodhyd.2017.11.015

Cui, W., & Mazza, G. (1996). Physicochemical characteristics of flaxseed gum. *Food Research International*, *29*(3–4), 397–402. https://doi.org/10.1016/0963-9969(96)00005-1

Da Costa, J. M. G., Borges, S. V., Hijo, A. A. C. T., Silva, E. K., Marques, G. R., Cirillo, M. Â., & De Azevedo, V. M. (2013). Matrix structure selection in the microparticles of essential oil oregano produced by spray dryer. *Journal of Microencapsulation*, *30*(8), 717–727. https://doi.org/10.3109/02652048.2013.778909

Dagorn-Scaviner, C., Gueguen, J., & Lefebvre, J. (1986). A comparison of interfacial behaviours of pea (Pisum sativum L.) legumin and vicilin at air/water interface. *Food / Nahrung*, *30*(3–4), 337–347. https://doi.org/10.1002/food.19860300332

de Camargo, A. C., Franchin, M., & Shahidi, F. (2019). Tocopherols and Tocotrienols: Sources, Analytical Methods, and Effects in Food and Biological Systems. In *Encyclopedia of Food Chemistry*, 561-570. https://doi.org/10.1016/b978-0-08-100596-5.22358-5

Desiderio, E., Shanmugam, K., & Östergren, K. (2023). Plant based meat alternative, from cradle to company-gate: A case study uncovering the environmental impact of the Swedish pea protein value chain. *Journal of Cleaner Production*, *418*, 138173. https://doi.org/10.1016/J.JCLEPRO.2023.138173

Di Mattia, C., Balestra, F., Sacchetti, G., Neri, L., Mastrocola, D., & Pittia, P. (2015). Physical and structural properties of extra-virgin olive oil based mayonnaise. *Lwt*, *62*(1), 764–770. https://doi.org/10.1016/j.lwt.2014.09.065

Dickinson, E. (2009). Hydrocolloids as emulsifiers and emulsion stabilizers. *Food Hydrocolloids*, *23*(6), 1473–1482. https://doi.org/10.1016/j.foodhyd.2008.08.005

Dima, C., Assadpour, E., Dima, S., & Jafari, S. M. (2020). Bioavailability of nutraceuticals: Role of the food matrix, processing conditions, the gastrointestinal tract, and nanodelivery systems. *Comprehensive Reviews in Food Science and Food Safety*, *19*(3), 954–994. https://doi.org/10.1111/1541-4337.12547

Dima, C., Pətraşcu, L., Cantaragiu, A., Alexe, P., & Dima, Ş. (2016). The kinetics of the swelling process and the release mechanisms of Coriandrum sativum L. essential oil from chitosan/alginate/inulin microcapsules. *Food Chemistry*, *195*, 39–48. https://doi.org/10.1016/j.foodchem.2015.05.044

Ding, H. H., Qian, K., Goff, H. D., Wang, Q., & Cui, S. W. (2018). Structural and conformational characterization of arabinoxylans from flaxseed mucilage. *Food Chemistry*, *254*, 266–271. https://doi.org/10.1016/j.foodchem.2018.01.159

Donsì, F. (2018). Applications of Nanoemulsions in Foods. *Nanoemulsions: Formulation, Applications, and Characterization*, 349–377. https://doi.org/10.1016/B978-0-12-811838-2.00011-4

Donsì, F., Sessa, M., & Ferrari, G. (2013). Nanometric-Size Delivery Systems for Bioactive Compounds for the Nutraceutical and Food Industries. *Bionanotechnology*, 619–666. https://doi.org/10.1002/9781118451915.ch37

Donsì, F., Sessa, M., Mediouni, H., Mgaidi, A., & Ferrari, G. (2011). Encapsulation of bioactive compounds in nanoemulsion- based delivery systems. *Procedia Food Science*, *1*, 1666–1671. https://doi.org/10.1016/j.profoo.2011.09.246

Donsì, F., & Velikov, K. P. (2019). Encapsulation of food ingredients by single O/W and W/O nanoemulsions. In *Lipid-Based Nanostructures for Food Encapsulation Purposes*, 37-87. https://doi.org/10.1016/b978-0-12-815673-5.00002-7

Donsì, F., Wang, Y., & Huang, Q. (2011). Freeze-thaw stability of lecithin and modified starch-based nanoemulsions. *Food Hydrocolloids*, *25*(5), 1327–1336. https://doi.org/10.1016/j.foodhyd.2010.12.008

Elboutachfaiti, R., Delattre, C., Quéro, A., Roulard, R., Duchêne, J., Mesnard, F., & Petit, E. (2017). Fractionation and structural characterization of six purified rhamnogalacturonans type I from flaxseed mucilage. *Food Hydrocolloids*, *62*, 273–279. https://doi.org/10.1016/j.foodhyd.2016.08.005

Fang, Z., & Bhandari, B. (2012). Comparing the efficiency of protein and maltodextrin on spray drying of bayberry juice. *Food Research International*, *48*(2), 478–483. https://doi.org/10.1016/j.foodres.2012.05.025

Farshi, P., Mirmohammadali, S. N., Rajpurohit, B., Smith, J. S., & Li, Y. (2024). Pea protein and starch: Functional properties and applications in edible films. *Journal of Agriculture and Food Research*, *15*, 100927. https://doi.org/10.1016/J.JAFR.2023.100927

Feng, X., Dai, H., Yu, Y., Wei, Y., Tan, H., Tang, M., Ma, L., & Zhang, Y. (2022). Adjusting the interfacial property and emulsifying property of cellulose nanofibrils by ultrasonic treatment combined with gelatin addition. *Food Hydrocolloids*, *133*, 107905. https://doi.org/10.1016/J.FOODHYD.2022.107905

Fernandes, R. V. D. B., Borges, S. V., & Botrel, D. A. (2014). Gum arabic/starch/maltodextrin/inulin as wall materials on the microencapsulation of rosemary essential oil. *Carbohydrate Polymers*, *101*(1), 524–532. https://doi.org/10.1016/j.carbpol.2013.09.083

Fernandez-Avila, C., Gutierrez-Merida, C., & Trujillo, A. J. (2017). Physicochemical and sensory characteristics of a UHT milk-based product enriched with conjugated linoleic acid emulsified by Ultra-High Pressure Homogenization. *Innovative Food Science and Emerging Technologies*, *39*, 275–283. https://doi.org/10.1016/j.ifset.2017.01.001

Ferreira, C. D., da Conceição, E. J. L., Machado, B. A. S., Hermes, V. S., de Oliveira Rios, A., Druzian, J. I., & Nunes, I. L. (2016). Physicochemical Characterization and Oxidative Stability of Microencapsulated Crude Palm Oil by Spray Drying. *Food and Bioprocess Technology*, *9*(1), 124–136. https://doi.org/10.1007/s11947-015-1603-z

Fioramonti, S. A., Martinez, M. J., Pilosof, A. M. R., Rubiolo, A. C., & Santiago, L. G. (2015). Multilayer emulsions as a strategy for linseed oil microencapsulation: Effect of pH and alginate concentration. *Food Hydrocolloids*, *43*, 8–17. https://doi.org/10.1016/j.foodhyd.2014.04.026

Fioramonti, S. A., Rubiolo, A. C., & Santiago, L. G. (2017). Characterisation of freeze-dried flaxseed oil microcapsules obtained by multilayer emulsions. *Powder Technology*, *319*, 238–244. https://doi.org/10.1016/j.powtec.2017.06.052

Foegeding, E. A., & Davis, J. P. (2011). Food protein functionality: A comprehensive approach. *Food Hydrocolloids*, *25*(8), 1853–1864. https://doi.org/10.1016/j.foodhyd.2011.05.008

Fu, J. Y., Che, H. L., Tan, D. M. Y., & Teng, K. T. (2014). Bioavailability of tocotrienols: Evidence in human studies. *Nutrition and Metabolism*, *11*(1), 1–10. https://doi.org/10.1186/1743-7075-11-5

Gao, P., & Morozowich, W. (2006). Development of supersaturatable self-emulsifying drug delivery system formulations for improving the oral absorption of poorly soluble drugs. *Expert Opinion on Drug Delivery*, *3*(1), 97–110. https://doi.org/10.1517/17425247.3.1.97

Garnero, C., Aloisio, C., & Longhi, M. (2013). Ibuprofen-Maltodextrin Interaction: Study of Enantiomeric Recognition and Complex Characterization. *Pharmacology & Pharmacy*, *4*(1), 18–30. https://doi.org/10.4236/pp.2013.41003

Georgantelis, D., Ambrosiadis, I., Katikou, P., Blekas, G., & Georgakis, S. A. (2007). Effect of rosemary extract, chitosan and α-tocopherol on microbiological parameters and lipid oxidation of fresh pork sausages stored at 4 °C. *Meat Science*, *76*(1), 172–181. https://doi.org/10.1016/J.MEATSCI.2006.10.026

Gharsallaoui, A., Roudaut, G., Chambin, O., Voilley, A., & Saurel, R. (2007). Applications of spray-drying in microencapsulation of food ingredients: An overview. *Food Research International*, *40*(9), 1107–1121. https://doi.org/10.1016/j.foodres.2007.07.004

Ghosh, N., Das, A., & Khanna, S. (2020). Vitamin E: Tocopherols and tocotrienol and their role in health and disease. *Essential and Toxic Trace Elements and Vitamins in Human Health*, 283–293. https://doi.org/10.1016/B978-0-12-805378-2.00020-6

Gibbs, B. F., Kermasha, S., Alli, I., & Mulligan, C. N. (1999). Encapsulation in the food industry: A review. *International Journal of Food Sciences and Nutrition*, *50*(3), 213–224. https://doi.org/10.1080/096374899101256

Gibis, M., Rahn, N., & Weiss, J. (2013). Physical and oxidative stability of uncoated and chitosan-coated liposomes containing grape seed extract. *Pharmaceutics*, *5*(3), 421–433. https://doi.org/10.3390/pharmaceutics5030421

Goh, P. S., Ng, M. H., Choo, Y. M., Boyce, A. N., & Chuah, C. H. (2015). Production of nanoemulsions from palm-based tocotrienol rich fraction by microfluidization. *Molecules*, *20*(11), 19936–19946. https://doi.org/10.3390/molecules201119666

Gorji, S. G., Smyth, H. E., Sharma, M., & Fitzgerald, M. (2016). Lipid oxidation in mayonnaise and the role of natural antioxidants: a review. *Trends in Food Science & Technology*, *56*, 88-102. https://doi.org/10.1016/j.tifs.2016.08.002

Gothsch, T., Schilcher, C., Richter, C., Beinert, S., Dietzel, A., Büttgenbach, S., & Kwade, A. (2015). High-pressure microfluidic systems (HPMS): flow and cavitation measurements in supported silicon microsystems. *Microfluidics and Nanofluidics*, *18*(1), 121–130. https://doi.org/10.1007/s10404-014-1419-6

Graves, S., Meleson, K., Wilking, J., Lin, M. Y., & Mason, T. G. (2005). Structure of concentrated nanoemulsions. *Journal of Chemical Physics*, *122*(13), 134703. https://doi.org/10.1063/1.1874952

Guan, C., Wu, Y., Luo, L., Qiao, F., Zhu, J., Lin, Q., & Liu, C. (2023). Improvement of delivery properties of soybean 7S protein by high-pressure homogenization: In the case of curcumin. *International Journal of Biological Macromolecules*, *250*, 126255. https://doi.org/10.1016/J.IJBIOMAC.2023.126255

Guerra-Rosas, M. I., Morales-Castro, J., Cubero-Márquez, M. A., Salvia-Trujillo, L., & Martín-Belloso, O. (2017). Antimicrobial activity of nanoemulsions containing essential oils and high methoxyl pectin during long-term storage. *Food Control*, *77*, 131–138. https://doi.org/10.1016/j.foodcont.2017.02.008

Gumus, C. E., Decker, E. A., & McClements, D. J. (2017). Formation and Stability of ω-3 Oil Emulsion-Based Delivery Systems Using Plant Proteins as Emulsifiers: Lentil, Pea, and Faba Bean Proteins. *Food Biophysics*, *12*(2), 186–197. https://doi.org/10.1007/s11483-017-9475-6

Guo, L., Fan, L., Zhou, Y., & Li, J. (2023). Constitution and reconstitution of microcapsules with high diacylglycerol oil loading capacity based on whey protein isolate / octenyl succinic anhydride starch/ inulin matrix. *International Journal of Biological Macromolecules*, *242*, 124667. https://doi.org/10.1016/J.IJBIOMAC.2023.124667

Guo, Q., & Mu, T. H. (2011). Emulsifying properties of sweet potato protein: Effect of protein concentration and oil volume fraction. *Food Hydrocolloids*, *25*(1), 98–106. https://doi.org/10.1016/j.foodhyd.2010.05.011

Gursoy, R. N., & Benita, S. (2004). Self-emulsifying drug delivery systems (SEDDS) for improved oral delivery of lipophilic drugs. *Biomedicine & Pharmacotherapy*, *58*(3), 173–182. https://doi.org/10.1016/J.BIOPHA.2004.02.001

Gutiérrez, G., Matos, M., Barrero, P., Pando, D., Iglesias, O., & Pazos, C. (2016). Iron-entrapped niosomes and their potential application for yogurt fortification. *LWT*, *74*, 550–556. https://doi.org/10.1016/J.LWT.2016.08.025

Håkansson, A. (2018). Fabrication of Nanoemulsions by High-Pressure Valve Homogenization. In *Nanoemulsions: Formulation, Applications, and Characterization*, 175-206. https://doi.org/10.1016/B978-0-12-811838-2.00007-2

Håkansson, A., & Rayner, M. (2018). General Principles of Nanoemulsion Formation by High-Energy Mechanical Methods. In *Nanoemulsions: Formulation, Applications, and Characterization*. https://doi.org/10.1016/B978-0-12-811838-2.00005-9

Hermund, D. B., & Yes, B. (2015). *Characterisation and antioxidant evaluation of Icelandic F . vesiculosus extracts in vitro and in fish-oil-enriched milk and mayonnaise*, *19*, 828-841. https://doi.org/10.1016/j.jff.2015.02.020

Hill, S. E., Krishnamurthy, R. G., Hossain, A., & Shahidi, F. (2020). Cooking Oils, Salad Oils, and Dressings. In *Bailey's Industrial Oil and Fat Products*. https://doi.org/10.1002/047167849x.bio058.pub2

Hou, P., Pu, F., Zou, H., Diao, M., Zhao, C., Xi, C., & Zhang, T. (2019). Whey protein stabilized nanoemulsion: A potential delivery system for ginsenoside Rg3 whey protein stabilized nanoemulsion: Potential Rg3 delivery system. *Food Bioscience*, *31*, 100427. https://doi.org/10.1016/j.fbio.2019.100427

Hu, H., Wu, J., Li-Chan, E. C. Y., Zhu, L., Zhang, F., Xu, X., Fan, G., Wang, L., Huang, X., & Pan, S. (2013). Effects of ultrasound on structural and physical properties of

soy protein isolate (SPI) dispersions. *Food Hydrocolloids*, *30*(2), 647–655. https://doi.org/10.1016/j.foodhyd.2012.08.001

Hu, L., Hu, Q., & Yang, C. (2018). Spray-dried curcumin nanoemulsion: A new road to improvement of oral bioavailability of curcumin. *Pakistan Journal of Pharmaceutical Sciences*, *31*(1), 169–173.

Hu, X., Liu, L., Zhong, J., Liu, X., & Qin, X. (2024). Improved physicochemical properties and in vitro digestion of walnut oil microcapsules with soy protein isolate and highly oxidized konjac glucomannan as wall materials. *Food Chemistry*, *444*, 138640. https://doi.org/10.1016/J.FOODCHEM.2024.138640

Huang, X., Kakuda, Y., & Cui, W. (2001). Hydrocolloids in emulsions: Particle size distribution and interfacial activity. *Food Hydrocolloids*, *15*(4–6), 533–542. https://doi.org/10.1016/S0268-005X(01)00091-1

Huck-Iriart, C., Álvarez-Cerimedo, M. S., Candal, R. J., & Herrera, M. L. (2011). Structures and stability of lipid emulsions formulated with sodium caseinate. *Current Opinion in Colloid and Interface Science*, *16*(5), 412–420. https://doi.org/10.1016/j.cocis.2011.06.003

Ishwarya, S. P., & Anandharamakrishnan, C. (2015). Spray-Freeze-Drying approach for soluble coffee processing and its effect on quality characteristics. In *Journal of Food Engineering*, *149*, 171-180. https://doi.org/10.1016/j.jfoodeng.2014.10.011

Jafari, S. M., & McClements, D. J. (2017). Nanotechnology Approaches for Increasing Nutrient Bioavailability. In *Advances in Food and Nutrition Research, 81* (1), 1-30. https://doi.org/10.1016/bs.afnr.2016.12.008

Jafari, Seid Mahdi, Arpagaus, C., Cerqueira, M. A., & Samborska, K. (2021). Nano spray drying of food ingredients; materials, processing and applications. *Trends in Food Science and Technology*, *109*, 632–646. https://doi.org/10.1016/j.tifs.2021.01.061

Jafari, Seid Mahdi, Assadpoor, E., He, Y., & Bhandari, B. (2008). Encapsulation efficiency of food flavours and oils during spray drying. *Drying Technology*, *26*(7), 816–835. https://doi.org/10.1080/07373930802135972

Jaiswal, M., Dudhe, R., & Sharma, P. K. (2015). Nanoemulsion: an advanced mode of drug delivery system. *3 Biotech*, *5*(2), 123–127. https://doi.org/10.1007/s13205-014-0214-0

Jiang, J., Chen, J., & Xiong, Y. L. (2009). Structural and emulsifying properties of soy protein isolate subjected to acid and alkaline pH-shifting processes. *Journal of Agricultural and Food Chemistry*, *57*(16), 7576–7583. https://doi.org/10.1021/jf901585n

Jiang, J., Xiong, Y. L., & Chen, J. (2010). PH shifting alters solubility characteristics and thermal stability of soy protein isolate and its globulin fractions in different pH, salt concentration, and temperature conditions. *Journal of Agricultural and Food Chemistry*, *58*(13), 8035–8042. https://doi.org/10.1021/jf101045b

Jiang, J., Zhu, B., Liu, Y., & Xiong, Y. L. (2014). Interfacial structural role of pH-shifting processed pea protein in the oxidative stability of oil/water emulsions. *Journal of Agricultural and Food Chemistry*, *62*(7), 1683–1691. https://doi.org/10.1021/jf405190h

Jiang, S., Yildiz, G., Ding, J., Andrade, J., Rababahb, T. M., Almajwalc, A., Abulmeatyc, M. M., & Feng, H. (2019). Pea Protein Nanoemulsion and Nanocomplex as Carriers for Protection of Cholecalciferol (Vitamin D3). *Food and Bioprocess Technology*, *12*(6), 1031–1040. https://doi.org/10.1007/s11947-019-02276-0

Jourdain, L. S., Schmitt, C., Leser, M. E., Murray, B. S., & Dickinson, E. (2009). Mixed layers of sodium caseinate + dextran sulfate: Influence of order of addition to oil-water interface. *Langmuir*, *25*(17), 10026–10037. https://doi.org/10.1021/la900919w

Joye, I. J., & McClements, D. J. (2013). Production of nanoparticles by anti-solvent precipitation for use in food systems. *Trends in Food Science and Technology*, *34*(2), 109–123. https://doi.org/10.1016/j.tifs.2013.10.002

Julian McClements, D., Henson, L., Popplewell, L. M., Decker, E. A., & Jun Choi, S. (2012). Inhibition of Ostwald ripening in model beverage emulsions by addition of poorly water soluble triglyceride oils. *Journal of Food Science*, *77*(1), 33–38. https://doi.org/10.1111/j.1750-3841.2011.02484.x

Jyothi, N. V. N., Prasanna, P. M., Sakarkar, S. N., Prabha, K. S., Ramaiah, P. S., & Srawan, G. Y. (2010). Microencapsulation techniques, factors influencing encapsulation efficiency. *Journal of Microencapsulation*, *27*(3), 187–197. https://doi.org/10.3109/02652040903131301

Kalman, H. (2021). Effect of moisture content on flowability: Angle of repose, tilting angle, and Hausner ratio. *Powder Technology*, *393*, 582–596. https://doi.org/10.1016/j.powtec.2021.08.010

Kamer, D. D. A. (2024). Synergistic formulation approach for developing pea protein and guar gum enriched olive oil-in-water emulsion gels as solid fat substitutes: Formulation optimization, characterization, and molecular simulation. *International Journal of Biological Macromolecules*, *257*, 128718. https://doi.org/10.1016/J.IJBIOMAC.2023.128718

Karaca, A. C., Low, N., & Nickerson, M. (2011). Emulsifying properties of chickpea, faba bean, lentil and pea proteins produced by isoelectric precipitation and salt extraction. *Food Research International*, *44*(9), 2742–2750. https://doi.org/10.1016/j.foodres.2011.06.012

Karaca, A. C., Nickerson, M., & Low, N. H. (2013). Microcapsule production employing chickpea or lentil protein isolates and maltodextrin: Physicochemical properties and oxidative protection of encapsulated flaxseed oil. *Food Chemistry*, *139*(1–4), 448–457. https://doi.org/10.1016/j.foodchem.2013.01.040

Kato, A., Sato, T., & Kobayashi, K. (1989). Emulsifying properties of protein–polysaccharide complexes and hybrids. *Agricultural and Biological Chemistry*, *53*(8), 2147–2152. https://doi.org/10.1080/00021369.1989.10869639

Katouzian, I., & Jafari, S. M. (2016). Nano-encapsulation as a promising approach for targeted delivery and controlled release of vitamins. *Trends in Food Science and Technology*, *53*, 34–48. https://doi.org/10.1016/j.tifs.2016.05.002

Katsaros, G., Tsoukala, M., Giannoglou, M., & Taoukis, P. (2020). Effect of storage on the rheological and viscoelastic properties of mayonnaise emulsions of different oil droplet size. *Heliyon*, *6*(12), e05788. https://doi.org/10.1016/J.HELIYON.2020.E05788

Kelemen, K., Schuch, A. C., & Schuchmann, H. P. (2014). Influence of Flow Conditions in High-Pressure Orifices on Droplet Disruption of Oil-in-Water Emulsions. *Chemical Engineering and Technology*, *37*(7), 1227–1234. https://doi.org/10.1002/ceat.201400037

Kha, T. C., Nguyen, M. H., Roach, P. D., & Stathopoulos, C. E. (2015). A storage study of encapsulated gac (Momordica cochinchinensis) oil powder and its fortification into foods. *Food and Bioproducts Processing*, *96*, 113–125. https://doi.org/10.1016/J.FBP.2015.07.009

Kibici, D., & Kahveci, D. (2019). Effect of Emulsifier Type, Maltodextrin, and β-Cyclodextrin on Physical and Oxidative Stability of Oil-In-Water Emulsions. *Journal of Food Science*, *84*(6), 1273–1280. https://doi.org/10.1111/1750-3841.14619

Kim, W., Wang, Y., & Selomulya, C. (2022). Impact of sodium alginate on binary whey/pea protein-stabilised emulsions. *Journal of Food Engineering*, *321*, 110978. https://doi.org/10.1016/j.jfoodeng.2022.110978

Kim, Y. J., Kim, B. K., & Lee, M. H. (2022). Improving curcumin retention in oil-in-water emulsions coated by chitosan and their disperse stability exposed to thermal treatments. *Journal of Food Engineering*, *319*, 110918. https://doi.org/10.1016/J.JFOODENG.2021.110918

Kim, Y. J., Yong, H. I., Chun, Y. G., Kim, B. K., & Lee, M. H. (2024). Physicochemical characterization and environmental stability of a curcumin-loaded Pickering nanoemulsion using a pea protein isolate-dextran conjugate via the Maillard reaction. *Food Chemistry*, *436*, 137639. https://doi.org/10.1016/J.FOODCHEM.2023.137639

Ko, S. N., Kim, C. J., Kim, C. T., Kim, Y., & Kim, I. H. (2010). Effects of tocopherols and tocotrienols on the inhibition of autoxidation of conjugated linoleic acid. *European Journal of Lipid Science and Technology*, *112*(4), 496–501. https://doi.org/10.1002/ejlt.200900177

Komaiko, J. S., & Mcclements, D. J. (2016). Formation of Food-Grade Nanoemulsions Using Low-Energy Preparation Methods: A Review of Available Methods. *Comprehensive Reviews in Food Science and Food Safety*, *15*(2), 331–352. https://doi.org/10.1111/1541-4337.12189

Kong, M., Chen, X. G., Kweon, D. K., & Park, H. J. (2011). Investigations on skin permeation of hyaluronic acid based nanoemulsion as transdermal carrier.

Carbohydrate Polymers, *86*(2), 837–843. https://doi.org/10.1016/j.carbpol.2011.05.027

Korbelik, M., & Cooper, P. D. (2007). Potentiation of photodynamic therapy of cancer by complement: The effect of γ-inulin. *British Journal of Cancer*, *96*(1), 67–72. https://doi.org/10.1038/sj.bjc.6603508

Kornsteiner, M., Wagner, K. H., & Elmadfa, I. (2006). Tocopherols and total phenolics in 10 different nut types. *Food Chemistry*, *98*(2), 381–387. https://doi.org/10.1016/j.foodchem.2005.07.033

Kosasih, E. A., Dzaky, M. I., Zikri, A., Rachmanudiputra, A., Abizar, F., Fauzi, M. B., & Suharyadi, Y. S. (2023). Microencapsulation of maltodextrin and gelatin using spray drying with double-condenser compression refrigeration systems. *Case Studies in Thermal Engineering*, *45*, 102931. https://doi.org/10.1016/J.CSITE.2023.102931

Koyoro, H., & Powers, J. (1987). Functional Properties of Pea Globulin Fractions. In *Cereal chemistry*, *64*(2), 97-101.

Kuhn, K. R., Cavallieri, Â. L. F., & da Cunha, R. L. (2011). Cold-set whey protein-flaxseed gum gels induced by mono or divalent salt addition. *Food Hydrocolloids*, *25*(5), 1302–1310. https://doi.org/10.1016/j.foodhyd.2010.12.005

Kumar, H., & Kumar, V. (2018). Ultrasonication assisted formation and stability of water-in-oil nanoemulsions: Optimization and ternary diagram analysis. *Ultrasonics Sonochemistry*, *49*, 79–88. https://doi.org/10.1016/j.ultsonch.2018.07.022

Kumar, M., Bishnoi, R. S., Shukla, A. K., & Jain, C. P. (2019). Techniques for formulation of nanoemulsion drug delivery system: A review. *Preventive Nutrition and Food Science*, *24*(3), 225–234. https://doi.org/10.3746/pnf.2019.24.3.225

Lacerda, E. C. Q., Calado, V. M. D. A., Monteiro, M., Finotelli, P. V., Torres, A. G., & Perrone, D. (2016). Starch, inulin and maltodextrin as encapsulating agents affect the quality and stability of jussara pulp microparticles. *Carbohydrate Polymers*, *151*, 500–510. https://doi.org/10.1016/j.carbpol.2016.05.093

Lam, A. C. Y., Can Karaca, A., Tyler, R. T., & Nickerson, M. T. (2018). Pea protein isolates: Structure, extraction, and functionality. *Food Reviews International*, *34*(2), 126–147. https://doi.org/10.1080/87559129.2016.1242135

Lam, R. S. H., & Nickerson, M. T. (2013). Food proteins: A review on their emulsifying properties using a structure-function approach. *Food Chemistry*, *141*(2), 975–984. https://doi.org/10.1016/j.foodchem.2013.04.038

Laureanti, E. J. G., Paiva, T. S., de Matos Jorge, L. M., & Jorge, R. M. M. (2023). Microencapsulation of bioactive compound extracts using maltodextrin and gum arabic by spray and freeze-drying techniques. *International Journal of Biological Macromolecules*, *253*, 126969. https://doi.org/10.1016/J.IJBIOMAC.2023.126969

Lavine, E., & Ben-Shoshan, M. (2019). Anaphylaxis to hidden pea protein: A Canadian pediatric case series. *The Journal of Allergy and Clinical Immunology: In Practice*, *7*(6), 2070–2071. https://doi.org/10.1016/J.JAIP.2019.02.010

Le Priol, L., Dagmey, A., Morandat, S., Saleh, K., El Kirat, K., & Nesterenko, A. (2019). Comparative study of plant protein extracts as wall materials for the improvement of the oxidative stability of sunflower oil by microencapsulation. *Food Hydrocolloids*, *95*, 105–115. https://doi.org/10.1016/j.foodhyd.2019.04.026

Leal-Calderon, F., Thivilliers, F., & Schmitt, V. (2007). Structured emulsions. *Current Opinion in Colloid and Interface Science*, *12*(4–5), 206–212. https://doi.org/10.1016/j.cocis.2007.07.003

Lee, W. J., Tan, C. P., Sulaiman, R., Hee, Y. Y., & Chong, G. H. (2020). Storage stability and degradation kinetics of bioactive compounds in red palm oil microcapsules produced with solution-enhanced dispersion by supercritical carbon dioxide: A comparison with the spray-drying method. *Food Chemistry*, *304*, 125427. https://doi.org/10.1016/j.foodchem.2019.125427

Lefebvre, G., Riou, J., Bastiat, G., Roger, E., Frombach, K., Gimel, J. C., Saulnier, P., & Calvignac, B. (2017). Spontaneous nano-emulsification: Process optimization and modeling for the prediction of the nanoemulsion's size and polydispersity. *International Journal of Pharmaceutics*, *534*(1–2), 220–228. https://doi.org/10.1016/J.IJPHARM.2017.10.017

Leonard, S. W., Paterson, E., Atkinson, J. K., Ramakrishnan, R., Cross, C. E., & Traber, M. G. (2005). Studies in humans using deuterium-labeled α- and γ-tocopherols demonstrate faster plasma γ-tocopherol disappearance and greater γ-metabolite production. *Free Radical Biology and Medicine*, *38*(7), 857–866. https://doi.org/10.1016/j.freeradbiomed.2004.12.001

Let, M. B., Jacobsen, C., & Meyer, A. S. (2007). Ascorbyl palmitate, γ-tocopherol, and EDTA affect lipid oxidation in fish oil enriched salad dressing differently. *Journal of Agricultural and Food Chemistry*, *55*(6), 2369–2375. https://doi.org/10.1021/jf062675c

Leyva-porras, C., López-pablos, A. L., Alvarez-salas, C., & Pérez-urizar, J. (2014). Polysaccharides. *Polysaccharides*, 1–22. https://doi.org/10.1007/978-3-319-03751-6

Li, C. Y., Kim, H. W., Li, H., Lee, D. C., & Rhee, H. I. (2014). Antioxidative effect of purple corn extracts during storage of mayonnaise. *Food Chemistry*, *152*, 592–596. https://doi.org/10.1016/j.foodchem.2013.11.152

Li, S., Zhu, Y., Hao, X., Su, H., Chen, X., & Yao, Y. (2024). High internal phase Pickering emulsions stabilized by the complexes of ultrasound-treated pea protein isolate/mung bean starch for delivery of β-carotene. *Food Chemistry*, *440*, 138201. https://doi.org/10.1016/J.FOODCHEM.2023.138201

Li, Z., Cao, Y., Wang, Y., Li, Y., Liu, Z., Zhu, Z., Zhang, H., Huang, J., & Xiong, Y. (2024). The effects of resonance acoustic mixing modulation on the structural and

emulsifying properties of pea protein isolate. *Food Chemistry*, 138541. https://doi.org/10.1016/J.FOODCHEM.2024.138541

Liang, S., Huang, Y., Shim, Y. Y., Ma, X., Reaney, M. J. T., & Wang, Y. (2018). Novel Flaxseed Gum Nanocomposites Are Slow Release Iron Supplements. *Journal of Agricultural and Food Chemistry*, *66*(20), 5167–5177. https://doi.org/10.1021/acs.jafc.8b01347

Lim, S. S., Baik, M. Y., Decker, E. A., Henson, L., Michael Popplewell, L., McClements, D. J., & Choi, S. J. (2011). Stabilization of orange oil-in-water emulsions: A new role for ester gum as an Ostwald ripening inhibitor. *Food Chemistry*, *128*(4), 1023–1028. https://doi.org/10.1016/j.foodchem.2011.04.008

Lim, W. S., Lim, N., Kim, Y. J., Woo, J. H., Park, H. J., & Lee, M. H. (2024). A cholecalciferol-loaded emulsion stabilized by a pea protein isolate–inulin complex and its application in 3D food printing. *Journal of Food Engineering*, *364*, 111811. https://doi.org/10.1016/J.JFOODENG.2023.111811

Liu, Caihua, Sun, F., Tian, Y., Jiang, L., Wang, Z., & Zhou, L. (2024). Recovery of soy whey protein from soy whey wastewater at various cavitation jet pretreatment time and their structural and emulsifying properties. *Food Chemistry: X*, *21*, 101122. https://doi.org/10.1016/J.FOCHX.2024.101122

Liu, Chang, Pei, R., Peltonen, L., & Heinonen, M. (2020). Assembling of the interfacial layer affects the physical and oxidative stability of faba bean protein-stabilized oil-in-water emulsions with chitosan. *Food Hydrocolloids*, *102*, 105614. https://doi.org/10.1016/j.foodhyd.2019.105614

Liu, J., Shim, Y. Y., Poth, A. G., & Reaney, M. J. T. (2016). Conlinin in flaxseed (Linum usitatissimum L.) gum and its contribution to emulsification properties. *Food Hydrocolloids*, *52*, 963–971. https://doi.org/10.1016/j.foodhyd.2015.09.001

Liu, J., Shim, Y. Y., Shen, J., Wang, Y., Ghosh, S., & Reaney, M. J. T. (2016). Variation of composition and functional properties of gum from six Canadian flaxseed (Linum usitatissimum L.) cultivars. *International Journal of Food Science and Technology*, *51*(10), 2313–2326. https://doi.org/10.1111/ijfs.13200

Liu, J., Shim, Y. Y., Shen, J., Wang, Y., & Reaney, M. J. T. (2017). Whey protein isolate and flaxseed (Linum usitatissimum L.) gum electrostatic coacervates: Turbidity and rheology. *Food Hydrocolloids*, *64*, 18–27. https://doi.org/10.1016/j.foodhyd.2016.10.006

Liu, J., Shim, Y. Y., Tse, T. J., Wang, Y., & Reaney, M. J. T. (2018a). Flaxseed gum a versatile natural hydrocolloid for food and non-food applications. *Trends in Food Science and Technology*, *75*, 146–157. https://doi.org/10.1016/j.tifs.2018.01.011

Liu, J., Shim, Y. Y., Wang, Y., & Reaney, M. J. T. (2015). Intermolecular interaction and complex coacervation between bovine serum albumin and gum from whole flaxseed (Linum usitatissimum L.). *Food Hydrocolloids*, *49*, 95–103. https://doi.org/10.1016/j.foodhyd.2015.02.035

Liu, S., Elmer, C., Low, N. H., & Nickerson, M. T. (2010). Effect of pH on the functional behaviour of pea protein isolate-gum Arabic complexes. *Food Research International*, *43*(2), 489–495. https://doi.org/10.1016/j.foodres.2009.07.022

Liu, X. Y., He, T. S., Wang, C. C., Xu, B. C., Feng, R., Zhang, B., & Tao, H. (2024). Modulation of pea protein isolate nanoparticles by interaction with OSA-corn starch: Enhancing the stability of the constructed Pickering emulsions. *Food Chemistry*, *437*, 137766. https://doi.org/10.1016/J.FOODCHEM.2023.137766

Long, H., Bi, Y., Pu, L., Xu, W., Xue, H., Fu, G., & Prusky, D. (2022). Preparation of chitosan/ fennel seed essential oil/ starch sodium octenyl succinate composite films for apple fruit preservation. *Lwt*, *167*, 113826. https://doi.org/10.1016/j.lwt.2022.113826

López-Molina, D., Chazarra, S., How, C. W., Pruidze, N., Navarro-Perán, E., García-Cánovas, F., García-Ruiz, P. A., Rojas-Melgarejo, F., & Rodríguez-López, J. N. (2015). Cinnamate of inulin as a vehicle for delivery of colonic drugs. *International Journal of Pharmaceutics*, *479*(1), 96–102. https://doi.org/10.1016/j.ijpharm.2014.12.064

Luo, H., Zhou, X., Ellingford, C., Zhang, Y., Chen, S., Zhou, K., Zhang, D., Bowen, C. R., & Wan, C. (2019). Interface design for high energy density polymer nanocomposites. *Chemical Society Reviews*, *48*(16), 4424–4465. https://doi.org/10.1039/c9cs00043g

Łupina, K., Kowalczyk, D., Lis, M., Raszkowska-Kaczor, A., & Drozłowska, E. (2022). Controlled release of water-soluble astaxanthin from carboxymethyl cellulose/gelatin and octenyl succinic anhydride starch/gelatin blend films. *Food Hydrocolloids*, *123*, 107179. https://doi.org/10.1016/j.foodhyd.2021.107179

Makri, E., Papalamprou, E., & Doxastakis, G. (2005). Study of functional properties of seed storage proteins from indigenous European legume crops (lupin, pea, broad bean) in admixture with polysaccharides. *Food Hydrocolloids*, *19*(3), 583–594. https://doi.org/10.1016/j.foodhyd.2004.10.028

Maqsoudlou, A., Sadeghi Mahoonak, A., Mohebodini, H., & Koushki, V. (2020). Stability and structural properties of bee pollen protein hydrolysate microencapsulated using maltodextrin and whey protein concentrate. *Heliyon*, *6*(5), e03731. https://doi.org/10.1016/J.HELIYON.2020.E03731

Marion M. Bradford. (1976). A rapid and sensitive method for the quantitation of microgram quantities of protein utilizing the principle of protein-dye binding. *Analytical Biochemistry*, *72*(5), 248–254. https://doi.org/10.1016/0003-2697(76)90527-3

Mba, O. I., Dumont, M. J., & Ngadi, M. (2018). Characterization of tocopherols, tocotrienols and total carotenoids in deep-fat fried French fries. *Journal of Food Composition and Analysis*, *69*, 78–86. https://doi.org/10.1016/J.JFCA.2018.02.011

McClements, D. J. (2004). Food emulsions: Principles, practices, and techniques: Second edition. In *Food Emulsions: Principles, Practices, and Techniques, Second Edition*.

McClements, D. J. (2011). Edible nanoemulsions: Fabrication, properties, and functional performance. *Soft Matter*, *7*(6), 2297–2316. https://doi.org/10.1039/c0sm00549e

McClements, D. J., Bai, L., & Chung, C. (2017). Recent Advances in the Utilization of Natural Emulsifiers to Form and Stabilize Emulsions. *Annual Review of Food Science and Technology*, *8*(1), 205–236. https://doi.org/10.1146/annurev-food-030216-030154

McClements, D. J., & Gumus, C. E. (2016). Natural emulsifiers — Biosurfactants, phospholipids, biopolymers, and colloidal particles: Molecular and physicochemical basis of functional performance. *Advances in Colloid and Interface Science*, *234*, 3–26. https://doi.org/10.1016/j.cis.2016.03.002

McClements, D. J., & Jafari, S. M. (2018). Improving emulsion formation, stability and performance using mixed emulsifiers: A review. *Advances in Colloid and Interface Science*, *251*, 55–79. https://doi.org/10.1016/j.cis.2017.12.001

McClements, D. J., & Rao, J. (2011). Food-Grade nanoemulsions: Formulation, fabrication, properties, performance, Biological fate, and Potential Toxicity. *Critical Reviews in Food Science and Nutrition*, *51*(4), 285–330. https://doi.org/10.1080/10408398.2011.559558

McClements, D. J., & Xiao, H. (2012). Potential biological fate of ingested nanoemulsions: Influence of particle characteristics. *Food and Function*, *3*(3), 202–220. https://doi.org/10.1039/c1fo10193e

McClements, J. D., Decker, E. A., & Weiss, J. (2007). Emulsion-based delivery systems for lipophilic bioactive components. *Journal of Food Science*, *72*(8), 109–124. https://doi.org/10.1111/j.1750-3841.2007.00507.x

Meganathan, P., & Fu, J. Y. (2016). Biological properties of tocotrienols: Evidence in human studies. *International Journal of Molecular Sciences*, *17*(11), 1682. https://doi.org/10.3390/ijms17111682

Melchior, S., Codrich, M., Gorassini, A., Mehn, D., Ponti, J., Verardo, G., Tell, G., Calzolai, L., & Calligaris, S. (2023). Design and advanced characterization of quercetin-loaded nano-liposomes prepared by high-pressure homogenization. *Food Chemistry*, *428*, 136680. https://doi.org/10.1016/J.FOODCHEM.2023.136680

Miguel, G. A., Jacobsen, C., Prieto, C., Kempen, P. J., Lagaron, J. M., Chronakis, I. S., & García-Moreno, P. J. (2019). Oxidative stability and physical properties of mayonnaise fortified with zein electrosprayed capsules loaded with fish oil. *Journal of Food Engineering*, *263*, 348–358. https://doi.org/10.1016/j.jfoodeng.2019.07.019

Moretton, M., Alongi, M., Renoldi, N., & Anese, M. (2023). Steering protein and carbohydrate digestibility by food design to address elderly needs: The case of pea protein enriched bread. *LWT*, *190*, 115530. https://doi.org/10.1016/J.LWT.2023.115530

Murúa-Pagola, B., Beristain-Guevara, C. I., & Martínez-Bustos, F. (2009). Preparation of starch derivatives using reactive extrusion and evaluation of modified starches as

shell materials for encapsulation of flavoring agents by spray drying. *Journal of Food Engineering*, *91*(3), 380–386. https://doi.org/10.1016/j.jfoodeng.2008.09.035

Musa, I., Khaza'ai, H., Abdul Mutalib, M. S., Yusuf, F., Sanusi, J., & Chang, S. K. (2017). Effects of oil palm tocotrienol rich fraction on the viability and morphology of astrocytes injured with glutamate. *Food Bioscience*, *20*, 168–177. https://doi.org/10.1016/j.fbio.2017.10.005

Nakano, Y., Tajima, M., Sugiyama, E., Sato, V. H., & Sato, H. (2019). Development of a Novel Nano-emulsion Formulation to Improve Intestinal Absorption of Cannabidiol. *Medical Cannabis and Cannabinoids*, *2*(1), 35–42. https://doi.org/10.1159/000497361

Nankar, R. P., Raman, M., & Doble, M. (2016). Nanoformulations of polyphenols for prevention and treatment of cardiovascular and metabolic disorders. In *Emulsions. 3*, 107-151. https://doi.org/10.1016/b978-0-12-804306-6.00004-0

Nguyen, Q. D., Dang, T. T., Nguyen, T. V. L., Nguyen, T. T. D., & Nguyen, N. N. (2022). Microencapsulation of roselle (Hibiscus sabdariffa L.) anthocyanins: Effects of different carriers on selected physicochemical properties and antioxidant activities of spray-dried and freeze-dried powder. *International Journal of Food Properties*, *25*(1), 359–374. https://doi.org/10.1080/10942912.2022.2044846

Nunes, G. L., Etchepare, M. de A., Cichoski, A. J., Zepka, L. Q., Jacob Lopes, E., Barin, J. S., Flores, É. M. de M., da Silva, C. de B., & de Menezes, C. R. (2018). Inulin, hi-maize, and trehalose as thermal protectants for increasing viability of Lactobacillus acidophilus encapsulated by spray drying. *LWT*, *89*, 128–133. https://doi.org/10.1016/J.LWT.2017.10.032

O'Sullivan, J., Murray, B., Flynn, C., & Norton, I. (2016). The effect of ultrasound treatment on the structural, physical and emulsifying properties of animal and vegetable proteins. *Food Hydrocolloids*, *53*, 141–154. https://doi.org/10.1016/j.foodhyd.2015.02.009

Ozcelik, M., Ambros, S., Heigl, A., Dachmann, E., & Kulozik, U. (2019). Impact of hydrocolloid addition and microwave processing condition on drying behavior of foamed raspberry puree. In *Journal of Food Engineering 240*, 83-91. https://doi.org/10.1016/j.jfoodeng.2018.07.001

Ozturk, B., Argin, S., Ozilgen, M., & McClements, D. J. (2014). Formation and stabilization of nanoemulsion-based vitamin e delivery systems using natural surfactants: Quillaja saponin and lecithin. *Journal of Food Engineering*, *142*, 57–63. https://doi.org/10.1016/j.jfoodeng.2014.06.015

Ozturk, B., Argin, S., Ozilgen, M., & McClements, D. J. (2015). Nanoemulsion delivery systems for oil-soluble vitamins: Influence of carrier oil type on lipid digestion and vitamin D3 bioaccessibility. *Food Chemistry*, *187*, 499–506. https://doi.org/10.1016/j.foodchem.2015.04.065

Ozturk, B., & McClements, D. J. (2016). Progress in natural emulsifiers for utilization in food emulsions. *Current Opinion in Food Science*, *7*, 1–6. https://doi.org/10.1016/j.cofs.2015.07.008

Padial-Domínguez, M., Espejo-Carpio, F. J., Pérez-Gálvez, R., Guadix, A., & Guadix, E. M. (2020). Optimization of the emulsifying properties of food protein hydrolysates for the production of fish oil-in-water emulsions. *Foods*, *9*(5), 636. https://doi.org/10.3390/foods9050636

Pang, K. L., & Chin, K. Y. (2019). The role of tocotrienol in protecting against metabolic diseases. *Molecules*, *24*(5), 923. https://doi.org/10.3390/molecules24050923

Park, S. H., Hong, C. R., & Choi, S. J. (2020). Prevention of Ostwald ripening in orange oil emulsions: Impact of surfactant type and Ostwald ripening inhibitor type. *LWT*, *134*, 110180. https://doi.org/10.1016/J.LWT.2020.110180

Park, S. K., Sanders, B. G., & Kline, K. (2010). Tocotrienols induce apoptosis in breast cancer cell lines via an endoplasmic reticulum stress-dependent increase in extrinsic death receptor signaling. *Breast Cancer Research and Treatment*, *124*(2), 361–375. https://doi.org/10.1007/s10549-010-0786-2

Paulo, F., & Santos, L. (2017). Design of experiments for microencapsulation applications: A review. *Materials Science and Engineering C*, *77*, 1327–1340. https://doi.org/10.1016/j.msec.2017.03.219

Paulo, L. A. de O., Fernandes, R. N., Simiqueli, A. A., Rocha, F., Dias, M. M. dos S., Minim, V. P. R., Minim, L. A., & Vidigal, M. C. T. R. (2023). Baru oil (Dipteryx alata vog.) applied in the formation of O/W nanoemulsions: A study of physical-chemical, rheological and interfacial properties. *Food Research International*, *170*, 112961. https://doi.org/10.1016/J.FOODRES.2023.112961

Peh, H. Y., Tan, W. S. D., Liao, W., & Wong, W. S. F. (2016). Vitamin E therapy beyond cancer: Tocopherol versus tocotrienol. *Pharmacology and Therapeutics*, *162*, 152–169. https://doi.org/10.1016/j.pharmthera.2015.12.003

Pennock, J. F. (1964). A Reassessment of Tocopherol Chemistry. *Journal of Chemical Information and Modeling*, *17*(5), 542–548. https://doi.org/10.1017/CBO9781107415324.004

Perrechil, F. A., & Cunha, R. L. (2010). Oil-in-water emulsions stabilized by sodium caseinate: Influence of pH, high-pressure homogenization and locust bean gum addition. *Journal of Food Engineering*, *97*(4), 441–448. https://doi.org/10.1016/j.jfoodeng.2009.10.041

Pierpaoli, E., Viola, V., Pilolli, F., Piroddi, M., Galli, F., & Provinciali, M. (2010). γ- and δ-tocotrienols exert a more potent anticancer effect than α-tocopheryl succinate on breast cancer cell lines irrespective of HER-2/neu expression. *Life Sciences*, *86*(17–18), 668–675. https://doi.org/10.1016/j.lfs.2010.02.018

Plankensteiner, L., Hennebelle, M., Vincken, J. P., & Nikiforidis, C. V. (2024). Insights into the emulsification mechanism of the surfactant-like protein oleosin. *Journal of Colloid and Interface Science*, *657*, 352–362. https://doi.org/10.1016/J.JCIS.2023.11.165

Poozesh, S., Jafari, S. M., & Akafuah, N. K. (2020). d powders of a lab-scale spray dryer. *Powder Technology*, *373*, 590–598. https://doi.org/10.1016/j.powtec.2020.07.012

Pratt, D. A., Tallman, K. A., & Porter, N. A. (2011). Free radical oxidation of polyunsaturated lipids: New mechanistic insights and the development of peroxyl radical clocks. *Accounts of Chemical Research*, *44*(6), 458–467. https://doi.org/10.1021/ar200024c

Qian, K. Y., Cui, S. W., Wu, Y., & Goff, H. D. (2012). Flaxseed gum from flaxseed hulls: Extraction, fractionation, and characterization. *Food Hydrocolloids*, *28*(2), 275–283. https://doi.org/10.1016/j.foodhyd.2011.12.019

Quek, S. Y., Chok, N. K., & Swedlund, P. (2007). The physicochemical properties of spray-dried watermelon powders. *Chemical Engineering and Processing: Process Intensification*, *46*(5), 386–392. https://doi.org/10.1016/j.cep.2006.06.020

Rabbani, M., Pezeshki, A., Ahmadi, R., Mohammadi, M., Tabibiazar, M., Ahmadzadeh Nobari Azar, F., & Ghorbani, M. (2021). Phytosomal nanocarriers for encapsulation and delivery of resveratrol- Preparation, characterization, and application in mayonnaise. *Lwt*, *151*, 112093. https://doi.org/10.1016/j.lwt.2021.112093

Rafiee, Z., & Jafari, S. M. (2018). *Application of Lipid Nanocarriers for the Food Industry BT - Bioactive Molecules in Food*. https://doi.org/10.1007/978-3-319-54528-8_93-1

Rautenberg, A., & Lamprecht, A. (2022). Spray-freeze-dried lyospheres: Solid content and the impact on flowability and mechanical stability. *Powder Technology*, *411*, 117905. https://doi.org/10.1016/j.powtec.2022.117905

Rehman, A., Tong, Q., Jafari, S. M., Korma, S. A., Khan, I. M., Mohsin, A., Manzoor, M. F., Ashraf, W., Mushtaq, B. S., Zainab, S., & Cacciotti, I. (2021). Spray dried nanoemulsions loaded with curcumin, resveratrol, and borage seed oil: The role of two different modified starches as encapsulating materials. *International Journal of Biological Macromolecules*, *186*, 820–828. https://doi.org/10.1016/j.ijbiomac.2021.07.076

Ribes, S., Fuentes, A., & Barat, J. M. (2019). Effect of oregano (Origanum vulgare L. ssp. hirtum)and clove (Eugenia spp.)nanoemulsions on Zygosaccharomyces bailii survival in salad dressings. *Food Chemistry*, *295*, 630–636. https://doi.org/10.1016/j.foodchem.2019.05.173

Ribes, S., Fuentes, A., Talens, P., & Barat, J. M. (2017). Application of cinnamon bark emulsions to protect strawberry jam from fungi. *LWT - Food Science and Technology*, *78*, 265–272. https://doi.org/10.1016/j.lwt.2016.12.047

Ricaurte, L., Perea-Flores, M. D. J., Martinez, A., & Quintanilla-Carvajal, M. X. (2016). Production of high-oleic palm oil nanoemulsions by high-shear homogenization (microfluidization). *Innovative Food Science and Emerging Technologies*, *35*(March), 75–85. https://doi.org/10.1016/j.ifset.2016.04.004

Richard, C., Jacquenet, S., Sergeant, P., & Moneret-Vautrin, D. A. (2015). Cross-reactivity of a new food ingredient, dun pea, with legumes, and risk of anaphylaxis in legume allergic children. *European Annals of Allergy and Clinical Immunology*, *47*(4), 118–125.

Rosolen, M. D., Bordini, F. W., de Oliveira, P. D., Conceição, F. R., Pohndorf, R. S., Fiorentini, Â. M., da Silva, W. P., & Pieniz, S. (2019). Symbiotic microencapsulation of Lactococcus lactis subsp. lactis R7 using whey and inulin by spray drying. *LWT*, *115*, 108411. https://doi.org/10.1016/J.LWT.2019.108411

Saavedra-Leos, M. Z., Román-Aguirre, M., Toxqui-Terán, A., Espinosa-Solís, V., Franco-Vega, A., & Leyva-Porras, C. (2022). Blends of Carbohydrate Polymers for the Co-Microencapsulation of Bacillus clausii and Quercetin as Active Ingredients of a Functional Food. *Polymers*, *14*(2), 236. https://doi.org/10.3390/polym14020236

Saavedra-Leos, Z., Leyva-Porras, C., Araujo-Díaz, S. B., Toxqui-Terán, A., & Borrás-Enríquez, A. J. (2015). Technological application of maltodextrins according to the degree of polymerization. *Molecules*, *20*(12), 21067–21081. https://doi.org/10.3390/molecules201219746

Sabliov, C. M., Fronczek, C., Astete, C. E., Khachaturyan, M., Khachatryan, L., & Leonardi, C. (2009). Effects of Temperature and UV Light on Degradation of α-Tocopherol in Free and Dissolved Form. *JAOCS, Journal of the American Oil Chemists' Society*, *86*(9), 895–902. https://doi.org/10.1007/s11746-009-1411-6

Saénz, C., Tapia, S., Chávez, J., & Robert, P. (2009). Microencapsulation by spray drying of bioactive compounds from cactus pear (Opuntia ficus-indica). *Food Chemistry*, *114*(2), 616–622. https://doi.org/10.1016/j.foodchem.2008.09.095

Sail, A. M., Wan Mustapha, W. A., Yusop, S. M., Maskat, M. Y., & Shamsuddin, A. F. (2018). Optimisation of cinnamaldehyde-in-water nanoemulsion formulation using central composite rotatable design. *Sains Malaysiana*, *47*(9), 1999–2008. https://doi.org/10.17576/jsm-2018-4709-07

Saini, R. K., & Keum, Y. S. (2016). Tocopherols and tocotrienols in plants and their products: A review on methods of extraction, chromatographic separation, and detection. *Food Research International*, *82*, 59–70. https://doi.org/10.1016/j.foodres.2016.01.025

Samborska, K., Witrowa-Rajchert, D., & Gonçalves, A. (2005). Spray-drying of α-amylase - The effect of process variables on the enzyme inactivation. *Drying Technology*, *23*(4), 941–953. https://doi.org/10.1081/DRT-200054243

Santiago-Adame, R., Medina-Torres, L., Gallegos-Infante, J. A., Calderas, F., González-Laredo, R. F., Rocha-Guzmán, N. E., Ochoa-Martínez, L. A., & Bernad-Bernad, M. J. (2015). Spray drying-microencapsulation of cinnamon infusions (Cinnamomum zeylanicum) with maltodextrin. *Lwt*, *64*(2), 571–577. https://doi.org/10.1016/j.lwt.2015.06.020

Saricaoglu, F. T., Atalar, I., Yilmaz, V. A., Odabas, H. I., & Gul, O. (2019). Application of multi pass high pressure homogenization to improve stability, physical and bioactive properties of rosehip (Rosa canina L.) nectar. *Food Chemistry*, *282*, 67–75. https://doi.org/10.1016/J.FOODCHEM.2019.01.002

Selvaraju, T. R., Khaza'ai, H., Vidyadaran, S., Mutalib, M. S. A., & Vasudevan, R. (2014). The neuroprotective effects of tocotrienol rich fraction and alpha tocopherol

against glutamate injury in astrocytes. *Bosnian Journal of Basic Medical Sciences*, *14*(4), 195–204. https://doi.org/10.17305/bjbms.2014.4.91

Sen, C. K., Rink, C., & Khanna, S. (2010). Palm oil–derived natural vitamin e α-tocotrienol in brain health and disease. *Journal of the American College of Nutrition*, *29*, 314S-323S. https://doi.org/10.1080/07315724.2010.10719846

Sha, L., Koosis, A. O., Wang, Q., True, A. D., & Xiong, Y. L. (2021). Interfacial dilatational and emulsifying properties of ultrasound-treated pea protein. *Food Chemistry*, *350*, 129271. https://doi.org/10.1016/J.FOODCHEM.2021.129271

Shahidi, F., & De Camargo, A. C. (2016). Tocopherols and tocotrienols in common and emerging dietary sources: Occurrence, applications, and health benefits. *International Journal of Molecular Sciences*, *17*(10), 1–29. https://doi.org/10.3390/ijms17101745

Shahidi, F., & Han, X. Q. (1993). Encapsulation of Food Ingredients. *Critical Reviews in Food Science and Nutrition*, *33*(6), 501–547. https://doi.org/10.1080/10408399309527645

Shantha, N. C., & Decker, E. A. (1994). Rapid, sensitive, iron-based spectrophotometric methods for determination of peroxide values of food lipids. *Journal of AOAC International*, *77*(2), 421–424. https://doi.org/10.1093/jaoac/77.2.421

Shao, Y., Tang, C. H., Almajwal, A. M., Abulmeaty, M. M. A., Feng, H., Alruwaili, N. W., Dominguez-Uscanga, A., Andrade, J. E., Razak, S., Elsadek, M. F., Li, Y., Jin, H., Sun, X., Sun, J., Liu, C. C., Liu, C. C., Xu, J., Walia, N., Chen, L., Nickerson, M. T. (2019). Physicochemical properties and storage stability of food protein-stabilized nanoemulsions. *Food Research International*, *12*(1), 175–185. https://doi.org/10.1016/j.foodres.2017.11.033

Sharif, H. R., Williams, P. A., Sharif, M. K., Khan, M. A., Majeed, H., Safdar, W., Shamoon, M., Shoaib, M., Haider, J., & Zhong, F. (2017). Influence of OSA-starch on the physico chemical characteristics of flax seed oil-eugenol nanoemulsions. *Food Hydrocolloids*, *66*, 365–377. https://doi.org/10.1016/j.foodhyd.2016.12.002

Shepherd, R., Robertson, A., & Ofman, D. (2000). Dairy glycoconjugate emulsifiers: Casein-maltodextrins. *Food Hydrocolloids*, *14*(4), 281–286. https://doi.org/10.1016/S0268-005X(99)00067-3

Shevkani, K., Singh, N., Kaur, A., & Rana, J. C. (2015). Structural and functional characterization of kidney bean and field pea protein isolates: A comparative study. *Food Hydrocolloids*, *43*, 679–689. https://doi.org/10.1016/j.foodhyd.2014.07.024

Silva, E. K., Zabot, G. L., Bargas, M. A., & Meireles, M. A. A. (2016). Microencapsulation of lipophilic bioactive compounds using prebiotic carbohydrates: Effect of the degree of inulin polymerization. *Carbohydrate Polymers*, *152*, 775–783. https://doi.org/10.1016/j.carbpol.2016.07.066

Simonazzi, A., Cid, A. G., Villegas, M., Romero, A. I., Palma, S. D., & Bermúdez, J. M. (2018). Nanotechnology applications in drug controlled release. In *Drug Targeting*

and Stimuli Sensitive Drug Delivery Systems, 81-116. https://doi.org/10.1016/B978-0-12-813689-8.00003-3

Solans, C., & Solé, I. (2012). Nano-emulsions: Formation by low-energy methods. *Current Opinion in Colloid and Interface Science*, *17*(5), 246–254. https://doi.org/10.1016/j.cocis.2012.07.003

Song, F., Li, Y., Wang, B., Shen, X., Wang, H., Li, R., & Xia, Q. (2022). Effect of drying method and wall material composition on the characteristics of camellia seed oil microcapsule powder. *JAOCS, Journal of the American Oil Chemists' Society*, *99*(4), 353–364. https://doi.org/10.1002/aocs.12569

Song, H. Y., & McClements, D. J. (2021). Nano-enabled-fortification of salad dressings with curcumin: Impact of nanoemulsion-based delivery systems on physicochemical properties. *Lwt*, *145*, 111299. https://doi.org/10.1016/j.lwt.2021.111299

Song, X., He, G., Ruan, H., & Chen, Q. (2006). Preparation and properties of octenyl succinic anhydride modified early indica rice starch. *Starch/Staerke*, *58*(2), 109–117. https://doi.org/10.1002/star.200500444

Stone, A. K., Avarmenko, N. A., Warkentin, T. D., & Nickerson, M. T. (2015). Functional properties of protein isolates from different pea cultivars. *Food Science and Biotechnology*, *24*(3), 827–833. https://doi.org/10.1007/s10068-015-0107-y

Stone, A. K., & Nickerson, M. T. (2012). Formation and functionality of whey protein isolate-(kappa-, iota-, and lambda-type) carrageenan electrostatic complexes. *Food Hydrocolloids*, *27*(2), 271–277. https://doi.org/10.1016/j.foodhyd.2011.08.006

Sultana, M., Chan, E. S., Janarthanan, P., & Choo, W. S. (2023). Functional orange juice with Lactobacillus casei and tocotrienol-enriched flaxseed oil co-encapsulation: Physicochemical properties, probiotic viability, oxidative stability, and sensorial acceptability. *Lwt*, *188*, 115388. https://doi.org/10.1016/j.lwt.2023.115388

Sun, H., Ma, Y., Huang, X., Song, L., Guo, H., Sun, X., Li, N., & Qiao, M. (2023). Stabilization of flaxseed oil nanoemulsions based on flaxseed gum: Effects of temperature, pH and NaCl on stability. *LWT*, *176*, 114512. https://doi.org/10.1016/J.LWT.2023.114512

Sun, M., Li, X., McClements, D. J., Xiao, M., Chen, H., Zhou, Q., Xu, S., Chen, Y., & Deng, Q. (2022). Reducing off-flavors in plant-based omega-3 oil emulsions using interfacial engineering: Coating algae oil droplets with pea protein/flaxseed gum. *Food Hydrocolloids*, *122*, 107069. https://doi.org/10.1016/J.FOODHYD.2021.107069

Sun, Z., Yin, S., Zhao, C., Fan, L., & Hu, H. (2022). Biochemical and Biophysical Research Communications Inhibition of PD-L1-mediated tumor-promoting signaling is involved in the anti-cancer activity of b -tocotrienol. *Biochemical and Biophysical Research Communications*, *617*, 33–40. https://doi.org/10.1016/j.bbrc.2022.05.082

Surjit Singh, C. K., Lim, H. P., Khoo, J. Y. P., Tey, B. T., & Chan, E. S. (2022). Effects of high-energy emulsification methods and environmental stresses on emulsion

stability and retention of tocotrienols encapsulated in Pickering emulsions. *Journal of Food Engineering*, *327*, 111061. https://doi.org/10.1016/j.jfoodeng.2022.111061

Syväoja, E. L., Pilronen, V., Varo, P., Koivistoinen, P., & Salminen, K. (1986). Tocopherols and tocotrienols in Finnish foods: Oils and fats. *Journal of the American Oil Chemists' Society*, *63*(3), 328–329. https://doi.org/10.1007/BF02546039

Tan, P. Y., Tan, T. B., Chang, H. W., Tey, B. T., Chan, E. S., Lai, O. M., Baharin, B. S., Nehdi, I. A., & Tan, C. P. (2018). Effects of storage and yogurt matrix on the stability of tocotrienols encapsulated in chitosan-alginate microcapsules. *Food Chemistry*, *241*, 79–85. https://doi.org/10.1016/j.foodchem.2017.08.075

Tan, P. Y., Tey, B. T., Chan, E. S., Lai, O. M., Chang, H. W., Tan, T. B., Liu, Y., Wang, Y., Tan, C. P., Olives Barba, A. I., Cámara Hurtado, M., Sánchez Mata, M. C., Fernández Ruiz, V., López Sáenz De Tejada, M., Darnoko, D., Cheryan, M., Moros, E., Jerrel, J., Perkins, E. G., Choi, H. K. (2000). Stabilization and Release of Palm Tocotrienol Emulsion Fabricated Using pH Sensitive Calcium Carbonate. *Food Chemistry*, *8*(2), 1873–1885. https://doi.org/10.3390/foods10020358

Tanford, C., Bunville, L. G., & Nozaki, Y. (1959). The Reversible Transformation of β-Lactoglobulin at pH 7.5. *Journal of the American Chemical Society*, *81*(15), 4032–4036. https://doi.org/10.1021/ja01524a054

Tarhini, M., Greige-Gerges, H., & Elaissari, A. (2017). Protein-based nanoparticles: From preparation to encapsulation of active molecules. *International Journal of Pharmaceutics*, *522*(1–2), 172–197. https://doi.org/10.1016/j.ijpharm.2017.01.067

Teo, A., Lam, Y., Lee, S. J., & Goh, K. K. T. (2021). Spray drying of whey protein stabilized nanoemulsions containing different wall materials – maltodextrin or trehalose. *Lwt*, *136*, 110344. https://doi.org/10.1016/j.lwt.2020.110344

Theodore P. Labuza, T., & Dugan. Jr, L. R. (1971). Kinetics of lipid oxidation in foods. *C R C Critical Reviews in Food Technology*, *2:3*, 355–405. https://doi.org/10.1080/10408397109527127

Timilsena, Y. P., Adhikari, R., Barrow, C. J., & Adhikari, B. (2017). Digestion behaviour of chia seed oil encapsulated in chia seed protein-gum complex coacervates. *Food Hydrocolloids*, *66*, 71–81. https://doi.org/10.1016/j.foodhyd.2016.12.017

Tomotake, H., Shimaoka, I., Kayashita, J., Nakajoh, M., & Kato, N. (2002). Physicochemical and functional properties of buckwheat protein product. *Journal of Agricultural and Food Chemistry*, *50*(7), 2125–2129. https://doi.org/10.1021/jf011248q

Tripodo, G., & Mandracchia, D. (2019). Inulin as a multifaceted (active)substance and its chemical functionalization: From plant extraction to applications in pharmacy, cosmetics and food. *European Journal of Pharmaceutics and Biopharmaceutics*, *141*, 21–36. https://doi.org/10.1016/j.ejpb.2019.05.011

Turchiuli, C., Jimenez Munguia, M. T., Hernandez Sanchez, M., Cortes Ferre, H., & Dumoulin, E. (2014). Use of different supports for oil encapsulation in powder by

spray drying. *Powder Technology*, *255*, 103–108. https://doi.org/10.1016/j.powtec.2013.08.026

Vinceković, M., Viskić, M., Jurić, S., Giacometti, J., Bursać Kovačević, D., Putnik, P., Donsì, F., Barba, F. J., & Režek Jambrak, A. (2017). Innovative technologies for encapsulation of Mediterranean plants extracts. *Trends in Food Science and Technology*, *69*, 1–12. https://doi.org/10.1016/j.tifs.2017.08.001

Walia, N., & Chen, L. (2020). Pea protein based vitamin D nanoemulsions: Fabrication, stability and in vitro study using Caco-2 cells. *Food Chemistry*, *305*, 125475. https://doi.org/10.1016/j.foodchem.2019.125475

Walker, R. M., Decker, E. A., & McClements, D. J. (2015). Physical and oxidative stability of fish oil nanoemulsions produced by spontaneous emulsification: Effect of surfactant concentration and particle size. *Journal of Food Engineering*, *164*, 10–20. https://doi.org/10.1016/j.jfoodeng.2015.04.028

Walstra, P. (1993). Principles of emulsion formation. *Chemical Engineering Science*, *48*(2), 333–349. https://doi.org/10.1016/0009-2509(93)80021-H

Wang, B., Li, D., Wang, L.-J., Adhikari, B., & Shi, J. (2010). Ability of flaxseed and soybean protein concentrates to stabilize oil-in-water emulsions. *Journal of Food Engineering*, *100*(3), 417–426. https://doi.org/10.1016/j.jfoodeng.2010.04.026

Wang, L., Song, Y., Parikh, A., Joyce, P., Chung, R., Liu, L., Afinjuomo, F., Hayball, J. D., Petrovsky, N., Barclay, T. G., & Garg, S. (2019). Doxorubicin-loaded delta inulin conjugates for controlled and targeted drug delivery: Development, characterization, and in vitro evaluation. *Pharmaceutics*, *11*(11), 581. https://doi.org/10.3390/pharmaceutics11110581

Wang, S., Yang, J., Shao, G., Liu, J., Wang, J., Yang, L., Li, J., Liu, H., Zhu, D., Li, Y., & Jiang, L. (2020). pH-induced conformational changes and interfacial dilatational rheology of soy protein isolated/soy hull polysaccharide complex and its effects on emulsion stabilization. *Food Hydrocolloids*, *109*, 106075. https://doi.org/10.1016/J.FOODHYD.2020.106075

Wang, X., Jiang, Y., Wang, Y. W., Huang, M. T., Ho, C. T., & Huang, Q. (2008). Enhancing anti-inflammation activity of curcumin through O/W nanoemulsions. *Food Chemistry*, *108*(2), 419–424. https://doi.org/10.1016/j.foodchem.2007.10.086

Wang, Yifan, Bai, C., McClements, D. J., Xu, X., Sun, Q., Jiao, B., Wang, Q., & Dai, L. (2023). Improvement of 3D printing performance of pea protein isolate Pickering emulsion gels by regulating electrostatic interaction between protein and polysaccharide. *Food Hydrocolloids*, *145*, 109097. https://doi.org/10.1016/J.FOODHYD.2023.109097

Wang, Yingxin, Ghosh, S., & Nickerson, M. T. (2022). Effect of biopolymer mixing ratios and aqueous phase conditions on the interfacial and emulsifying properties of lentil protein isolate–κ-carrageenan and lentil protein isolate–ι-carrageenan complexes. *Cereal Chemistry*, *99*(1), 169–183. https://doi.org/10.1002/cche.10465

Wei, Z., & Huang, Q. (2019). Assembly of Protein-Polysaccharide Complexes for Delivery of Bioactive Ingredients: A Perspective Paper. *Journal of Agricultural and Food Chemistry*, *67*(5), 1344–1352. https://doi.org/10.1021/acs.jafc.8b06063

Whittle, K. J., Dunphy, P. J., & Pennock, J. F. (1966). The isolation and properties of delta-tocotrienol from Hevea latex. *The Biochemical Journal*, *100*(1), 138–145. https://doi.org/10.1042/bj1000138

Wibowo, S., Vervoort, L., Tomic, J., Santiago, J. S., Lemmens, L., Panozzo, A., Grauwet, T., Hendrickx, M., & Van Loey, A. (2015). Colour and carotenoid changes of pasteurised orange juice during storage. *Food Chemistry*, *171*, 330–340. https://doi.org/10.1016/j.foodchem.2014.09.007

Wijekoon, M. M. J. O., Mahmood, K., Ariffin, F., Mohammadi Nafchi, A., & Zulkurnain, M. (2023). Recent advances in encapsulation of fat-soluble vitamins using polysaccharides, proteins, and lipids: A review on delivery systems, formulation, and industrial applications. *International Journal of Biological Macromolecules*, *241*, 124539. https://doi.org/10.1016/J.IJBIOMAC.2023.124539

Wlodarkievicz, M. E., Maria, B., Puton, S., Fischer, B., Fernandes, I. A., Junges, A., & Paroul, N. (2022). Microencapsulation of Citronella Essential Oil (Cymbopogon winterianus) with Different Wall Materials Using Spray Drying. *Letters in Applied NanoBioScience*, *12*(3), 71. https://doi.org/10.33263/lianbs123.071

Wong, B. T., Day, L., & Augustin, M. A. (2011). Deamidated wheat protein-dextran Maillard conjugates: Effect of size and location of polysaccharide conjugated on steric stabilization of emulsions at acidic pH. *Food Hydrocolloids*, *25*(6), 1424–1432. https://doi.org/10.1016/j.foodhyd.2011.01.017

Wong, W. Y., Ward, L. C., Fong, C. W., Yap, W. N., & Brown, L. (2017). Anti-inflammatory γ- and δ-tocotrienols improve cardiovascular, liver and metabolic function in diet-induced obese rats. *European Journal of Nutrition*, *56*(1), 133–150. https://doi.org/10.1007/s00394-015-1064-1

Wu, W., He, W., Tan, Y., Tian, Z., Chen, L., Hu, F.-Q., & Wu, W. (2011). Food protein-stabilized nanoemulsions as potential delivery systems for poorly water-soluble drugs: preparation, in vitro characterization, and pharmacokinetics in rats. *International Journal of Nanomedicine*, *6*, 521—533. https://doi.org/10.2147/ijn.s17282

Xavier dos Santos, D., Casazza, A. A., Aliakbarian, B., Bedani, R., Saad, S. M. I., & Perego, P. (2019). Improved probiotic survival to in vitro gastrointestinal stress in a mousse containing Lactobacillus acidophilus La-5 microencapsulated with inulin by spray drying. *LWT*, *99*, 404–410. https://doi.org/10.1016/J.LWT.2018.10.010

Xiao, Z., Xia, J., Zhao, Q., Niu, Y., & Zhao, D. (2022). Maltodextrin as wall material for microcapsules: A review. *Carbohydrate Polymers*, *298*, 120113. https://doi.org/10.1016/j.carbpol.2022.120113

Xu, D., Qi, Y., Wang, X., Li, X., Wang, S., Cao, Y., Wang, C., Sun, B., Decker, E., & Panya, A. (2017). The influence of flaxseed gum on the microrheological properties

and physicochemical stability of whey protein stabilized β-carotene emulsions. *Food and Function*, *8*(1), 415–423. https://doi.org/10.1039/c6fo01357k

Xu, F., Pandya, J. K., Chung, C., McClements, D. J., & Kinchla, A. J. (2018). Emulsions as delivery systems for gamma and delta tocotrienols: Formation, properties and simulated gastrointestinal fate. *Food Research International*, *105*, 570–579. https://doi.org/10.1016/j.foodres.2017.11.033

Xu, Z. (2005). Analysis of Tocopherols and Tocotrienols. *Handbook of Food Analytical Chemistry*, *1–2*, 479–490. https://doi.org/10.1002/0471709085.ch12

Yang, M., Peng, J., Zi, Y., Shi, C., Kan, G., Wang, X., & Zhong, J. (2023). Encapsulation of fish oil by complex coacervation and freeze drying with modified starch aid. *Food Hydrocolloids*, *137*, 108371. https://doi.org/10.1016/j.foodhyd.2022.108371

Yang, Y., & McClements, D. J. (2013). Encapsulation of vitamin E in edible emulsions fabricated using a natural surfactant. *Food Hydrocolloids*, *30*(2), 712–720. https://doi.org/10.1016/j.foodhyd.2012.09.003

Yap, S. P., Yuen, K. H., & Wong, J. W. (2001). Pharmacokinetics and bioavailability of α-, γ- and δ-tocotrienols under different food status. *Journal of Pharmacy and Pharmacology*, *53*(1), 67–71. https://doi.org/10.1211/0022357011775208

Yap, Siew Ping, & Yuen, K. H. (2004). Influence of lipolysis and droplet size on tocotrienol absorption from self-emulsifying formulations. *International Journal of Pharmaceutics*, *281*(1–2), 67–78. https://doi.org/10.1016/j.ijpharm.2004.05.015

Yesiltas, B., García-Moreno, P. J., Sørensen, A. D. M., Soria Caindec, A. M., Hyldig, G., Anankanbil, S., Guo, Z., & Jacobsen, C. (2021). Enrichment of mayonnaise with a high fat fish oil-in-water emulsion stabilized with modified DATEM C14 enhances oxidative stability. *Food Chemistry*, *341*, 128141. https://doi.org/10.1016/j.foodchem.2020.128141

Yi, H., Cho, H., Hwang, K. T., & Shin, B. S. (2015). Physical and Oxidative Stability of Flaxseed Oil-Fructooligosaccharide Emulsion. *Journal of Food Processing and Preservation*, *39*(6), 2348–2355. https://doi.org/10.1111/jfpp.12482

Yi, J., Gan, C., Wen, Z., Fan, Y., & Wu, X. (2021). Development of pea protein and high methoxyl pectin colloidal particles stabilized high internal phase pickering emulsions for β-carotene protection and delivery. *Food Hydrocolloids*, *113*, 106497. https://doi.org/10.1016/j.foodhyd.2020.106497

Yi, J., Huang, H., Liu, Y., Lu, Y., Fan, Y., & Zhang, Y. (2020). Fabrication of curcumin-loaded pea protein-pectin ternary complex for the stabilization and delivery of β-carotene emulsions. *Food Chemistry*, *313*, 126118. https://doi.org/10.1016/j.foodchem.2019.126118

Yin, X., Hu, Q., Chen, X., Tan, S., Niu, A., Qiu, W., & Wang, G. (2023). Inclusion complexes of clove essential oil with sodium caseinate and gum arabic prepared by high-pressure homogenization: Characterization and non-contact antimicrobial activity. *Food Control*, *150*, 109765. https://doi.org/10.1016/J.FOODCONT.2023.109765

Yousf, N., Nazir, F., Salim, R., Ahsan, H., & Sirwal, A. (2017). Water solubility index and water absorption index of extruded product from rice and carrot blend. *Journal of Pharmacognosy and Phytochemistry JPP*, *6*(66), 2165–2168. http://www.phytojournal.com/archives/2017/vol6issue6/PartAD/6-6-326-909.pdf

Yu, Y., Wei, R., Jia, X., Zhang, X., Liu, H., Xu, B., & Xu, B. (2022). Preparation of Piper nigrum Microcapsules by Spray Drying and Optimization with Response Surface Methodology. *Journal of Oleo Science*, *71*(12), 1789–1797. https://doi.org/10.5650/jos.ess21299

Yuan, Y., Gao, Y., Zhao, J., & Mao, L. (2008). Characterization and stability evaluation of β-carotene nanoemulsions prepared by high pressure homogenization under various emulsifying conditions. *Food Research International*, *41*(1), 61–68. https://doi.org/10.1016/j.foodres.2007.09.006

Zang, X., Wang, J., Yu, G., & Cheng, J. (2019). Addition of anionic polysaccharides to improve the stability of rice bran protein hydrolysate-stabilized emulsions. *LWT*, *111*, 573–581. https://doi.org/10.1016/J.LWT.2019.04.020

Zha, F., Dong, S., Rao, J., & Chen, B. (2019). Pea protein isolate-gum Arabic Maillard conjugates improves physical and oxidative stability of oil-in-water emulsions. *Food Chemistry*, *285*, 130–138. https://doi.org/10.1016/j.foodchem.2019.01.151

Zhang, J., Bing, L., & Reineccius, G. A. (2016). Comparison of modified starch and Quillaja saponins in the formation and stabilization of flavor nanoemulsions. *Food Chemistry*, *192*, 53–59. https://doi.org/10.1016/j.foodchem.2015.06.078

Zhang, L., & Li, L. (2022). The interaction between anionic polysaccharides and legume protein and their influence mechanism on emulsion stability. *Food Hydrocolloids*, *131*(April), 107814. https://doi.org/10.1016/j.foodhyd.2022.107814

Zhang, X., Wang, Q., Liu, Z., Zhi, L., Jiao, B., Hu, H., Ma, X., Agyei, D., & Shi, A. (2023). Plant protein-based emulsifiers: Mechanisms, techniques for emulsification enhancement and applications. *Food Hydrocolloids*, *144*, 109008. https://doi.org/10.1016/J.FOODHYD.2023.109008

Zhang, Y., Li, D., Wang, L. J., & Adhikari, B. (2013). Rheological and Microstructural Characteristics of Thermally Produced Flaxseed Gum-Whey Protein Isolate Mixed Solutions and Gels. *Drying Technology*, *31*(13–14), 1635–1642. https://doi.org/10.1080/07373937.2013.771652

Zhu, J., Li, X., Liu, L., Li, Y., Qi, B., & Jiang, L. (2022). Preparation of spray-dried soybean oil body microcapsules using maltodextrin: Effects of dextrose equivalence. *Lwt*, *154*, 112874. https://doi.org/10.1016/j.lwt.2021.112874

Zou, L., & Akoh, C. C. (2015). Antioxidant activities of annatto and palm tocotrienol-rich fractions in fish oil and structured lipid-based infant formula emulsion. *Food Chemistry*, *168*, 504–511. https://doi.org/10.1016/j.foodchem.2014.07.098

APPENDICES

Appendix A1

Production of TRF-based Nanoemulsion

Appendix A2

TRF-based Nanoemulsion

Appendix A3

TRF-based Microcapsule

Appendix A4

Wall Materials of Maltodextrin, Starch Sodium Octenyl Succinate, and Inulin

Appendix A5

Control Mayonnaise, Mayonnaise Containing TRF-based Microcapsule, and Mayonnaise Containing TRF bulk oil

Appendix B1

Hedonic Sensory Questionnaire (UPM Students)

SENSORY EVALUATION OF TOCOTRIENOL-FORTIFIED MAYONNAISE

Instructions:

a) Each sample has been coded with three-digit numbers.
b) Please evaluate all sensory attributes of each sample by giving a score ranging from 1 (dislike extremely) to 9 (like extremely) as listed in TABLE 1.
c) Please rinse your mouth before tasting each sample.
d) Please rate the sensory attributes for each sample from **left to right** as listed in TABLE 2.

TABLE 1

Sensory score	Description
1	Dislike extremely
2	Dislike very much
3	Dislike moderately
4	Dislike slightly
5	Neither like or dislike
6	Like slightly
7	Like moderately
8	Like very much
9	Like extremely

TABLE 2

Sensory attributes			
Colour			
Aroma			
Taste			
Creaminess			
Sourness			
Overall acceptability			

THANK YOU FOR YOUR TIME AND KIND COOPERATION

Appendix C1

Formulations of TRF-based Nanoemulsion (Total 300g)

Oil phase	Aqueous phase					Total
TRF-oil	**TPPI-FG Ratio**	**TPPI**	**FG**	**Distilled Water**	**Sodium azide**	
10% 30 g	3:1 2.0% 6.0 g	1.5% 4.50 g	0.5% 1.50 g	88% 264 g	0.01% 0.03 g	100% 300 g
10% 30 g	5:1 2.0% 6.0 g	1.67% 5.01 g	0.33% 0.99 g	88% 264 g	0.01% 0.03 g	100% 300 g
10% 30 g	7:1 2.0% 6.0 g	1.75% 5.25 g	0.25% 0.75 g	88% 264 g	0.01% 0.03 g	100% 300 g
10% 30 g	9:1 2.0% 6.0 g	1.8% 5.40 g	0.2% 0.60 g	88% 264 g	0.01% 0.03 g	100% 300 g
10% 30 g	11:1 2.0% 6.0 g	1.83% 5.49 g	0.167% 0.50 g	88% 264 g	0.01% 0.03 g	100% 300 g

Abbreviations: TRF: Tocotrienol-rich fraction; TPPI: Treated pea protein isolate; FG: Flaxseed gum.

Example of calculation:

To prepare a total 300g of nanoemulsion using TPPI-FG at ratio 3:1,
1) Total oil phase (10% TRF-oil)
= 300 g × 10%
= 30g

2) Total TPPI-FG complex (2%)
= 300 g × 2%
= 6 g

3) TPPI-FG ratio 3:1
a) TPPI
= 2% × (3/4)
= 1.5 %
= 4.5 g

b) FG
= 2% × (1/4)
= 0.5%
= 1.5 g

4) Sodium azide (0.01%)
= 300 g × 0.01%
= 0.003 g

5) Distilled water (88%)
= 300 g × 88%
= 264 g

Appendix C2

Formulations of TRF-based Microcapsule (Total 300g)

Formulas	Core-to-wall ratios	TRF-oil	Mixing ratio	Wall materials			TPPI-FG complex (3:1)	Distilled water	Total
				M	OSS	INU			
1:2 M	1:2 30g:60g	10% 30 g	1:0	18.0% 54.0 g	-	-	2.0% 6.0 g	70% 210 g	100% 300 g
1:3 M	1:3 30g:90g	10% 30 g	1:0	28.0% 2 84.0 g	-	-	2.0% 6.0 g	60% 180 g	100% 300 g
1:4 M	1:4 30g:120g	10% 30 g	1:0	38.0% 114.0 g	-	-	2.0% 6.0 g	50% 150 g	100% 300 g
1:4 M:OSS (9:1)	1:4 30g:120g	10% 30 g	9:1	34.2% 102.6 g	3.8% 11.4 g	-	2.0% 6.0 g	50% 150 g	100% 300 g
1:4 M:OSS (8:2)	1:4 30g:120g	10% 30 g	8:2	30.4% 91.2 g	7.6% 22.8 g	-	2.0% 6.0 g	50% 150 g	100% 300 g
1:4 M:INU (9:1)	1:4 30g:120g	10% 30 g	9:1	34.2% 102.6 g	-	3.8% 11.4 g	2.0% 6.0 g	50% 150 g	100% 300 g
1:4 M:INU (8:2)	1:4 30g:120g	10% 30 g	8:2	30.4% 91.2 g	-	7.6% 22.8 g	2.0% 6.0 g	50% 150 g	100% 300 g

Abbreviations: TRF: Tocotrienol-rich fraction; TPPI: Treated pea protein isolate; FG: Flaxseed gum; M: Maltodextrin; OSS: Starch sodium octenyl succinate; INU: Inulin.

Example of calculation:

To prepare a total 300g of solution using TPPI-FG at ratio 3:1, core-to-wall ratio of 1:2 using maltodextrin.

1) Core-to-wall ratio is 1:2 = 30 g : 60 g
   a) Core material consists of 10% TRF-oil
      = 300 g × 10%
      = 30 g
   b) Wall material consists of 20% dry solid (18% of M and OSS and 2% TPPI-FG complex)
      = 300 g × 20%
      = 60 g

2) Mixing ratio of wall materials, M is 1:0
   Maltodextrin
   = 300 g × 18%
   = 54 g

3) TPPI-FG complex (2%)
   = 300 g × 2%
   = 6 g

4) Distilled water
   = 100% – 10% – 18% – 2%
   = 70 %
   = 210 g

Example of calculation:

To prepare a total 300g of solution using TPPI-FG at ratio 3:1, core-to-wall ratio of 1:4, using M: OSS at mixing ratio of 1:9.

1) Core-to-wall ratio is 1:4 = 30 g : 120 g
   a) Core material consists of 10% TRF-oil
      = 300 g × 10%
      = 30 g
   b) Wall material consists of 40% dry solid (38% of M and OSS and 2% TPPI-FG complex)
      = 300 g × 40%
      = 120 g

2) Mixing ratio of wall material, M: OSS is 1:9
   a) Maltodextrin
      = 38% × (9/10)
      = 34.2%
      = 102.6 g
   b) OSS
      = 38% × (1/10)
      = 3.8%
      = 11.4 g

3) TPPI-FG complex (2%)
   = 300 g × 2%
   = 6 g

4) Distilled water
   = 100% – 10% – 38% – 2%
   = 50%
   = 150 g

BIODATA OF STUDENT

Teow Shuh Jun was born on November 6, 1994, in Kuala Lumpur, Malaysia. She received her primary and secondary education at SJK(C) On Pong and SMK Pandan Mewah, Kuala Lumpur, from 2001 to 2011, respectively. Following her secondary education, she pursued her Cambridge A-Level in Science from 2012 to 2013 at Universiti Kolej Tunku Abdul Rahman, Setapak. From 2014 to 2017, she continued her academic journey at the same institution and graduated with First Class Honors in a Bachelor of Science (Honours) Degree in Food Science. During her undergraduate studies, she engaged in a research project focused on the development of low glycemic index-high fiber noodle. In 2017, she participated in the Innovation Food Product Development Competition organized by the Malaysian Institute of Food Technology (MIFT) as part of a group. She was awarded with the first prize in the said competition. In 2018 to 2019, she pursued her Master of Food Technology at Universiti Putra Malaysia, under the guidance of Prof. Dr. Jamilah Binti Bakar. She successfully completed a research project that investigated the properties of foam-mat dried *Clitorea Ternatea* powder, examining variations resulting from the use of different foaming agents and drying temperatures.

.

LIST OF PUBLICATIONS

Teow, S. J., Choy, H. W., Khor, Y. P., Tan, T. B., Gholivand, S., Mat Yusoff, M., & Tan, C. P. (2025). Storage stability and sensory evaluation of tocotrienol-rich fraction fortified mayonnaise. *International Food Research Journal,* 32*(1)*: 41–52.

Teow, S. J., Choy, H. W., Khor, Y. P., Tan, T. B., Gholivand, S., Mat Yusoff, M., & Tan, C. P. (2025). Storage stability, release characteristics, and bioaccessibility of the tocotrienol-rich fraction encapsulated in maltodextrin-starch sodium octenyl succinate microcapsules. Food *and Bioproducts Processing,* 151: 11-19.